PhD PROCEEDINGS

ANNUAL ISSUES OF THE DOCTORAL SCHOOL

FACULTY OF INFORMATION TECHNOLOGY & BIONICS

2019

PhD PROCEEDINGS

ANNUAL ISSUES OF THE DOCTORAL SCHOOL

FACULTY OF INFORMATION TECHNOLOGY & BIONICS
PÁZMÁNY PÉTER CATHOLIC UNIVERSITY

PhD PROCEEDINGS

ANNUAL ISSUES OF THE DOCTORAL SCHOOL

FACULTY OF INFORMATION TECHNOLOGY & BIONICS

2019

PÁZMÁNY UNIVERSITY *e*PRESS
BUDAPEST, 2019

HU ISSN 2064-7271

Kiadja a Pázmány Egyetem eKiadó
Budapest, 2019

Felelős kiadó
Ft. Dr. Szuromi Szabolcs Anzelm O. Praem.
a Pázmány Péter Katolikus Egyetem rektora

The publication of this volume was supported by the European Union,
co-financed by the European Social Fund (EFOP-3.6.3-VEKOP-16-2017-00002)
and by the New National Excellence Program of the Ministry of Human Capacities

Cover image by Ádám Nagy: *Optical-flow-based respiration signal extraction*

Contents

Introduction

It is our pleasure to publish this Annual Proceedings again to demonstrate the genuine interdisciplinary research done at the Jedlik Laboratories by young talents working in the Roska Tamás Doctoral School of Sciences and Technology of the Faculty of Information Technology and Bionics at Pázmány Péter Catholic University. The scientific results of our PhD students show the main recent research directions in which our faculty is engaged. Thanks are also due to the supervisors and consultants, as well as to the five collaborating National Research Laboratories of the Hungarian Academy of Sciences, the Semmelweis Medical School and the University of Pannonia. The collaborative work with the partner universities, especially, Katolieke Universiteit Leuven, Politecnico di Torino, Technische Universität München, University of California at Berkeley, University of Notre Dame, Universidad de Sevilla, Universita di Catania, Université de Bordeaux, Universidad Autonoma de Madrid is gratefully acknowledged.

We acknowledge the many sponsors of the research reported here. Namely,

- the Hungarian National Research Fund (OTKA),
- the Hungarian Academy of Sciences (MTA),
- UNKP Programme, Ministry of Human Capacities, Hungarian Government,
- the National Research, Development and Innovation Office (NKFIH),
- the Gedeon Richter Co.,
- the Office of Naval Research (ONR) of the US,
- NVIDIA Ltd.,
- Verizon Computer Vision Group (Eutecus Inc.), Berkeley, CA,
- MorphoLogic Ltd., Budapest,
- Analogic Computers Ltd., Budapest,
- AnaFocus Ltd., Seville,

and some other companies and individuals.

Needless to say, the resources and support of the Pázmány Péter Catholic University is gratefully acknowledged.

Budapest, June 2019.

GÁBOR PRÓSZÉKY
Chairman of the Board of the Doctoral School

PÉTER SZOLGAY
Head of the Doctoral School

.

PROGRAM 1
BIONICS, BIO-INSPIRED WAVE COMPUTERS, NEUROMORPHIC MODELS

Heads: Tamás FREUND, György KARMOS, Zsolt LIPOSITS, Sándor PONGOR

Overcoming the blood-brain barrier by different intranasal formulations of quinidine, a P-gp model substrate.

Luca Anna BORS
(Supervisor: Franciska ERDŐ)
Pázmány Péter Catholic University, Faculty of Information Technology and Bionics
50/a Práter street, 1083 Budapest, Hungary
bors.luca.anna@itk.ppke.hu

Statement of originality - *This proceeding report describes the work of the doctoral student during the academic year 2018/2019. Parts of this work might be under submission to scientific conferences and journals.*

Summary

To understand the pathogenesis of blood brain barrier (BBB) related diseases, this study was made to open a new alternative to investigate the BBB and its function by using intranasal drug delivery. The intranasal administration of drugs has become an innovative way to deliver CNS medication without too much peripheral exposure, as the drug is administered as a spray, drop or gel into the nasal cavity where the olfactory nerves can absorb the drug and transport it directly to the brain. Due to this drug delivery route the unwanted side effects in the periphery can be reduced significantly. The mucosa of the nasal cavity is also takes part as an absorption site as it is rich in small veins and capillaries that can also absorb and distribute molecules.

Methods

We tried to find the best formulation to deliver quinidine (QND) into the central nervous system (CNS) through the nasal route; three different vehicles were compared to each other: nasal drops, a silicon-gel (recipe got from the Institute of Behavioral Neuroscience, Heinrich Heine University of Düsseldorf) and another gel manufactured by MetP Pharma, Switzerland, a company that specialized in intranasal delivery methods. These formulations were used to deliver QND, our P-glycoprotein (P-gp) substrate to the CNS in rat models.

Results and discussion

After trying out multiple formulations of intranasal QND, the more viscous vehicles seems to be more practical for intranasal drug delivery than nasal drops, but it has to be noted that more viscous substances get harder to be delivered into the nasal cavity. In case of QND the "'home-made"' silicon gel showed better results than the MetP Pharma gel, but we have to consider that both the administration technique may have some error.

Fig. 1. Intranasal administration of viscous substances. The gel was delivered with Gilson Microman pipette with a specialized piston-like tip that is necessary to deliver the exact amount of gel into the nose. The olfactory region marked with yellow.

References

[1] F. Erdő, L. Denes, and E. de Lange, "Age-associated physiological and pathological changes at the blood-brain barrier: A review.," *J Cereb Blood Flow Metab.*, vol. 37, no. 1, pp. 4-24, 2017.

[2] A. M. Dolberg and S. Reichl, "Expression of P-glycoprotein in excised human nasal mucosa and optimized models of RPMI 2650 cells.," *Int J Pharm.*, vol. 508, no. 1-2, pp. 22-33, 2016.

[3] F. Erdő, L. A. Bors, D. Farkas, Á. Bajza, S. Gizurarson "Evaluation of intranasal delivery route of drug administration for brain targeting" *Brain Res Bull.*, vol. 143, pp.155-170, 2018.

L. BORS, "Overcoming the blood-brain barrier by different intranasal formulations of quinidine, a P-gp model substrate." in *PhD Proceedings – Annual Issues of the Doctoral School, Faculty of Information Technology and Bionics, Pázmány Péter Catholic University – 2019.* G. Prószéky, P. Szolgay Eds. Budapest: Pázmány University ePress, 2019, pp. 12–12. This research has been partially supported by the European Union, co-financed by the European Social Fund (EFOP-3.6.3-VEKOP-16-2017-00002).

Reducing the Effects of Biological Noise by Coupled Feed Forward Loops

Suchana CHAKRAVARTY
(Supervisor: Attila CSIKÁSZ-NAGY)
Pázmány Péter Catholic University, Faculty of Information Technology and Bionics
50/a Práter street, 1083 Budapest, Hungary
chakravarty.suchana@itk.ppke.hu

***Abstract*—The dynamics of various cellular networks are important due to their diverse and special role played in biology. Due to presence of cellular noise the cells behave stochastically. Underlying mechanisms of cellular networks can be explained by mathematical modelling and computational simulations. Earlier research has reported about the dynamics of simple feed forward loops. Here we are interested in investigating the underlying dynamics and the effects on cellular noise by coupling of feed forward loop. We test by computational simulation how our models of coupled feed forward loops can reduce cellular noise and try to explain the quantitative as well as qualitative behavior of these systems.**

***Keywords*-Cellular noise; computational simulation; mathematical modelling; feed forward loops.**

Discussion

Cellular processes are noisy due to the inherent stochastic behavior of biochemical reactions. The stochastic fluctuation can be originated either extrinsically or intrinsically. The extrinsic noise arises due to the interaction with the neighboring environmental processes. The intrinsic noise depends on the low copy number of metabolites present in a cell or it can be present because of the noise in the time scale of the individual reactions [1].

The feed forward loop is generally three node networks, where a species regulates the second species and they jointly regulate the third target species through the direct and indirect arms. When the direct and indirect arms possess same sign, it is called coherent and when they have different sign it is called incoherent feed forward loop[2]. The key functions of simple feed forward loop such as acceleration of response time by implementing incoherent feed forward loop or sign sensitive time delay in the case of coherent feed forward loop has been shown earlier [2]. The most biological abundant reaction motif, coherent feed forward loop can be useful in the case of reduction of noise [3]. It has been shown earlier that negative feedback loops could be also useful for reducing cellular noise [1]. The attenuation of noise is also attained by the simultaneous degradation of two chemical species which are co-expressed [1].

We have developed a mathematical model of a coupled feed forward loop and investigated the dynamics of the coupled feed forward loop through stochastic simulation. Our preliminary results suggest that if we choose the species to switch back and forth between active and inactive states then it can reduce the noise quite well.

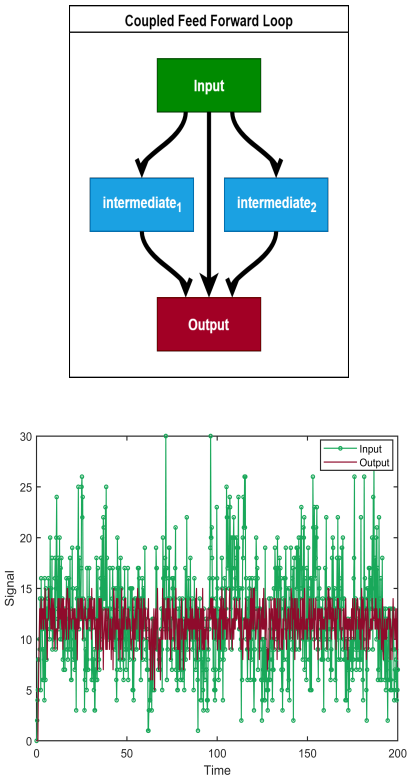

Fig. 1. In the upper panel the influential diagram of coupled feed forward loops is depicted; In the lower panel the stochastic time course simulation of the model is provided. The green color denotes the input signal and red denotes output signals. The noise is much less in the output compared to the input

Reference

[1] Luca Laurenti, Attila Csikász-Nagy, Marta Kwiatkowska, and Luca Cardelli, "Molecular Filters for Noise Reduction. " , *Biophysical Journal* , vol.114, no. 12, pp. 3000–3011, 2018.

[2] S. Mangan and U. Alon, "Structure and function of the feed-forward loop network motif. " , *PNAS* , vol. 100, no. 21, pp. 11980–11985, 2003.

[3] Rong Gui, Quan Liu , Yuangen Yao, Haiyou Deng, Chengzhang Ma, Ya Jia and Ming Yi, "Noise Decomposition Principle in a Coherent Feed-Forward Transcriptional Regulatory Loop." *Frontiers in Physiology*, vol. 7, no. 600, pp. 1-11, 2016.

S. CHAKRAVARTY, "Reducing the Effects of Biological Noise by Coupled Feed Forward Loops" in *PhD Proceedings – Annual Issues of the Doctoral School, Faculty of Information Technology and Bionics, Pázmány Péter Catholic University – 2019.* G. Prószéky, P. Szolgay Eds. Budapest: Pázmány University ePress, 2019, pp. 13–13. This research has been partially supported by the European Union, co-financed by the European Social Fund (EFOP-3.6.3-VEKOP-16-2017-00002).

Secretin modulates excitatory GABAergic neurotransmission to GnRH neurons via retrograde NO signaling pathway in male mice

Veronika CSILLAG
(Supervisors: Imre FARKAS, Zsolt LIPOSITS)
Pázmány Péter Catholic University, Faculty of Information Technology and Bionics
50/a Práter street, 1083 Budapest, Hungary
csillag.veronika@itk.ppke.hu

Metabolic hormones influence reproduction in accordance with the actual energy balance. This control may occur at multiple levels of the reproductive axis, although the majority of these interactions takes place centrally in the hypothalamus. It has been shown earlier, that secretin, a member of the gut-brain hormone family, modulates the luteinizing hormone (LH) level, albeit the underlying mechanisms have not been examined till date (Kimura et al., 1987). In order to elucidate the involved intracellular mechanisms, in vitro electrophysiological experiments were carried out in GnRH-GFP neurons of male mice. Whole-cell patch-clamp measurements demonstrated increased frequency of the spontaneus postsynaptic currents (sPSCs) and that of the GABAergic miniature postsynaptic currents (mPSCs) after 100 nM secretin administration. Resting membrane potential also became depolarized and the frequency of evoked action potentials also increased after adding secretin in to the slice chamber. The elevation of the frequency of mPSCs after secretin treatment was prevented by using either a secretin receptor antagonist (3M) or intracellularly applied G-protein-coupled receptor blocker (GDP-β-S) supporting the involvement of secretin receptor in the mechanism. Concerning the known downstream pathway to secretin receptor, intracellular blockade of protein kinase A (PKA) activity with KT-5720 abolished the effect of secretin. Intracellular inhibition of the neuronal nitric oxide synthase (nNOS) by NPLA also prevented the stimulatory effect of secretin on mPSCs. These data suggest that the direct activation of GnRH neurons via secretin receptor occurs through the cAMP/PKA/nNOS signaling pathway, resulting in nitric oxide release. In turn, NO can bind to its only known receptor, the soluble guanylyl cyclase (sGC), expressed in GABAergic axon terminals innervating GnRH neurons (Farkas et al., 2016; Farkas et al., 2018). Presumably, the NO-sGC interaction in the presynaptic axon terminals leads to increased vesicular GABA release which, in turn, excites GnRH neurons via $GABA_A$ receptors.

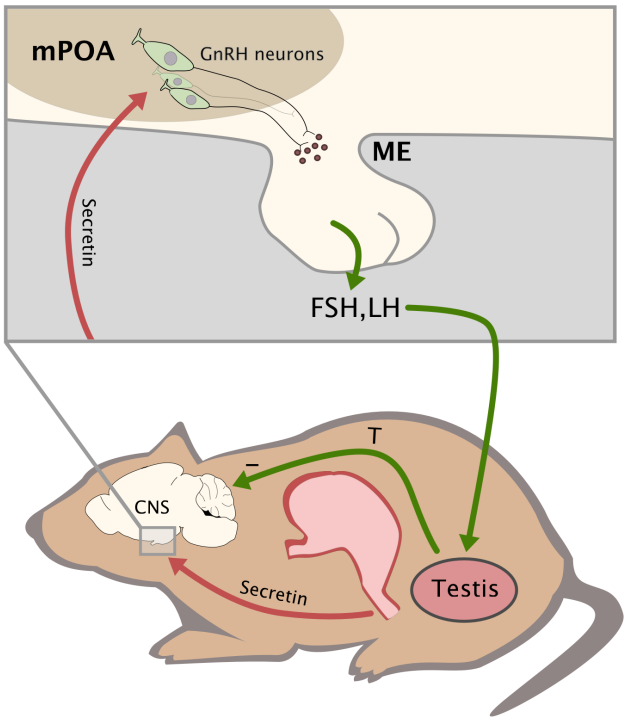

Fig. 1. **Shematic figure of HPG axis in male mice.** Fusiform GnRH neurons are located in the mPOA of the hypothalamus and their axons terminate in the median eminence (ME) where they secrete GnRH into the portal circulation. Red arrows show the relationship between secretin and the reproductive axis. Secretin is produced in the duodenum into the peripheral circulation, and after entering the CNS, it can affect GnRH neurons and reproduction. **T**: Testoserone, **CNS**: central nervous system, **FSH**: Follicle stimulating hormone, LH:Luteinizing hormone, **ME**: mediane eminence, **mPOA:**medial preoptic area

Acknowledgements

The author wishes to acknowledge Dr. Imre Farkas and Prof. Zsolt Liposits for their excellent supervision.This research was supported by the National Research, Development and Innovative Office (K115984 and K128278).

References

[1] Farkas, I., Balint, F., Farkas, E., Vastagh, C., Fekete, C. Liposits, Z. (2018) Estradiol Increases Glutamate and GABA Neurotransmission into GnRH Neurons via Retrograde NO-Signaling in Proestrous Mice during the Positive Estradiol Feedback Period. eNeuro, 5.

[2] Farkas, I., Vastagh, C., Farkas, E., Balint, F., Skrapits, K., Hrabovszky, E., Fekete, C. Liposits, Z. (2016) Glucagon-Like Peptide-1 Excites Firing and Increases GABAergic Miniature Postsynaptic Currents (mPSCs) in Gonadotropin-Releasing Hormone (GnRH) Neurons of the Male Mice via Activation of Nitric Oxide (NO) and Suppression of Endocannabinoid Signaling Pathways. Frontiers in cellular neuroscience, 10, 214.

[3] Kimura, F., Mitsugi, N., Arita, J., Akema, T. Yoshida, K. (1987) Effects of preoptic injections of gastrin, cholecystokinin, secretin, vasoactive intestinal peptide and PHI on the secretion of luteinizing hormone and prolactin in ovariectomized estrogen-primed rats. Brain research, 410, 315-322.

V. CSILLAG, “Secretin modulates excitatory GABAergic neurotransmission to GnRH neurons via retrograde NO signaling pathway in mice” in *PhD Proceedings – Annual Issues of the Doctoral School, Faculty of Information Technology and Bionics, Pázmány Péter Catholic University – 2019.* G. Prószéky, P. Szolgay Eds. Budapest: Pázmány University ePress, 2019, pp. 14–14. This research has been partially supported by the European Union, co-financed by the European Social Fund (EFOP-3.6.3-VEKOP-16-2017-00002).

Investigation of Classification methods for EEG-based BCI using Neural Networks

Ward FADEL

(Supervisors: István ULBERT, Lucia WITTNER)
Pázmány Péter Catholic University, Faculty of Information Technology and Bionics
50/a Práter street, 1083 Budapest, Hungary
fadel.ward@itk.ppke.hu

***Abstract*—Classification of motor imagery EEG-based Brain-computer interface (BCI) signals is a cornerstone in building BCI systems. Many approaches have been developed, but neural networks approach is not investigated well although it is the prominent approach in other fields such as computer vision. In this study, we investigated applying neural networks as classifiers and we tried to apply one approach in which the EEG data is translated into sequence of 2-D images that form the input of a Recurrent Convolutional Neural network. The results can be improved by processing the dataset differently, and by choosing different network architectures and parameters.**

***Keywords*-Brain-Computer Interface (BCI); Classifcation; Neural Networks; motor imagery.**

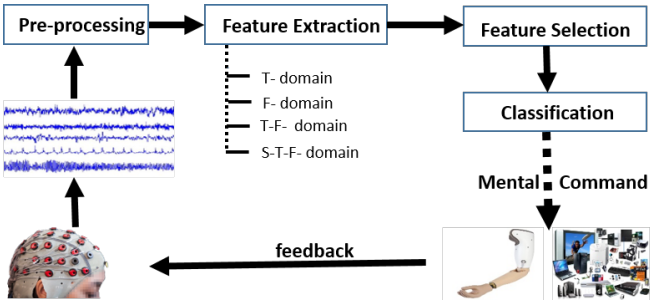

Fig. 1. General EEG-based BCI system.

I. Summary

A Brain-Computer Interface (BCI) is a communication system that translates brain activity patterns of a user into commands for an interactive application [1]. In order to use a BCI, firstly, an offline training phase is needed so the system can be collaborated. Secondly, the online phase in which the brain activity is translated into commands. fig.1 shows a general EEG-based BCI system.

The classification of motor imagery activity is a challenging task due to the low signal-to-noise ratio of EEG signals and their non-stationary nature for the same subject and among subjects, the high sensitivity for artifacts, the limited number of training data, and the low reliability of current BCI systems [2]. Therefore, the classification algorithms mainly aim to overcome one or more of these challenges.

Neural networks are prominent in image classification, for this reason, many studies suggested to transform the EEG signals into 2-D images before classification using a specific neural network architecture.

Pouya Bashivan et al [3] transformed the EEG data into 2-D images in a topology preserving manner to preserve the spatial structure, then, multiple color channels were used to represent the spectral dimension. finally, the sequence of images was used to preserve the temporal dimension which used to train a deep recurrent convolutional neural network to learn to classify the EEG data which represent the cognitive load for the working memory (4 classes). They used 15 participants, each one has been tested for 14 minutes to recognize the amount of mental workload. The brain activity related to memory operations primarily exits in three frequency bands; theta, alpha, and beta. We followed the same approach applied in [3] which was used for mental workload classification. We applied the approach for motor imagery classification. For this reason,we modified the input of the Recurrent Convolutional Neural Network as follows: a) Instead of filtering the EEG signals into theta, alpha, and beta bands, we chose Mu and beta bands, and thus we obtained two(color) channel 2-D images instead of three-channel ones, which reduces complexity.

b) WE used motor imagery EEG datasets from Physiobank Motor/mental imagery database which consists of 109 subjects who performed left and right hand tasks and also both fists and both feet tasks, each subject performed tasks for approximately 26 minutes.We excluded subjects(S088, S092, S100, S104) because they have damaged recordings. Each subject performed 9 different tasks (4 imagery, 4 real, and 1 rest), each task(with relaxation after it). We train the network over 85 subjects, while 10 subjects were used for validation and 10 subjects for testing. The maximum training accuracy was 67.04%, while the maximum accuracy over validation set was 58.22% and for test set it was 57.13%. The results can be improved by choosing different network architectures and parameters. We expect improved results if we make the time window one seventh its value. For motor imagery classification it is also important to choose a subset of the electrodes for classification so to reduce complexity and increase accuracy.

Acknowledgements

I would like to thank Prof. CSURGAY Árpád, Prof. SZOLGAY Péter, Prof. ULBERT István, and Dr. WITTNER Lucia for their support and help.

References

[1] *Reza Abiri et al, A comprehensive review of EEG-based brain–computer interface paradigms,J. Neural Eng.2019, 16, 011001* ,

[2] *F Lotte1 , L Bougrain, A Cichocki, M Clerc, M Congedo, A Rakotomamonjy and F Yger, A review of classification algorithms for EEG-based brain–computer interfaces: a 10 year update,J. Neural Eng. 2018, 15, 031005* ,

[3] Pouya Bashivan, Irina Rish, Mohammed Yeasin, Noel Codella, *Learning Representations from EEG with Deep Recurrent-COonvolutional Neural Networks*, ICLR Conference, 2016.

W. FADEL, "Investigation of Classification methods for EEG-based BCI using Neural Networks" in *PhD Proceedings – Annual Issues of the Doctoral School, Faculty of Information Technology and Bionics, Pázmány Péter Catholic University – 2019.* G. Prószéky, P. Szolgay Eds. Budapest: Pázmány University ePress, 2019, pp. 15–15. This research has been partially supported by the European Union, co-financed by the European Social Fund (EFOP-3.6.3-VEKOP-16-2017-00002).

Describing the ion passage through the CFTR ion channel

Bianka Vivien FARKAS
(Supervisor:Tamás HEGEDŰS, Zoltán GÁSPÁRI)
Pázmány Péter Catholic University, Faculty of Information Technology and Bionics
50/a Práter street, 1083 Budapest, Hungary
farkas.bianka.vivien@itk.ppke.hu

The CFTR/ABCC7 chloride channel is a member of the ATP-Binding Cassette (ABC) protein superfamily. Mutations affecting the coding gene of this protein could lead to reduced expression or impaired function of the protein in the epithelial cells causing cystic fibrosis (CF), a lethal disease. In the interest of understanding protein function and developing more efficient drug molecules, a high-resolution protein structure is required. Even though the recently published zebrafish and human CFTR cryo-EM structures (PDBID:5W81 [1] and 6MSM [2]) are solved in the active (ATP-bound, phosphorylated) conformation, both lack an open channel for chloride passage. Our goal is to characterize the CFTR structure and dynamics based on both experimental and homology models, using *in silico* methods. Therefore, in our study we performed molecular dynamics (MD) simulations to generate a conformational ensemble of the CFTR protein. We applied pore detecting algorithms on the resulting ensemble to discover conformations with open channel and we analyzed the possible pathways in detail. Considering that chloride ions penetrated the identified pore in our equilibrium simulations without passing through a bottleneck region, we carried out metadynamics simulations to characterize the energetics of this crossing event. Our study and methodology can help to understand the transport mechanism of the wild type and mutant CFTR proteins.

References

[1] Z. Zhang, F. Liu, and J. Chen, "Conformational Changes of CFTR upon Phosphorylation and ATP Binding," *Cell*, vol. 170, pp. 483–491.e8, July 2017.

[2] Z. Zhang, F. Liu, and J. Chen, "Molecular structure of the ATP-bound, phosphorylated human CFTR," *Proceedings of the National Academy of Sciences of the United States of America*, vol. 115, no. 50, pp. 12757–12762, 2018.

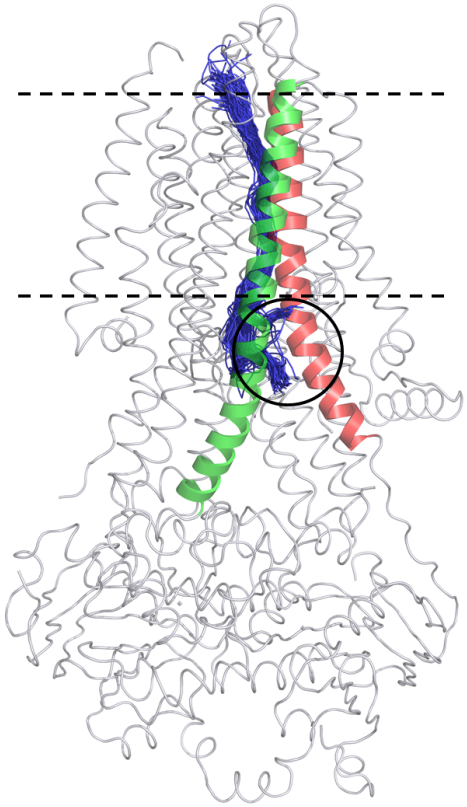

Fig. 1. The tunnels (blue lines) identified in the frames from the simulations are shown in the context of he initial structure of the zebrafish CFTR protein (PDBID:5W81). The intracellular entry between the transmembrane helix 4 (green) and 6 (red) is marked by the black circle. The dashed lines indicate the membrane boundaries.

B. FARKAS, "Describing the ion passage through the CFTR ion channel" in *PhD Proceedings – Annual Issues of the Doctoral School, Faculty of Information Technology and Bionics, Pázmány Péter Catholic University – 2019.* G. Prószéky, P. Szolgay Eds. Budapest: Pázmány University ePress, 2019, pp. 16–16.
This research has been partially supported by the European Union, co-financed by the European Social Fund (EFOP-3.6.3-VEKOP-16-2017-00002).

Quantifying growth of *S. cerevisiae* strains in co-cultures

Tünde GAIZER
(Supervisor: Attila CSIKÁSZ-NAGY)
Pázmány Péter Catholic University, Faculty of Information Technology and Bionics
50/a Práter street, 1083 Budapest, Hungary
3in Research Group, Faculty of Information Technology and Bionics, Pázmány Péter Catholic University, Esztergom, Hungary
gaizer.tunde.eva@itk.ppke.hu

***Abstract*—Natural microbial communities consist of multiple strains that live and grow together and directly or indirectly affect each other. Interactions that arise between these co-existing species shape the future of the whole community. Despite of their importance, traditional microbial growth kinetics experiments have been focusing on single strain growth only and our understanding of intra-strain interactions are limited. Our goal is to gain a better understanding of the interactions that arise between natural *S. cerevisiae* strains to be able to explain the variety of strains that coexist i.e. in the same vineyard. To achieve this, a high-throughput methodology is being developed that can be used to screen pairs of interacting strains.**

***Keywords*-high-throughput screening; yeast growth; fluorescence; systems biology**

Introduction

Microbial communities can be found around us in nature nearly everywhere, playing a crucial role in health, biotechnology or global climate regulation [1]. Controlling these communities could give rise to many useful applications, from decreasing environmental pollution to improving human health however our understanding and ability to predict the behavior of these communities in various environment or composition is still insufficient [1]. The integration of mathematical modeling and directed experiments are proposed and applied by many to improve understanding and predictability of microbial communities [1], [2].

S. cerevisiae is an important research and industrial microorganism. It has proven many times besides wine and beer industry, in fundamental research and biotechnological applications as well [3]. Lab optimized strains of budding yeast has been a model for many discoveries regarding eukaryotic cellular processes, but recently the great diversity of natural strains moved into focus too and sequencing data of more than 1000 strains are available now [4]. Interactions between natural strains have been shown previously [5]. We would like to extend this knowledge with an approach of combining modeling and high-throughput experiments. We started developing our experimental methods to support parametrization of purposefully developed agent-based models. One of our challenges is to quantitatively measure growth of individual strains in co-culture with another. We have implemented a fluorescence based approach to simultaneously measure pairwise co-cultures in microtiter plates.

Discussion

High-throughput methodology based on 96-well plates have been well established, however most cases OD (optical density at 600 nm) was measured that determines total population size only. However this is not enough to differentiate between species or strains in co-cultures [2]. To make this possible, green and red fluorescence labels have been added. This way, growth curves for the total population as well as for the 2 subpopulations can be generated real time. Other possible methods include rt-PCR, cell counting or cell plating, these however are not providing 24 hour growth curve and difficult to manage in large scale. Both liquid and solid phase experiments are included in our studies to enable characterization of the potential local and global interactions, as demonstrated in [6]. Fluorescent intensity was found to correlate with OD during exponential phase but not later. Preliminary results are shown on figure 1.

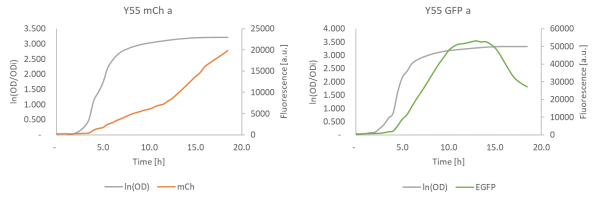

Fig. 1. Growth curve of fluorescently labeled Y55 strains obtained by measuring OD and fluorescence simultaneously (plotted on two separate ordinates).

Acknowledgements

Experimental work described were carried out together with Bíborka Pillér, Emese Nagy, Nóra Molnár. Model was developed by János Juhász, Bence Makove and Donát Pesti. The research has been supported by the European Union, co-financed by the European Social Fund (EFOP-3.6.2-16-2017-00013, Thematic Fundamental Research Collaborations Grounding Innovation in Informatics and Infocommunications).

References

[1] S. Widder and et. al, "Challenges in microbial ecology: building predictive understanding of community function and dynamics," *The ISME Journal*, vol. 10, no. 11, pp. 2557–2568, 2016.
[2] J. Friedman, L. M. Higgins, and J. Gore, "Community structure follows simple assembly rules in microbial microcosms," *Nature Ecology & Evolution*, vol. 1, p. 0109, may 2017.
[3] M. Cavaliere, S. Feng, O. S. Soyer, and J. I. Jiménez, "Cooperation in microbial communities and their biotechnological applications," *Environmental Microbiology*, vol. 19, pp. 2949–2963, aug 2017.
[4] J. Peter and et. al, "Genome evolution across 1,011 Saccharomyces cerevisiae isolates," *Nature*, vol. 556, pp. 339–344, apr 2018.
[5] D. Rivero, L. Berná, I. Stefanini, E. Baruffini, A. Bergerat, A. Csikász-Nagy, C. De Filippo, and D. Cavalieri, "Hsp12p and PAU genes are involved in ecological interactions between natural yeast strains," *Environmental Microbiology*, vol. 17, no. 8, pp. 3069–3081, 2015.
[6] B. Kerr, M. A. Riley, M. W. Feldman, and B. J. M. Bohannan, "Local dispersal promotes biodiversity in a real-life game of rock-paper-scissors.," *Nature*, vol. 418, no. 6894, pp. 171–174, 2002.

T. GAIZER, "Quantifying growth of S. cerevisiae strains in co-cultures" in *PhD Proceedings – Annual Issues of the Doctoral School, Faculty of Information Technology and Bionics, Pázmány Péter Catholic University – 2019.* G. Prószéky, P. Szolgay Eds. Budapest: Pázmány University ePress, 2019, pp. 17–17.
This research has been partially supported by the European Union, co-financed by the European Social Fund (EFOP-3.6.3-VEKOP-16-2017-00002).

Tyramide signal amplification technique in dermal fibroblasts

Anna HAJDARA
((Supervisors: Balázs MAYER, Miklós GYÖNGY)
Pázmány Péter Catholic University, Faculty of Information Technology and Bionics
50/a Práter street, 1083 Budapest, Hungary
hajdara.anna@itk.ppke.hu

***Abstract*—Immunhistochemistry (IHC) has been a standout method for nearly 40 years to localize cell surface proteins within tissues or proteins in cells or in cellular compartments. For protein detection various antibodies are used routinely from different species. However detecting more, than one protein requires more, than one primary antibodies, which are produced in two or more different species. Tyramid signal amplification (TSA) increases the sensitivity of IHC and also makes it possible to use the two antibodies from the same species [1]. TSA was developed in the early 1990s and uses horseradish peroxidase (HRP) to catalyze the deposition of labeled tyramide molecules at the site of probe or epitope detection [2]. In TSA technology, with the assistance of H2O2, HRP catalyzes the transformation of the reporter-labeled tyramide into a short-lived reactive intermediate [3]. These reactive intermediates can conjugate and deposit on the surrounding protein residues (including tryptophan, histidine and tyrosine residues), resulting the accumulation of large numbers of reporter molecules and thus an enhanced detection signal [1]. TSA relies on the rapid deposition of a reporter molecule-tyramide, at the site of the antigen and adjacent proteins to achieve amplification of signal [1]. In this manuscript I present the optimization of CD90 signal amplification in dermal fibroblasts.**

I. RESULTS

The highest concentration of Alexa Fluor 488 tyramide (1:5000) appeared to overamplify our CD90 signal. In the negative control plasmamembranes of the cells were visible. Lower concentration of Alexa Fluor 488 tyramide (1:10000) with 1:100 primary antibody dilution and 1:2 dilution of secondary anti-mouse polymer-HRP (ready to use solution) showed the most specific staining compared to negative control. Our lowest concentrated tyramide solutions (1:50000) dilution and (1:25000) dilution could not demonstrate specific staining, the amplified signal was not visible.

II. CONCLUSION

The optimal TSA conditions described above will be used for future immunohistochemical experiments on dermal tissue sections using TSA amplification in cases of cell markers with low expression or of high level tissue autofluorescence.

III. MATERIALS AND METHODS

Cell isolation

Dermal fibroblasts were isolated from surgical samples of naevus excison from healthy individuals according to an inhouse protocol.

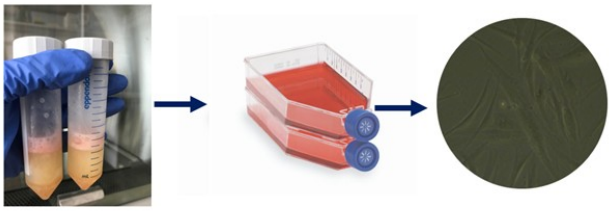

Fig. 1. *Dermal fibroblast isolation workflow*

Cell immunostaining and Tyramide signal amplification

Dermal fibroblast cells were placed in chamber slides in 5000 cell number. Cells were fixed with 2% formaldehyde, blocked with 1% bovine serum albumin or with Bloxall blocking reagent. Primary CD90 antibody was applied followed by polymer-HRP conjugated anti-mouse secondary antibody, then tyramide AlexaFluor 488 conjugate. Nuclei were stained with with 4′,6-diamidino-2-phenylindole (DAPI) for 10 minutes.

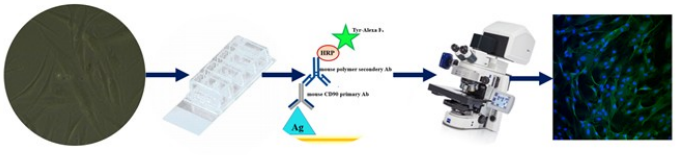

Fig. 2. *Immunostaining and tyramide signal amplification workflow*

REFERENCES

[1] B. Hunyady, K. Krempels, G. Harta, and É. Mezey, "Immunohistochemical signal amplification by catalyzed reporter deposition and its application in double immunostaining," J. Histochem. Cytochem., vol. 44, no. 12, pp. 1353–1362, 1996.
[2] A. Korosec et al., "Lineage Identity and Location within the Dermis Determine the Function of Papillary and Reticular Fibroblasts in Human Skin," J. Invest. Dermatol., vol. 139, no. 2, pp. 1–10, 2019.
[3] A. Stunova and L. Vistejnova, "Cytokine and Growth Factor Reviews Dermal fi broblasts — A heterogeneous population with regulatory function in wound healing," Cytokine Growth Factor Rev., no. January, pp. 0–1, 2018.

A. HAJDARA, "Tyramide signal amplification technique in dermal fibroblasts" in *PhD Proceedings – Annual Issues of the Doctoral School, Faculty of Information Technology and Bionics, Pázmány Péter Catholic University – 2019.* G. Prószéky, P. Szolgay Eds. Budapest: Pázmány University ePress, 2019, pp. 18–18. This research has been partially supported by the European Union, co-financed by the European Social Fund (EFOP-3.6.3-VEKOP-16-2017-00002).

Building the three-dimensional structural model of the postsynaptic protein GKAP

Zita HARMAT
(Supervisor: Zoltán GÁSPÁRI)
Pázmány Péter Catholic University, Faculty of Information Technology and Bionics
50/a Práter street, 1083 Budapest, Hungary
3in Research Group, Faculty of Information Technology and Bionics, Pázmány Péter Catholic University, Esztergom, Hungary
harmat.zita@itk.ppke.hu

In order to understand the molecular level processes of learning and memory it is crucial to unfold the structure-function relationship of the proteins taking part in these processes.

There are many neurons in the brain, making many connections, which are called synapses. From the point of view of the travelling of the stimulus, there is a presynaptic and a postsynaptic region. This work is concerned with the chemical synapses, where neurotransmitters transmit the stimulus via membrane-enclosed vesicles. These vesicles are emitted from the presynaptic region by exocitosis and taken up in the postsynaptic region by endocytosis. In the excitatory glutaminerg synapses there is a dense part made of visecles in the postsynaptic site on the axon terminal. On the other side, in the postsynaptic part, there is a thickening of the membrane in the dendritic spikes. This latter structure is called postsynaptic density (PSD). If the axon gets a stimulus it emits glutamate on the presynaptic site, and on the postsynaptic site, the glutamate binds to glutamate receptors, which in turn let ions inside the posysynaptic cell, depolarising it. This depolarisation signal is transmitted further by the postsynaptic density, which can be considered as a membrane-nested ”organelle” consisting of many proteins. Among the many proteins forming the postsynaptic density there are many scaffold and adaptor proteins. The scaffold proteins have many domains and they can bind to different proteins with their different domains forming quite huge complexes at times. This phenomenon regulates many cellular processes. The adaptor proteins bind cellular pathways together, aiding the molecular communication inside the cell. Apart from these proteins, there are many motor proteins, enzimes, cytoskeletal proteins, and protiens involved in translation are also part of the postsynaptic density. All these macromolecules form a network by interacting with each other. The changes in this network can lead to a change in the synapse.

The Guanilate KinaseAssociated Protein (GKAP, also known as DLGAP1) is found in the brain, mainly in the dendrites and in the postsynaptic parts of excitatory synapses: in the cortex, the hippocampus, the olfactury bulb, the striatum, the thalamus and the glanular and Purkinje cells of the cerebellum. It interacts with several proteins.

The GKAP has been reported to influence the signal transcription of the glutamate receptors. The protein has a role in the organisation and activity-dependent changes of the postsynaptic density, and hence in the synaptic scaling. The regulation of the functioning of the GKAP is achieved by phosphorilation.

The protein has three domains: a 14 amino acid repeat domain, (with a length varying from isoform to isoform). This domain lets GKAP bind to the DLG protein. Also it has a dinein light chain (DLC) domain, with which it binds to a motor protein called DLC, and it also has a GKAP homology domain (GH1) with yet unknown function. Only the GH1 domain has an experimentally determined structure obtained with x-ray crystallography. The malfunctioning of GKAP is plying a role in various central nervous system diseases, such as scisophrenia, fragile X chromosome mental retardation syndrome and major depression.

The phenomenon, that some proteins do not have a well defined three dimendional structure has been first described around the year 2000. Several studies have shown, that these proteins are also disordered *in vivo*. When binding to their partners, some of these disordered proteins acquire an ordered structure. The lack of a well-defined three-dimensional structure can be a great advantage in the forming of protein complexes. The malfunctioning of the intrinsically disordered proteins can cause many types of diseases, such as cancer, neurodegenerative diseases, heart diseases and diabetes and besides, they can aggregate, forming so called amyloids, which can lead to serious diseases, and they are also involved in virus infections. In drug discovery, the goal is to inhibit interaction of intrinsically disordered proteins with their partners through small molecules.

NMR measurements are a great way to characterise the three-dimensional structure and the dynamics of proteins. In these experiments, there are many conformations of the same protein in the test tube at the same time. This means, that the measured parameters are reflecting the mean of these conformations, and one given conformation cannot satisfy all the parameters, only an ensemble of structures can correspond to them. This leads to the conclusion, that if we would like to describe the three-dimensional structure of intrinsically disordered proteins, we have to work with structural ensembles.

We are exploring the possibility of building the sructure of the GKAP protein with fragment-based methods.

Acknowledgement

The research has been supported by the European Union, co-financed by the European Social Fund (EFOP-3.6.2-16-2017-00013, Thematic Fundamental Research Collaborations Grounding Innovation in Informatics and Infocommunications)

Z. HARMAT, “Building the three-dimensional structural model of the postsynaptic protein GKAP” in *PhD Proceedings – Annual Issues of the Doctoral School, Faculty of Information Technology and Bionics, Pázmány Péter Catholic University – 2019.* G. Prószéky, P. Szolgay Eds. Budapest: Pázmány University ePress, 2019, pp. 19–19. This research has been partially supported by the European Union, co-financed by the European Social Fund (EFOP-3.6.3-VEKOP-16-2017-00002).

How disease causing mutations perturb the structure of PSD proteins

Zsófia KÁLMÁN

(Supervisor: Zoltán GÁSPÁRI)
Pázmány Péter Catholic University, Faculty of Information Technology and Bionics
50/a Práter street, 1083 Budapest, Hungary
kalman.zsofia.etalka@itk.ppke.hu

I. Introduction

The postsynaptic density (PSD) is a specialized part of the postsynaptic neuron, and its primary function is to transduce the information between pre - and postsynaptic cells in the central nervous system. PSD is a complex, continuously and dynamically changing network of more than a thousand proteins with different functions [1]. The delicate balance of structured and disordered protein segments contribute to the maintenance of protein-protein interactions. The binding of different partners are also highly depending on the spatiotemporal control of the cell, often regulated through different post-translational modifications (PTMs), such as ubiquitination and phosphorylation [2].

Advancements in sequencing technologies resulted in not only the determination of the human genome but also the observation of naturally occurring variations. The phenotypic effect of mutations is on a wide-range spectrum from neutral polymorphisms through disease-causing germline mutations (DM) with serious consequences to the quality of life to often lethal somatic mutations. Most mutations are non-synonym single nucleotide variations (SNVs), resulting in an amino acid change on the protein level. Such changes can affect important functional and structural segments of the proteins, perturb their structure and the dynamics, and their outcome often alters different biological pathways required to maintain the synaptic plasticity [3].

Despite our increasingly growing knowledge about inherited SNVs and their outcome, molecular level understanding how these changes impair protein function greatly lacks behind, especially in the case of PSD proteins giving place to an extremely high amount of PPIs. By investigating those missense mutations that result in the loss of function structurally essential elements can be recognized, giving hints on how diseases emerge (Figure 1). Although analyzing cancer became one of the most popular topics in molecular biology and medicine, there are several benefits to exclude it from large scale analysis. The available rather noisy data makes it difficult to evaluate results properly, moreover, several medical branches greatly rely on data from Mendelian inherited mutations, such as prenatal diagnostics.

II. Materials and methods

We used Uniprot [4] as the primary database for both the mutations and the protein sequences. The list of proteins harboring the PSD was obtained from SynaptomeDB [5] and Genes2Cogniton [6]. Structural segments of proteins were determined using webservers, publicly available databases, and a pipeline developed in our research group.

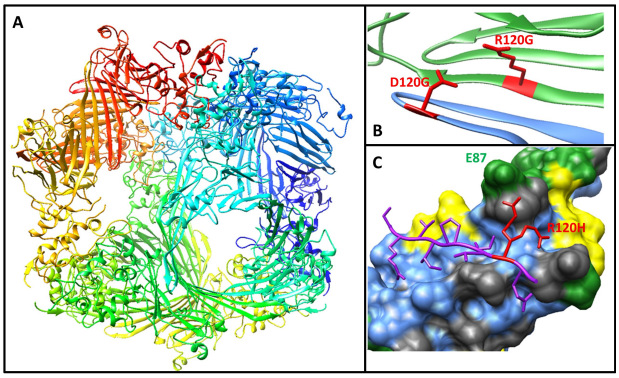

Fig. 1. A representative example of disease development caused by SNVs: -crystallin act as a molecular chaperone, although instead of renaturing proteins and release them they bind mature amyloid fibrils and prevent their elongation. Mutations affect self-assembly and lead to various diseases linked to forming of protein aggregates (e.g., Alzheimer disease). A: The protein assembles into homooligomers using a variable number of subunits. B: Perturbing the electrostatic interaction between Arg120 and Asp109 in the crystallin domain of two monomers result in toxic conformation. C: Similarly, electrostatic interaction aiding coupled binding and folding between the crystallin domain and the disordered C-terminal (Glu87 and Arg157, respectively) of two monomers may be impaired through DMs.

III. Results

Altogether we investigated more than 2100 germline DMs and more than 1800 polymorphisms in the proteins of PSD. We found DMs are somewhat more abundant in the PSD compared to the human proteome. We also found that the abundance of DMs in different structural regions differs between PSD and the proteome.

References

[1] M. Sheng and E. Kim, "The postsynaptic organization of synapses," *Cold Spring Harbor perspectives in biology*, vol. 3, no. 12, p. a005678, 2011.
[2] A. Kiss-Toth, L. Dobson, B. Peterfia, A. F. Angyan, B. Ligeti, G. Lukacs, and Z. Gaspari, "Occurrence of ordered and disordered structural elements in postsynaptic proteins supports optimization for interaction diversity," *Entrophy*, 2019.
[3] S. Sunyaev, V. Ramensky, and P. Bork, "Towards a structural basis of human non-synonymous single nucleotide polymorphisms," *Trends in Genetics*, vol. 16, no. 5, pp. 198–200, 2000.
[4] U. Consortium *et al.*, "Uniprot: the universal protein knowledgebase," *Nucleic acids research*, vol. 46, no. 5, p. 2699, 2018.
[5] M. Pirooznia, T. Wang, D. Avramopoulos, D. Valle, G. Thomas, R. L. Huganir, F. S. Goes, J. B. Potash, and P. P. Zandi, "Synaptomedb: an ontology-based knowledgebase for synaptic genes," *Bioinformatics*, vol. 28, no. 6, pp. 897–899, 2012.
[6] À. Bayés, M. O. Collins, C. M. Galtrey, C. Simonnet, M. Roy, M. D. Croning, G. Gou, L. N. van de Lagemaat, D. Milward, I. R. Whittle *et al.*, "Human post-mortem synapse proteome integrity screening for proteomic studies of postsynaptic complexes," *Molecular brain*, vol. 7, no. 1, p. 88, 2014.

Zs. KÁLMÁN, "How disease causing mutations perturb the structure of PSD proteins" in *PhD Proceedings – Annual Issues of the Doctoral School, Faculty of Information Technology and Bionics, Pázmány Péter Catholic University – 2019.* G. Prószéky, P. Szolgay Eds. Budapest: Pázmány University ePress, 2019, pp. 20–20. This research has been partially supported by the European Union, co-financed by the European Social Fund (EFOP-3.6.3-VEKOP-16-2017-00002).

Review of proteomics databases for protein complex simulations

Bence Márk KEÖMLEY-HORVÁTH
(Supervisors: Attila CSIKÁSZ-NAGY, István REGULY)
Pázmány Péter Catholic University, Faculty of Information Technology and Bionics
50/a Práter street, 1083 Budapest, Hungary
keomley-horvath.bence.mark@itk.ppke.hu

***Abstract*—Acquire the necessary data for large scale proteomics simulation is a hard task. Here, I collected bioinformatics databases that directly help protein complex assembly simulations. I have grouped these databases based on their contents into the following categories (i) protein abundance and structure, (ii) protein-protein interaction and (iii) complexome data.**

***Keywords*-Proteomics; Protein-Protein Interactions; Complexome**

I. Introduction

Nowadays several new, large scale, whole-cell level modeling simulation tools are emerging. For these kinds of simulations, we need need to identify the proper data sources. In our research group we are developing a tool, which can predict the protein complex formation on whole-cell level. To run the simulation, we need extensive protein-protein and domain-domain interaction data, furthermore, we need information on protein abundance and localization. Future plans to extend the tool would require deeper protein structure and protein degradation-synthesis data. To gain all of these datasets we need to extract data from multiple databases. To choose appropriate databases, here I collect and briefly describe some of the most relevant ones.

II. Proteins

A. Protein Abundance

There are different approaches to handle protein abundance data. Various number of processing steps have been performed on the raw data. In the PRIDE [1] data repository we can locate tens of thousands of Mass Spectrometry based human proteomics data. The paxDB [2] contains processed abundance data, in ppm (part per million) grouped by species. From this we can get the ratio of different protein abundances. More processed, human protein data can be found in Protein Atlas [3]. The data are grouped into three categories: the tissue specific transciptomics and protein abundance data. In the cell category we can get localization data and in the pathology category we can get information about the connection between the protein and the related diseases. The drawback of this database is that it contains only score-like value about the protein abundances.

B. Protein structure

The domain and binding site level structure of the proteins is also an important input data to the simulation. A general 3D protein structure database is the PDB (Protein Data Bank) [4], from which next to the structure we can also gain extensive annotation about its sequence and ligands. A more extensive annotation database is the Uniprot [5], which is often linked to other databases mentioned in this review.

III. Interactions

There are multiple different protein-protein interaction (PPI) databases. They are different in the data collection method and data extensiveness point of view. One of the broadest PPI database is the STRING [8], which contains more than 20 million proteins from around 5000 species. This amount of direct experimental data do not exists, but STRING also collects data by automatized literature research in scientific articles. The drawback of this is, that it contains lots of false positive interactions too. Another database is the BioGRID [9], which contains fewer proteins (still more than 1.5 million), but it describes the exact experimental method, that was used to get the data and it also manually curated.

IV. Complexome

To validate the predicted complexes we need a reference dataset about the complexes. The CORUM database [6] contains more than 4000 manually annotated protein complexes from mammalian organisms. Out of some functional annotations it lists the proteins in the complex and the interactions between them. Another database for similar purpose is the Complex Portal [7], which contains more extensive annotation data, than the CORUM - like 3D structure if available - but it is composed of fewer complexes.

References

[1] J. A. Vizcaíno et al., "2016 update of the PRIDE database and its related tools," Nucleic Acids Research, vol. 44, no. D1, pp. D447–D456, Nov. 2015.
[2] M. Wang, C. J. Herrmann, M. Simonovic, D. Szklarczyk, and C. von Mering, "Version 4.0 of PaxDb: Protein abundance data, integrated across model organisms, tissues, and cell-lines," PROTEOMICS, vol. 15, no. 18, pp. 3163–3168, Mar. 2015.
[3] M. Uhlen et al., "Tissue-based map of the human proteome," Science, vol. 347, no. 6220, pp. 1260419–1260419, Jan. 2015.
[4] Rose PW, Prlić A, Altunkaya A, Bi C, Bradley AR, Christie CH, et al. "The RCSB protein data bank: Integrative view of protein, gene and 3D structural information." Nucleic Acids Res. 2017;45: D271–D281. 10.1093/nar/gkw1000
[5] "UniProt: the universal protein knowledgebase," Nucleic Acids Research, vol. 45, no. D1, pp. D158–D169, Nov. 2016.
[6] M. Giurgiu et al., "CORUM: the comprehensive resource of mammalian protein complexes—2019," Nucleic Acids Research, vol. 47, no. D1, pp. D559–D563, Oct. 2018.
[7] B. H. M. Meldal et al., "The complex portal - an encyclopaedia of macromolecular complexes," Nucleic Acids Research, vol. 43, no. D1, pp. D479–D484, Oct. 2014.
[8] D. Szklarczyk et al., "STRING v10: protein–protein interaction networks, integrated over the tree of life," Nucleic Acids Research, vol. 43, no. D1, pp. D447–D452, Oct. 2014.
[9] A. Chatr-aryamontri et al., "The BioGRID interaction database: 2015 update," Nucleic Acids Research, vol. 43, no. D1, pp. D470–D478, Nov. 2014.

B. KEÖMLEY-HORVÁTH, "Review of proteomics databases for protein complex simulations" in *PhD Proceedings – Annual Issues of the Doctoral School, Faculty of Information Technology and Bionics, Pázmány Péter Catholic University – 2019.* G. Prószéky, P. Szolgay Eds. Budapest: Pázmány University ePress, 2019, pp. 21–21. This research has been partially supported by the European Union, co-financed by the European Social Fund (EFOP-3.6.3-VEKOP-16-2017-00002).

Developing of Brain-Computer Interfaces by using Deep Learning technologies

Csaba Márton KÖLLŐD
(Supervisor: István ULBERT)
Pázmány Péter Catholic University, Faculty of Information Technology and Bionics
50/a Práter street, 1083 Budapest, Hungary
kollod.csaba@itk.ppke.hu

***Abstract*—This report describes the start of the HUN BCI project. The aim of the project is to develop a Brain-Computer Interface System, which can classify the brain signals into 4 classes and with the classes control a computer game.**

I. Introduction

Brain-Computer Interfaces (BCI) are integrated software and hardware systems which record the bio-electrical signals of the brain. And by classifying the signals it controls an external device. (Fig. 1.)

Our research team, lead by István ULBERT, aims to create a BCI system, which will be challenged by other BCI devices of other research groups, in 2020 at the international Cybathlon competition.

II. Neural networks

For the translating algorithm (see on Fig. 1.) it is planned to test and use several, different type of neural networks. One of them is the DenseNet, developed by G. Huang et al. [1], which aims to further improve the efficiency of residual neural networks, by increasing the gradient-flow with additional connections between layers.

The other network is the Cascade convolutional recurrent neural network architecture, introduced by D. Zhang et al. [2]. This architecture combines the benefits of convolutioinal and LSTM networks on Electroencephalograph (EEG) signals.

III. Databases

In purpose to train deep neural networks, huge amount of data is required. On PhysioNet [3] I found an open access dataset. This dataset was created with the BCI2000 tool by G. Schalk et al. [4] and contains imagery motor movements of 109 subject.

According to further improve the database and the BCI system, we decided to create a similar dataset.

IV. Results

I planned a new paradigm with was reqiured for the new data recordings. I further developed a MATLAB code, which base on one of our lab member's, András BOHN's code, which leads the paradigm for the EEG subjects and registers the exact time of a given instruction. I also organised the experiments, which are required to create the new database. So far we made 23 EEG recordings with 7 subjects. Moreover I achieved to compensate them with credit points for their time and participation in the experiments. I also applied the team to the Cybathlon 2020 competition and we received a starting slot.

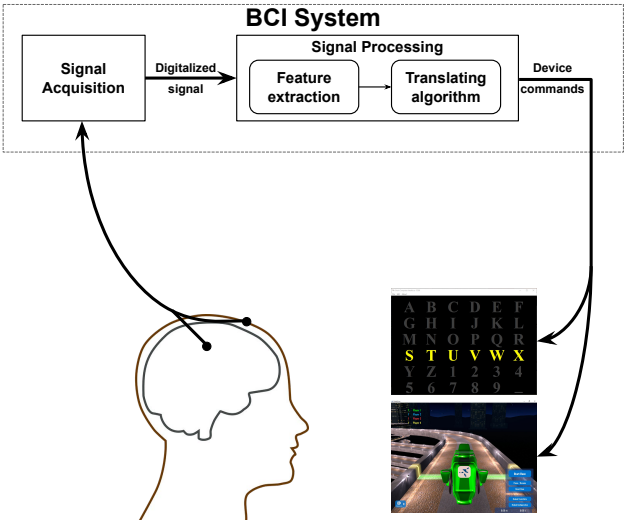

Fig. 1. BCI System workflow, based on J. R. Wolpaw et al. [5]

V. Conclusions

I have created the base to make high quality research by creating a paradigm and starting a new experiment process, to record sufficient number of EEG data. It is also decided, what kind of tools and neural network architectures will be used to create our BCI system. I continue the work in purpose to reach a good place in the Cybathlon 2020 competition.

References

[1] G. Huang, Z. Liu, L. Van Der Maaten, and K. Q. Weinberger, "Densely connected convolutional networks," in *Proceedings of the IEEE conference on computer vision and pattern recognition*, 2017, pp. 4700–4708.

[2] D. Zhang, L. Yao, X. Zhang, S. Wang, W. Chen, and R. Boots, "Eeg-based intention recognition from spatio-temporal representations via cascade and parallel convolutional recurrent neural networks," *arXiv preprint arXiv:1708.06578*, 2017.

[3] A. L. Goldberger, L. A. Amaral, L. Glass, J. M. Hausdorff, P. C. Ivanov, R. G. Mark, J. E. Mietus, G. B. Moody, C.-K. Peng, and H. E. Stanley, "Physiobank, physiotoolkit, and physionet: components of a new research resource for complex physiologic signals," *Circulation*, vol. 101, no. 23, pp. e215–e220, 2000.

[4] G. Schalk, D. J. McFarland, T. Hinterberger, N. Birbaumer, and J. R. Wolpaw, "Bci2000: a general-purpose brain-computer interface (bci) system," *IEEE Transactions on biomedical engineering*, vol. 51, no. 6, pp. 1034–1043, 2004.

[5] J. R. Wolpaw, N. Birbaumer, D. J. McFarland, G. Pfurtscheller, and T. M. Vaughan, "Brain–computer interfaces for communication and control," *Clinical neurophysiology*, vol. 113, no. 6, pp. 767–791, 2002.

Cs. KÖLLŐD, "Developing of Brain-Computer Interfaces by using Deep Learningtechnologies " in *PhD Proceedings – Annual Issues of the Doctoral School, Faculty of Information Technology and Bionics, Pázmány Péter Catholic University – 2019.* G. Prószéky, P. Szolgay Eds. Budapest: Pázmány University ePress, 2019, pp. 22–22. This research has been partially supported by the European Union, co-financed by the European Social Fund (EFOP-3.6.3-VEKOP-16-2017-00002).

Analyses of protein-protein interactions related to nNOS by stochastic simulations.

Marcell MISKI
(Supervisor: Attila CSIKÁSZ-NAGY)
Pázmány Péter Catholic University, Faculty of Information Technology and Bionics
50/a Práter street, 1083 Budapest, Hungary
miski.marcell@itk.ppke.hu

***Abstract*—The postsynaptic density has been considered as a key element creating the spectra of autistic behaviour. Not just the amount of the proteins can affect that spectra, but the interactions and binding between the proteins, since in some cases information can go through the connected proteins from the membrane receptor to the inner areas of the neural cell. In this article I will show which two software I will use to simulate those interactions *in-silico* and a possible pipeline between them.**

***Keywords*-keyword; postsynaptic density; SiComPre; Integrative Modeling; database**

I. Introduction

The postsynaptic density got its name from electron microscopy where one can observe a black region near the postsynaptic membrane inside the postsynaptic neuron which is dense in electrons. Those electrons are part of big protein complexes. These proteins are attached to the membrane receptors and transmit signals from the receptors towards the inside of the neuron where the signal is processed. Due to this important function the postsynaptic density has a key role in several neurological diseases.

This research focuses on the modeling of possible structures protein complexes. Inhibiting the NMDA/PSD-95/nNOS complex can restore poststroke damages of motoric functions.

II. The software

SiComPre was designed to give a quantitative prediction of possible protein combinations of complexes using advanced Gillespie algorithm and well defined diffusion in certain compartments. The software is easy to use by its GUI but needs a lot of experimental data to be given.

Unlike the previous program the Integrative Modeling Platform (hereinafter IMP) gives qualitative scored predictions of a certain complex. It models the proteins as bead chains and then makes a stochastic approximation of a desired complex (see figure 1) moving the bead chains closer to each other.

III. PipeLine

From literature there are several experimental data we can use for modeling a complex. Integrative Modeling itself is the method when one takes every available information and models from different sources and keep those which are consistent to each other. The information from experiments can be collected and organized into a releasable database. One of the main purpose of our database would be that it will generate the input files of all the used softwares automatically. Then quantitative simulations can be run by SiComPre which output gives a probability of every different complexes. The three dimensional structure of the complexes with high probability can be modeled by IMP to get qualitative information.

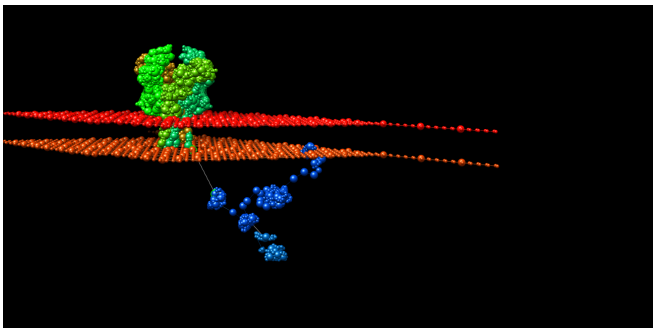

Fig. 1. **The 3D simulation of raw NMDA/PSD-95/nNOS structure.** The missing loops were not filled by refinement so the C-termini of the GluN2 is missing, there is no cytosolic part of the NMDA receptor. The dark blue is the PSD-95 which first PDZ domain is connected by the last available amino acid of the GluN2 just for illustration. The azure is the PDZ domain of nNOS trying to dimerize with the second PDZ domain of PSD-95. The most unrealistic part of the shown structure is that the C-termini of PSD-95 is touching the membrane (the membrane bead-chain structure is simulated like a graphene double-layer of alanines) while in reality the N-termini is tethered to the membrane.

Acknowledgements

I would like to express my special thanks of gratitude to supervisor Attila Csikász-Nagy for his patient guidance, enthusiastic encouragement and useful critiques of this research work. I would like to express my very great appreciation to Zoltán Gáspári for raising the questions and giving this wonderful topic to me. Assistance during IMP simulations provided by Kornél Komjáti was greatly appreciated. I am particularly grateful for the assistance given by Bence Márk Keömley-Horváth since he helped a lot learning SiComPre. I also wish to acknowledge the help provided by Simone Rizetto the developer of SiComPre.

Molecular graphics and analyses performed with UCSF Chimera, developed by the Resource for Biocomputing, Visualization, and Informatics at the University of California, San Francisco, with support from NIH P41-GM103311.

References

[1] Bach et al, *A high-affinity, dimeric inhibitor of PSD-95 bivalently interacts with PDZ1-2 and protects against ischemic brain damage* (2012) Proceedings of the National Academy of Sciences of the United States of America, 2nd edition, DOI: 10.1073/pnas.1113761109

[2] Rizzetto, S., Priami, C., Csikász-Nagy, A. (2015). *Qualitative and Quantitative Protein Complex Prediction Through Proteome-Wide Simulations.* PLOS Computational Biology, 11(10), e1004424. DOI:10.1371/journal.pcbi.1004424

[3] Russel D, Lasker K, Webb B, Velázquez-Muriel J, Tjioe E, Schneidman-Duhovny D, Peterson B, Sali A. *Putting the pieces together: integrative modeling platform software for structure determination of macromolecular assemblies.* PLoS Biol. 2012 Jan;10(1):e1001244. Epub 2012 Jan 17. DOI: 10.1371/journal.pbio.1001244.

M. MISKI, "Analyses of protein-protein interactions related to nNOS by stochastic simulations." in *PhD Proceedings – Annual Issues of the Doctoral School, Faculty of Information Technology and Bionics, Pázmány Péter Catholic University – 2019.* G. Prószéky, P. Szolgay Eds. Budapest: Pázmány University ePress, 2019, pp. 23–23. This research has been partially supported by the European Union, co-financed by the European Social Fund (EFOP-3.6.3-VEKOP-16-2017-00002).

Evaluating the performance of different methods for fitting the parameters of neuronal models

Máté MOHÁCSI
(Supervisor: Szabolcs KÁLI, Tamás FREUND)
Pázmány Péter Catholic University, Faculty of Information Technology and Bionics
50/a Práter street, 1083 Budapest, Hungary
mohacsi.mate@itk.ppke.hu

***Keywords*-neuronal modeling; model fitting; parallel optimization; algorithms; algorithm performance, multi-objective**

I. Introduction

Automated parameter fitting is becoming a widely used methodology in neuroscientific research. Several software packages have been successfully used for this purpose, but most of them are relatively difficult to master for non-specialists, and no systematic evaluation of their applicability to neural optimization problems has been performed.

We have created an extended and enhanced version of our previously described neural optimization tool. [1] The new version has an updated graphical user interface, which guides the user through the steps of defining a parameter fitting problem, running the optimization, and evaluating the results. The software provides a unified interface to many different algorithms for parameter optimization (including single- and multi-objective methods), implemented by four external packages. For many algorithms, parallel execution is also supported.

We used our unified framework to perform an extensive comparison of different algorithms and packages on a set of benchmark problems in neural optimization. Certain types of evolutionary and related algorithms provided the most consistently satisfactory results, but the relative performance of the different methods depended significantly on the nature of the problem, and sometimes also on the implementation. Our software tool and benchmarking results should make it easier for neuroscientists to select and use state-of-the-art parameter tuning methods for their research.

Cell populations in experiments contain a specific variability, which makes every individual neuron different. Typical network models contain copies of a single cell model that approximates the behavior of an average experimental neuron. However, it could be more suitable to construct a model population, which represents the distribution of the experimental data. In order to achieve this, we draw the parameters of a collection of virtual cells from a normal distribution, whose mean and covariance are set so that the resulting distribution of physiological features matches the experimentally measured distribution.

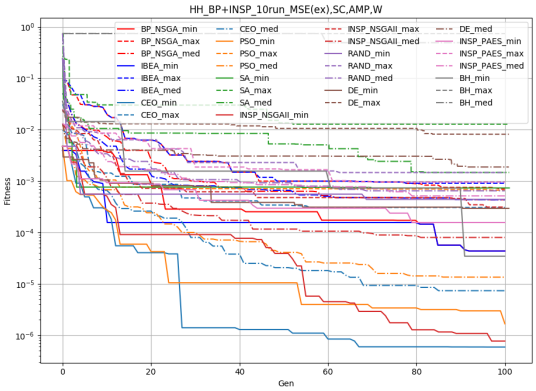

Fig. 1. Generation plot of 10 optimization, with 100 population and 100 generation. Inspyred, Scipy and Bluepyopt algorithms measured on Hodgkin-Huxley model, a less complex problem. Solid line represents the minimum, dashed line is maximum and dash-dot line for median. Fitnesses used for the optimization: Mean Squared Error, Spike Count, AP amplitude and AP width.

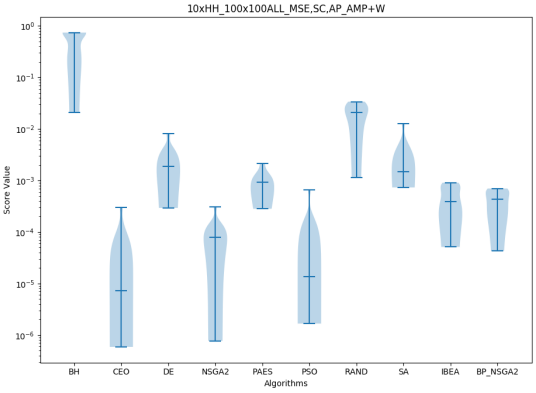

Fig. 2. 10 best evaluation of the algorithms represented on a violinplot. Algorithm names shown on the x-axis (Basinhopin, Evolutionary Algorithm, Differential Evolution,NSGA2, Pareto Archive Evolutional Strategy, Particle Swarm, Random Search, Simmulated Annealing, IBEA). The plot visualize the distribution of the fitness scores achieved by the algorithms.

Acknowledgements

I would like to thank to my supervisor Szabolcs Káli, Sára Sáray, Márk Patrik Török and Luca Tar for their help and support. Funding from the European Union's Horizon 2020 Framework Programme for Research and Innovation under the Specific Grant Agreements No. 720270 and No. 785907 (Human Brain Project SGA1 and SGA2), and from Széchenyi 2020 Program of the Human Resource Development Operational Program, and of the Program of Integrated Territorial Investments in Central-Hungary (EFOP-3.6.2-16-2017-00013 and 3.6.3-VEKOP- 16-2017-00002).

References

[1] P. Friedrich, M. Vella, A. I. Gulyás, T. F. Freund, and S. Káli, "A flexible, interactive software tool for fitting the parameters of neuronal models," *Frontiers in Neuroinformatics*, vol. 8, p. 63, 2014.

M. MOHÁCSI, "Evaluating the performance of different methods for fitting the parameters of neuronal models" in *PhD Proceedings – Annual Issues of the Doctoral School, Faculty of Information Technology and Bionics, Pázmány Péter Catholic University – 2019.* G. Prószéky, P. Szolgay Eds. Budapest: Pázmány University ePress, 2019, pp. 24–24. This research has been partially supported by the European Union, co-financed by the European Social Fund (EFOP-3.6.3-VEKOP-16-2017-00002).

Functional and structural investigation of the post-synaptic scaffold protein GKAP

Eszter NAGY-KANTA
(Supervisor: Zoltán GÁSPÁRI)
Pázmány Péter Catholic University, Faculty of Information Technology and Bionics
50/a Práter street, 1083 Budapest, Hungary
nagy-kanta.eszter@itk.ppke.hu

***Abstract*—GKAP, an essential member of the post-synaptic density (PSD), dynamically connects several proteins through its flexible disordered regions, which are not yet fully characterized. Production of isotope-labeled form of the disordered segments of GKAP enables detailed NMR (nuclear magnetic resonance spectroscopy) characterization of these regions and their interactions.**

***Keywords*-PSD; disordered protein structure; NMR**

I. Introduction

Even though the investigation of molecular mechanisms underlying memory and learning is accelerated, still many questions are to be answered regarding the details of synaptic transmission and neuronal signaling. PSD is a complex and dynamic network of many interacting proteins located in the dendritic spike of post-synaptic neurons. Scaffold proteins do not only maintain the spatial organization of this dynamic web but actively take part in the regulation and modulation of signaling through glutamate receptors. Guanylate kinase associated protein (GKAP, or DLGAP1 for discs large-associated protein 1) is an essential component of the PSD. It has an essential role in synaptic scaling by regulating the turnover of glutamate receptors in response to synaptic activity. It is linked to several psychological and neurological disorders [1].

Through its highly flexible disordered regions GKAP may link important interaction partners. On the N terminal, the GK-binding region (GKAP-GBR) associates with the GK region of the highly enriched PSD protein, the PSD-95 [2], while the dynein binding region (GKAP-DLC) binds the light chain of the dynein motor protein [3]. A globular, helical region called GH1 domain is located on the C terminal [4]. Besides the GH1 domain, the secondary-tertiary structure and the dynamics of the GKAP protein is yet to be characterized.

Intrinsically disordered proteins or regions do not adopt a single well-defined structure, rather exhibit large conformational variability and can only be represented by a conformational ensemble. The most suitable tool to characterize the structure and dynamics of disordered proteins is NMR spectroscopy [5]. For multidimensional NMR measurements non-radiant isotope-labeled (^{15}N and ^{13}C), high purity and concentrated protein samples are necessary.

II. Methods

Using *E. coli* bacteria, recombinant proteins corresponding to rat GKAP-GBR and GKAP-DLC were produced. After cell exploration, immobilized metal ion affinity chromatography and size-exclusion chromatography was performed. Control measurements include electronic circular dichroism spectroscopy and mass spectrometry. The functionality of the proteins are to be shown with their interaction partners with gel filtration, pull-down assay and isothermal titration calorimetry.

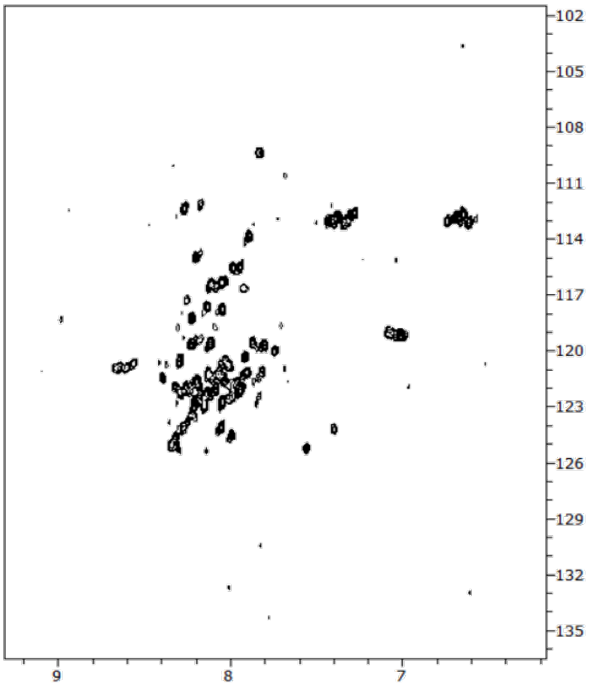

Fig. 1. HSQC NMR spectrum of the ^{15}N-labeled GKAP-DLC construct

III. Results

^{15}N single, and ^{15}N-^{13}C double-labeled production and preliminary NMR measurements of the constructs are on the way. We plan to focus on the detailed structural and functional characterization of the disordered regions of GKAP.

References

[1] A. H. Rasmussen, H. B. Rasmussen, and A. Silahtaroglu, "The dlgap family: neuronal expression, function and role in brain disorders," *Molecular brain*, vol. 10, no. 1, p. 43, 2017.

[2] J. Zhu, Q. Zhou, Y. Shang, H. Li, M. Peng, X. Ke, Z. Weng, R. Zhang, X. Huang, S. S. Li, *et al.*, "Synaptic targeting and function of sapaps mediated by phosphorylation-dependent binding to psd-95 maguks," *Cell reports*, vol. 21, no. 13, pp. 3781–3793, 2017.

[3] J.-B. Manneville, M. Jehanno, and S. Etienne-Manneville, "Dlg1 binds gkap to control dynein association with microtubules, centrosome positioning, and cell polarity," *The Journal of cell biology*, vol. 191, no. 3, pp. 585–598, 2010.

[4] J. Tong, H. Yang, S. H. Eom, C. Chun, and Y. J. Im, "Structure of the gh1 domain of guanylate kinase-associated protein from rattus norvegicus," *Biochemical and biophysical research communications*, vol. 452, no. 1, pp. 130–135, 2014.

[5] P. Tompa, "Intrinsically disordered proteins: a 10-year recap," *Trends in biochemical sciences*, vol. 37, no. 12, pp. 509–516, 2012.

E. NAGY-KANTA, "Functional and structural investigation of the post-synaptic scaffold protein GKAP" in *PhD Proceedings – Annual Issues of the Doctoral School, Faculty of Information Technology and Bionics, Pázmány Péter Catholic University – 2019.* G. Prószéky, P. Szolgay Eds. Budapest: Pázmány University ePress, 2019, pp. 25–25. This research has been partially supported by the European Union, co-financed by the European Social Fund (EFOP-3.6.3-VEKOP-16-2017-00002).

Particle separation in curved microchannels

Mihály SZŰCS
(Supervisor: Kristóf IVÁN)
Pázmány Péter Catholic University, Faculty of Information Technology and Bionics
50/a Práter street, 1083 Budapest, Hungary
szucs.mihaly@itk.ppke.hu

***Keywords*-microfluidics, particle separation, Dean flow, curved microchannel, cell separation**

I. Introduction

Microfluidic chips can use centrifugal effect to separate particles. There is a possibility to use inertial microfluidic platforms, where vortices are generated in the sample flow by special channel shapes. One type of these channel-designs use curved geometries, in which secondary Dean-vortices develop perpendicular to the main current. These vortices drift particles to one side of the channel.

II. Working principle

In curved pipes the curvature of the channel is influencing the behaviour of the flow. W.R. Dean proposed another number later named after him which takes this factor into account. In his two articles on this subject he introduces it as the function of the Reynolds number and the geometry of the curved channel. This number is named Dean number after him. If the Dean number is between 64 75 and 200, a pair of stable Dean vortices appear with opposite directions, which are perpendicular to the main flow, located at the bottom and the top of the channel.

In a laminar flow in a net lift force is present that drives the suspended particles from the center of the channel to the walls or at the vicinity of the wall at the other direction. In curved channels another lateral force also affects the particles: the Dean drag force. In curved channels the equilibrium of these two forces defines the place where a particle is focused. By creating microchannels with corresponding dimensions this phenomenon can be utilized to separate particles based on their size.

III. Design considerations

In the past decade many attempts were made to develop microfluidic separators for different tasks based on Dean force. While realizing the theory in practice many new problems and solutions appeared.

Prasad and Kim did a numerical simulation to find out which geometrical parameters are the most significant in the perspective of developing and maintaining Dean vortices in helical microchannels.

Another research investigated these parameters in particle separating experiments. They results showed that there is definitely an optimal flow rate above which defocusing occurs.

D. Di Carlo et al. defined some practical parameters to ease designing working separator channels for a given task. They investigated the ratio of particle size and channel diameter.

There are two main practices with the inputs of microfluidic separators based on Dean forces. One approach uses one inlet, where the particle-containing sample is injected into the curved channel.

Others design uses two inputs. One for the particle containing sample and one for sheath fluid. The sheath fluid is used to pinch the sample fluid to the wall of the channel.

These kind of separators require neither special materials nor fabrication techniques. Hence the fabrication methods used for these kind of microfluidic chips are usually the most common ones used for microfluidic chips. Soft lithography is the most common of these.

3D printing is also a viable option, because to induce Dean vortices one does not necessarily have micron-sized structures.

IV. Channel types

When designing a curved separator channel not only the aforementioned parameters need to be considered, but also practical possibilities and limitations. Hence different design types are invented to realize these channel systems.

A. One loop

The simplest method is to design a channel turning less than $360°$. This way the structure can easily fit onto a two-dimensional chip.

B. Helical channel

To design longer, more reliable separator channels one have to overcome the limitations of a two-dimensional plane. There are different approaches to this issue, one of them is using helical channels. This design needs three-dimensional fabrication methods, which are less common and precise, and the pitch of the helix can affect the development of Dean-vortices.

C. Spiral channel

The most common shape that is used to fit more than one channel turn on a two-dimensional chip is the spiral. It is a clearly two-dimensional structure, so it is suitable for conventional microfluidic chip fabrication methods, such as soft lithography or milling techniques.

D. Asymmetric sinusoid

The other way to fit multiple channel turns on a two-dimensional chip is to link then in a sinusoid manner. In a symmetric channel the Dean drag would change its direction from turn to turn, so every curve turning one direction have significantly less curvature radius then the ones turning the other direction, so the Dean drag is several times larger in the turns with smaller radius. This design results in a separator which have similar properties as the spiral channel.

M. SZŰCS, "Particle separation in curved microchannels" in *PhD Proceedings – Annual Issues of the Doctoral School, Faculty of Information Technology and Bionics, Pázmány Péter Catholic University – 2019.* G. Prószéky, P. Szolgay Eds. Budapest: Pázmány University ePress, 2019, pp. 26–26. This research has been partially supported by the European Union, co-financed by the European Social Fund (EFOP-3.6.3-VEKOP-16-2017-00002).

Analysis of ion channel models and possible implementations of long term plasticity in a detailed CA1 pyramidal cell model

Luca TAR
(Supervisor: Szabolcs KÁLI, Tamás FREUND)
Pázmány Péter Catholic University, Faculty of Information Technology and Bionics
50/a Práter street, 1083 Budapest, Hungary
tar.luca@itk.ppke.hu

***Keywords*-hippocampus; pyramidal cell; plasticity**

I. Introduction

In many cases, model parameters were tuned manually, and the effects of new parameter configurations were typically not assessed systematically. More recently, several tools have been developed that allow the automated determination of model parameters and support the systematic validation of the resulting models against experimental data. We used this approach to start developing morphologically and biophysically detailed models of CA1 pyramidal cells.

We considered multiple attributes of the cell determined by experiments, including the biophysics and distribution of ion channels, as well as the different electrophysiological characteristics of the soma and the dendrites. We gradually increased the complexity of our model, mainly by adding further types of ion channel, and monitored the ability of the model to capture both optimized and non-optimized features and behaviors. This method allowed us to determine the minimal set of mechanisms required to replicate particular neuronal behaviors and resulted in a new model of CA1 pyramidal neurons whose characteristics match a wide range of experimental results.

The dendrites of cortical pyramidal cells bear spines which receive most of the excitatory synaptic input, act as separate electrical and biochemical compartments, and play important roles in signal integration and plasticity. We also investigated ways to reduce the computational complexity of models of spiny neurons without altering their functional properties. Our models which show realistic electrical behavior in their dendrites and spines allow us to examine Ca-dynamics in dendritic spines in response to any combination of synaptic inputs and somatic action potentials. In combination with models of the critical molecular signaling pathways [1], this approach enables a comprehensive computational investigation of the mechanisms underlying activity-dependent synaptic plasticity in hippocampal pyramidal neurons.

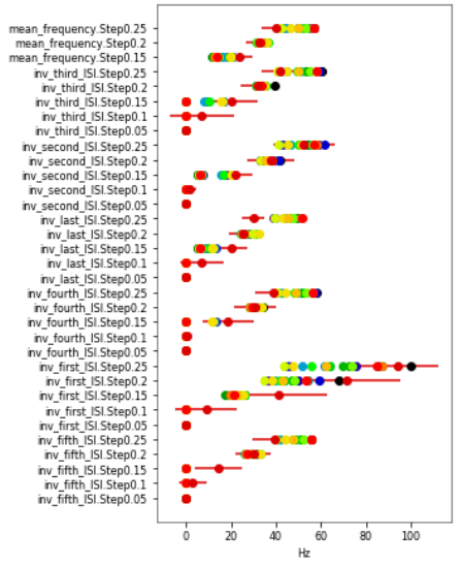

Fig. 1. The inters-spike intervals after the implementation of the new M-type potassium current. Each dot represent a model out of 20 parallel parameter optimization with different random seeds. The red dot is the experimental data. This plot clearly shows that most of the models are within the standard deviation (red line) of the target data.

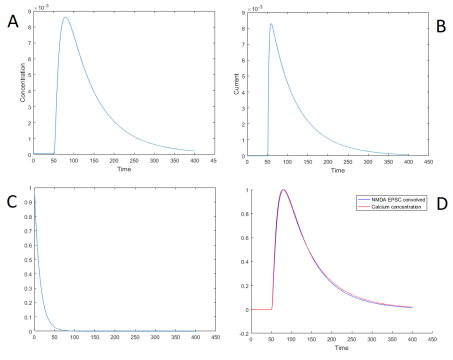

Fig. 2. Evaluation of the calcium dynamics. The parameters are acceptable, according to figure D. we could reproduce the observations Sabatini et al. A: Changes in the calcium concentration during a single synaptic event. B: The NMDA EPSC during a single synaptic event, under AMPA receptor block (the weight of AMPA was 0). C: A generated exponential with decay time constant matching the time constant of the calcium concentration decay (14 ms). D: The NMDA EPSC was convoluted with the exponential on figure C, then both the amplitude of the convoluted EPSC and the amplitude of the calcium concentration were normalized an plotted above each other.

References

[1] R. Lindroos, M. C. Dorst, K. Du, M. Filipović, D. Keller, M. Ketzef, A. K. Kozlov, A. Kumar, M. Lindahl, A. G. Nair, J. Pérez-Fernández, S. Grillner, G. Silberberg, and J. Hellgren Kotaleski, "Basal ganglia neuromodulation over multiple temporal and structural scales—simulations of direct pathway msns investigate the fast onset of dopaminergic effects and predict the role of kv4.2," *Frontiers in Neural Circuits*, vol. 12, p. 3, 2018. [Online]. Available: https://www.frontiersin.org/article/10.3389/fncir.2018.00003

L. TAR, "Analysis of ion channel models and possible implementations of long term plasticity in a detailed CA1 pyramidal cell model" in *PhD Proceedings – Annual Issues of the Doctoral School, Faculty of Information Technology and Bionics, Pázmány Péter Catholic University – 2019.* G. Prószéky, P. Szolgay Eds. Budapest: Pázmány University ePress, 2019, pp. 27–27. This research has been partially supported by the European Union, co-financed by the European Social Fund (EFOP-3.6.3-VEKOP-16-2017-00002).

Bio-stability study of liquid crystal polymer coated implants

Moutz WAHDOW
(Supervisor: Istvan ULBERT)
Pázmány Péter Catholic University, Faculty of Information Technology and Bionics
50/a Práter street, 1083 Budapest, Hungary
wahdow.moutz@itk.ppke.hu

***Abstract*—Bio-electronic implants are becoming increasingly important to human beings with the goal to improve longevity and quality of human life. The production of bioimplants involves an understanding of both biomedical science and electromechanical engineering to yield biocompatible products with sufficient lifespans. Selection of the constructional biomaterial is an essential requirement for a long-term and reliable service of the implants, which relies entirely on the comprehension of material properties. Our rule is to investigate the bio-stability and structural performance of biomaterials that are used now and might be in the future to build Bio-electronic Implants. Reviewing their performance under In vitro as well as In-vivo conditions for prolonged durations of time. As they must neither degrade or evoke any counter response from the host biological body. lately there has been an increased attention for Polymeric materials such as poly(p-xylylene), polyimide (PI), parylene-C, polydimethylsiloxane (PDMS) and Liquid Crystal Polymer (LCP). LCPs been reported to have the potential to laminate bio-implants by the measure of capabilities it can provide, such being easy to process and fabricate, has a decent resistivity to degrade over time, can provide MRI compatibility and miniaturization. For the degradation analysis: Impedance spectroscopy and two-photon microscopy are used to measure the passivation of the encapsulation layer. Tunneling microscopy and Cross-section analysis will be employed to evaluate any structural changes and quantify the reliability and integrity of the materials that cover medical devices before implanted in a human body.**

***Keywords*-Liquid Crystal Polymer (LCP); Polydimethylsiloxane (PDMS); Flexible electronics and Medical Implants.**

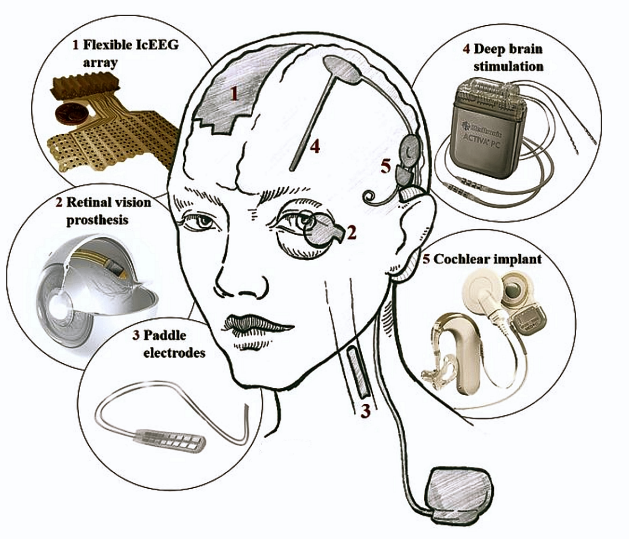

Fig. 1: Patients suffering from neuronal degenerative diseases are increasingly being equipped with neural implants to treat symptoms or restore functions [1].

Conclusion

LCPs have an appealing mechanical and chemical properties for neural prostheses applications. Such having chemical stability, low water and gas absorption rate, simultaneous flexibility and rigidity and easiness to process and fabricate. However, a particular obstacle in the long-term reliability of LCP-based neural implants is the LCP metal interface, Delamination in polymer-metal interface caused by ion diffusion and oxidation is of most impediment. Bio-stability testing for different Biomaterial is ongoing, LCP based device presumed to be robust and durable. New medical devices will be continually explored as biomaterial science and technology advances and alternatives to conventional implants will become more effective.

Acknowledgements

This research is conducted within POSITION-II. A pilot line for the next generation of smart catheters and implants. Funded by ECSEL Innovation Action contributed with more than 40 partners of research institutes, universities, industrial companies and technology leaders from all across Europe. In this pilot line scalable open technology platforms based on essential technologies will be integrated in one manufacturing network. POSITION-II will enable the electronic industry to take the lead in the development of these live saving instruments and to introduce open technology platforms for: miniaturization, in-tip AD conversion, wireless communication, MEMS transducer technology and encapsulation. These platforms are open to multiple users and for different applications. Open platforms will allow manufacturers to improve the performance of smart catheters at a lower cost. Additionally, it will enable the development of completely new smart minimally invasive instruments. Great respect and gratitude for Istvan Ulbert and his team and for all the administrators and tutors at Pazmany Peter Catholic University

References

[1] J. B. Erhardt, E. Fuhrer, O. G. Gruschke, J. Leupold, M. C. Wapler, J. Hennig, T. Stieglitz, and J. G. Korvink, "Should patients with brain implants undergo mri?" *Journal of neural engineering*, vol. 15, no. 4, p. 041002, 2018.

[2] V. Giagka and W. A. Serdijn, "Realizing flexible bioelectronic medicines for accessing the peripheral nerves–technology considerations," *Bioelectronic Medicine*, vol. 4, no. 1, p. 8, 2018.

[3] G.-T. Hwang, D. Im, S. E. Lee, J. Lee, M. Koo, S. Y. Park, S. Kim, K. Yang, S. J. Kim, K. Lee *et al.*, "In vivo silicon-based flexible radio frequency integrated circuits monolithically encapsulated with biocompatible liquid crystal polymers," *Acs Nano*, vol. 7, no. 5, pp. 4545–4553, 2013.

[4] Z. Dong, B. Duan, J. Li, and Y. Yang, "A stretchable flexible electronic platform for mechanical and electrical collaborative design," *Science China Information Sciences*, vol. 61, no. 6, p. 060418, 2018.

M. WAHDOW, "Bio-stability study of liquid crystal polymer coated implants" in *PhD Proceedings – Annual Issues of the Doctoral School, Faculty of Information Technology and Bionics, Pázmány Péter Catholic University – 2019.* G. Prószéky, P. Szolgay Eds. Budapest: Pázmány University ePress, 2019, pp. 28–28. This research has been partially supported by the European Union, co-financed by the European Social Fund (EFOP-3.6.3-VEKOP-16-2017-00002).

.

PROGRAM 2
COMPUTER TECHNOLOGY BASED ON MANY-CORE PROCESSOR CHIPS, VIRTUAL CELLULAR COMPUTERS, SENSORY AND MOTORIC ANALOG COMPUTERS

Head: Péter SZOLGAY

PID-based temperature control of a small satellite

Nawar AL-HEMEARY
(Supervisors: Gábor SZEDERKÉNYI, György CSEREY)
Pázmány Péter Catholic University, Faculty of Information Technology and Bionics
50/a Práter street, 1083 Budapest, Hungary
al.hemeary@itk.ppke.hu

***Abstract*—The CubeSat project is a collaborative effort of many universities and other communities. The design purpose of increasing space accessibility by reducing the cost and development time. To ensure a successful flight in space featuring gas propulsion system the ability to installing fuel tank inside the CubeSat should be sought at first. A thermal control subsystem is needed to be developed to effectively regulate the heat flow rate within the satellite orbit. Low power is the most concerning aspect of the CubeSats due to their small surface area which means a little amount of the solar cells are covering it. The goal of this paper is studying a heating power which has to be delivered for the system from the actuator and discuss its effect of the fuel tank temperature response with two types of the controllers: simple PID controller and anti-windup PID controller. Several simulation results are presented with those controllers for different values of the heating power to classify the adequate heating power to be delivered to the fuel tank to stabilize thermal fluctuations.**

***Keywords*-CubeSat; fuel tank; mathematical model; heating power; temperature control**

I. Introduction

CubeSats are the small satellites with the size of 10x10x10 cm^3 and a maximum mass about of 1.33 Kg designed of LEO orbit to explore the new space technologies. A typical CubeSat design uses solar cells for power generation and a small battery for storage. Nowadays, only a few CubeSats are boosted into space with an onboard propulsion system. These engines are used for flight formation, drags recovery, and other orbital maneuvers. The dynamical modeling and a simple PID-based temperature control design for a CubeSat have been derived and used to investigate the thermal hazards of installing the fuel tank inside the CubeSat [1], [2]. This model is formulated in the nonlinear ODEs form with a periodic disturbance input due to the orbital motion of the CubeSat. A small Surface area of the solar cell panel leads to a limited amount of the power generating at the CubeSats. Because of the power limits, the thermal control of CubeSat is challenging due to the low power consumption requirements. Therefore, the first choice in order to regulate the tank temperature with the required thermal limits along the satellite orbit was a passive control system [2]. Later on, the active control system was developed to achieve the optimal performance of the component and to control the fuel tank temperature at an assumed reference value. A PID controller might still be an advantageous choice even for certain nonlinear processes, while the anti-windup PID controller is stringently compensating the thermal oscillations of the fuel tank [1]. To avoid the power problems of installing the propellant tank inside the CubeSat, this paper studies the maximum and minimum limits of the heating power must be delivered to the fuel tank to keep its temperature at the defined input value by using PID controller and PID controller with anti-windup.

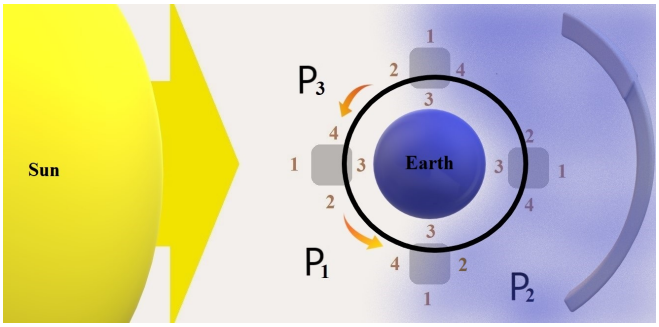

Fig. 1: CubeSat periodical motion.

References

[1] N. Al-Hemeary, M. Jaworski, J. Kindracki, and G. Szederkenyi, "Thermal model development for a cubesat," *Hungarian Journal of Industry and Chemistry*, vol. accepted, to appear, 2018.
[2] N. Al-Hemeary and G. Szederkenyi, "Fuel tank temperature control of a time-varying cubesat model," *IEEE 17th World Symposium on Applied Machine Intelligence and Informatics*, vol. accepted, to appear, 2019.

N. AL-HEMEARY, "PID-based temperature control of a small satellite " in *PhD Proceedings – Annual Issues of the Doctoral School, Faculty of Information Technology and Bionics, Pázmány Péter Catholic University – 2019.* G. Prószéky, P. Szolgay Eds. Budapest: Pázmány University ePress, 2019, pp. 30–30.
This research has been partially supported by the European Union, co-financed by the European Social Fund (EFOP-3.6.3-VEKOP-16-2017-00002).

Automatic parallelisation of scientific applications using high level abstractions with source-to-source translation

Gábor Dániel BALOGH
(Supervisor: István REGULY)
Pázmány Péter Catholic University, Faculty of Information Technology and Bionics
50/a Práter street, 1083 Budapest, Hungary
3in Research Group, Faculty of Information Technology and Bionics, Pázmány Péter Catholic University, Esztergom, Hungary
balogh.gabor.daniel@itk.ppke.hu

***Abstract*—Domain Specific Languages or Active Library frameworks have recently emerged as an important method for gaining performance portability. Embedded DSLs such as OP2 provides an API embedded in general purpose languages such as C/C++/Fortran. They rely on source-to-source translation to translate the higher-level API calls to platform specific parallel implementations. OP2 targets the solution of unstructured-mesh computations, where it can generate a variety of parallel implementations making use of a wide range of platform specific optimizations. Compiler tool-chains supporting source-to-source translation of code currently lack the capabilities to carry out such transformations. Clang/LLVM's Tooling library (LibTooling) has long been touted as having such capabilities but have only demonstrated its use in simple source refactoring tasks.**

During the first year of my PhD I have implemented a prototype for a source-to-source translator for OP2 with LibTooling utilizing the robustness and capabilities do a full fledged compiler architecture. I have tested the code generator on a set of unstructured applications and get near-identical parallel performance to that of OP2's current source-to-source translator.

***Keywords*-Source-to-source translation, Clang, LibTooling, CUDA, OpenMP, automatic parallelization, DSL, OP2, unstructured-mesh**

I. Summary

Domain Specific Languages or Active Library frameworks provide higher-level abstraction mechanisms, using which applications can be developed by scientists and engineers. In case of OP2 using this high-level API appears as calls to functions in a classical software library to the application developer. However OP2 then use extensive source-to-source translation to translate the higher-level API calls to platform specific parallel implementations.

OP2 currently uses Python to perform this translation step. However, the tools written in Python significantly lacks the robustness of compiler frameworks such as Clang/LLVM or GNU. They do only limited syntax or semantic checking, have even limited error/bug reporting to ease the development and becomes complicated very quickly when adding different optimizations, which in turn affect its maintainability and extensibility. The present work is motivated by the need to overcome these deficiencies and aims at making use of Clang/LLVM's LibTooling for full code analysis and synthesis.

II. Source-to-source translation with LibTooling

It is already shown that LibTooling is capable of perform source-to-source transformation as a series of local code replacements [1], [2]. taking advantage of the fact that the generated parallel loops with similar access patterns are structurally very similar, we created parallelisation skeletons and perform the code generation as a refactoring of these skeletons into the parallel implementation of the loops.

	SIMD	OpenMP	CUDA Global (AoS)	CUDA Global (SoA)	CUDA Hierarchical (AoS)	CUDA Hierarchical (SoA)
Airfoil	363.92s (-0.2%)	70.417s (1.2%)	12.77 s (-0.6%)	9.58 s (-0.4%)	9.85 s (0.2%)	7.30 s (1.8%)
Volna	95.39 s (0.3%)	14.84 s (-0.2%)	3.00 s (0.5%)	2.33 s (0.2%)	2.32 s (1.2%)	1.97 s (1.1%)

TABLE I
Performance of Airfoil and Volna on the Intel Xeon E5-1660 CPU (for OpenMP and SIMD) and on an NVIDIA P100 GPU with clang-op-translator.

With the new Clang based translator[3] I was able to generate parallel implementations using OpenMP and SIMD for CPUs and CUDA for GPUs for OP2. The performance of the generated implementation is near-identical to the Python generated versions as shown in Table I. I have CUDA results with two different colourings (global and hierarchical) and two data layouts presented. The values in parenthesis are the percentage difference in run time compared to the sources generated with OP2's current Python-based source-to-source translator (negative values means clang-op-translator has better performance). These results are promising, but we need to extend the translator to enable OPS applications to test the capabilities of the abstraction that we developed so far.

Acknowledgements

The research has been supported by the European Union, co-financed by the European Social Fund (EFOP-3.6.2-16-2017-00013, Thematic Fundamental Research Collaborations Grounding Innovation in Informatics and Infocommunications).
We are grateful to fellow engineers for their support: Gihan Mudalige, Samuel Antao and Carlo Bertolli.

References

[1] E. Bendersky, "Modern source-to-source transformation with clang and libtooling," 2014.
[2] E. Bendersky, "Ast matchers and clang refactoring tools," 2014.
[3] G. D. Balogh, G. R. Mudalige, I. Z. Reguly, S. Antao, and C. Bertolli, "Op2-clang: A source-to-source translator using clang/llvm libtooling," in *2018 IEEE/ACM 5th Workshop on the LLVM Compiler Infrastructure in HPC (LLVM-HPC)*, pp. 59–70, IEEE, 2018.

G. BALOGH, "Automatic parallelisation of scientific applications using high level abstractions with source-to-source translation" in *PhD Proceedings – Annual Issues of the Doctoral School, Faculty of Information Technology and Bionics, Pázmány Péter Catholic University – 2019.* G. Prószéky, P. Szolgay Eds. Budapest: Pázmány University ePress, 2019, pp. 31–31. This research has been partially supported by the European Union, co-financed by the European Social Fund (EFOP-3.6.3-VEKOP-16-2017-00002).

Light-Field 3D Videoconferencing

Aron CSERKASZKY
(Supervisor: Peter SZOLGAY)
Pázmány Péter Catholic University, Faculty of Information Technology and Bionics
50/a Práter street, 1083 Budapest, Hungary
cserkaszky.aron@itk.ppke.hu

***Abstract*—Videoconferencing and telepresence systems are not just an important tool in our fast paced modern life but also reduce climate impacting emissions. Thus the demand to improve the realism and productivity of this technology are both motivated by economic and environmental reasons. Light-field is the ultimate technology to allow multiple participants per location to seamlessly enjoy a realistic 3D videoconferencing experience, due to the lack of head mounted display component. In this paper we detail our implementation of 3D videoconferencing, consisting of a capture and a display light-field system.**

***Keywords*-light-field; videoconferencing; telepresence**

I. Introduction

The goal of videoconferencing is to multidirectonally transmit realistic realtime audiovisual content of mostly human participants to other participants at remote locations. Existing 2D video based solutions are abundant, the necessary hardware and software components are installed in virtually all smartphones and laptops sold nowadays. However the single view per participant, limits the realism and immersion of 2D systems and usually necessitates a separate videoconferencing device per participant. 3D solutions aim to transcend this limitation by capturing participants from more than one angle and to also show extra captured visual information to the other participants.

II. Existing solutions

While they are not technically 3D systems, we have to mention single camera based capture systems, where the camera is mounted on an interactively moving platform. As the moving platform, such as a remote controlled robot, shows different parts of the remote scene from different angles, it creates a time multiplexed 3D view of the scene for the remote participants. The interaction of this moving platform with its environment makes these complex, while only providing a marginally better realism than existing 2D solutions.

Dual camera based stereo systems are able to capture 3D visual information and to show it to remote participants, however stereo display technology requires glasses that select the appropriate view for each eye with their respective technology. The seamless immersion, while being less than ideal due to the glasses and the single point of view (POV), is also limited by the flat stereo displays for groups of participants on a single location.

Novel 360 capturing devices coupled with head mounted displays (HMD), improve yet again on the realism, by capturing every angle of the scene from a single point. The participants are able to control the view they see by the orientation of their own heads. This provides better visual content but also requires a participant to be isolated from its own real environment and potentially from other participants at the same location. The additional fact, that the participants facial features are obscured by the HMD, makes this technology suitable only for purely virtual meeting environments.

III. Light-Field 3D systems

Light-field capture systems use many cameras in a grid or a line to provide a baseline or baseplane, in which the POV of the observer is allowed to move freely. The amount of captured visual information might be limited by electrical, bandwidth, space or other constraints. But this provides still the most realistic telepresence experience, as existing light-field displays are able to show the correct 3D view to each observing participant, based on their physical location. There is also no need for glasses or HMDs, and participants are able to interact with their physical environment and other participants at the same location without hindrances. Should the observers move in their environment they will experience the change of perspective in the remote location as well, due to the continuous motion parallax provided by the light-field display. The density of the views emitted by the light-field display, determines the depth resolution, and the valid observing area, and should match the density and extent of the captured views.

IV. Our prototype

As a demonstration of this technology we have built a unidirectional light-field videoconferencing system. It consists of a capture and a display subsystem connected by a high throughput network. The goal of the prototype is to present a person to a remote group of observers in the most realistic way possible.

The capture subsystem consists of 96 cameras arranged on a 120 degree arc, pointing to the center, where a person may stand. The captured light-field allows observers to perceive an immersive 3D visual experience within this field of view (FOV). The realtime video feed of all cameras are synchronized and aggregated, then transmitted via the network to the display subsystem.

The display subsystem has a 1×1.8 meters holographic screen, to enable presenting a human. The display is able to emit 100 megarays of the input light-field, has a 2D equivalent resolution of 720×1280, and 0.9 degree angular resolution. The rendering computers on the displays side calculate the matching input light-field rays for each output light-field ray, and convert the captured light-field to the displayed one. We have achieved the low latency of approximately 100 ms in our prototype system.

Acknowledgements

The work in this paper was funded from the European Union's Horizon 2020 research and innovation program under the Marie Sklodowska-Curie grant agreement No 676401, European Training Network on Full Parallax Imaging.

Á. CSERKASZKY, "Light-Field 3D Videoconferencing" in *PhD Proceedings – Annual Issues of the Doctoral School, Faculty of Information Technology and Bionics, Pázmány Péter Catholic University – 2019.* G. Prószéky, P. Szolgay Eds. Budapest: Pázmány University ePress, 2019, pp. 32–32. This research has been partially supported by the European Union, co-financed by the European Social Fund (EFOP-3.6.3-VEKOP-16-2017-00002).

Image processing algorithms implementation on FPGA

Attila FEJÉR
(Supervisors: Péter SZOLGAY, Jenny BENOIS-PINEAU)
Pázmány Péter Catholic University, Faculty of Information Technology and Bionics
50/a Práter street, 1083 Budapest, Hungary
fejer.attila@itk.ppke.hu

***Abstract*—This paper discusses the control of a prosthetic arm based on egocentric view videos. The requirements of such application consist of real-time processing, low power usage, small architecture and device size. Considering these reasons FPGA (Field-programmable gate arrays) have been used as hardware acceleration for the required image processing tasks. In this paper, a partial implementation of the SIFT (Scale Invariant Feature Transform) algorithm on an FPGA-board is presented. Further possibilities of improvements are also proposed.**

***Keywords*-FPGA, SIFT, vision-guided prosthetic arm**

I. Introduction

There are many military conflicts, and different type of accidents throughout the world require the design and production of neuro-prosthetics within everyone's reach. To control this robotic arm is a hard task. We use computer vision and image processing algorithms and robotics techniques to solve this problem.

Our system has[1] three different video input sources. Tobii glass camera which is an eye tracker camera and the user can wear like eyeglasses. This eye tracker gives an egocentric view video as output. The other two cameras are GoPro action-cameras which gives two different views left and right. From Tobii eye tracker frames a CNN (Convolutional Neural Network) can predict the object what the patient tries to grasp. The output of this object recognition CNN is a bounding box which is the input of the object matching unit.

The object matching unit has four inputs: Tobii camera frames, GoPro cameras frames and a bounding box around the Tobii camera frames object of interest. The goal of the object matching part is to find the object of interest in the GoPro cameras frames. The method for that is the following:

1) Find SIFT[2] key points in Tobii and GoPro cameras frames
2) Extract SIFT descriptors
3) Use Bruteforce matcher between GoPro camera Left view and Tobii eye tracker descriptors and between GoPro right view and Tobii eye tracker descriptors
4) Estimate homography matrixes
5) Use the given bounding box and the homography matrices to calculate the left and right view frames bounding boxes

The next step is cut from the GoPro cameras frames the bounding boxes and use those as an input of the depth map.

The most time-consuming part of the object matching part is the SIFT keypoint and descriptor extraction. Because of that, we were starting to develop the SIFT algorithm on FPGA.

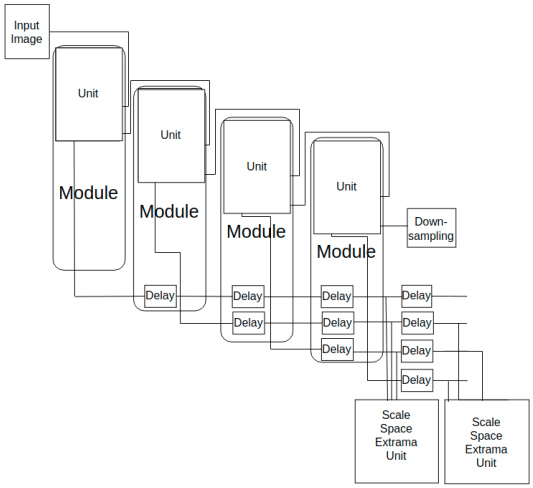

Fig. 1. Schematic chart of the proposed architecture

II. Proposed architecture

The proposed architecture is illustrated on Figure 1. The output of the units is a Gaussian filtered image and a difference of Gaussian image. The Gaussian filtered image is the input of the next unit. The Scale-Space Extrema Unit can calculate whether a pixel is a possible minimum or maximum or not.

III. Results and Conclusions

Current results show there are enough free resources left[3] on the FPGA to develop more image processing algorithms.

Real-time processing (> 25 fps) also achievable on low and high-end FPGAs.

Power dissipation of FPGAs is very low less than 3 Watts which makes them a better choice than GPUs, and CPUs in wearable device development.

IV. Acknowledgement

The contribution of Mr Zoltán Nagy and Mr Aymar de Rugy is kindly acknowledged.

References

[1] I. González-Díaz, J. Benois-Pineau, J.-P. Domenger, D. Cattaert, and A. de Rugy, "Perceptually-guided deep neural networks for ego-action prediction: Object grasping," *Pattern Recognition*, vol. 88, pp. 223 – 235, 2019.

[2] D. G. Lowe, "Object recognition from local scale-invariant features," in *Computer vision, 1999. The proceedings of the seventh IEEE international conference on*, vol. 2, pp. 1150–1157, Ieee, 1999.

[3] A. Fejér, Z. Nagy, J. Benois-Pineau, P. Szolgay, A. de Rugy, and J.-P. Domenger, "Fpga-based sift implementation for wearable computing," in *2019 22nd International Symposium on Design and Diagnostics of Electronic Circuits and Systems (DDECS)*, 2019.

A. FEJÉR, "Image processing algorithms implementation on FPGA" in *PhD Proceedings – Annual Issues of the Doctoral School, Faculty of Information Technology and Bionics, Pázmány Péter Catholic University – 2019.* G. Prószéky, P. Szolgay Eds. Budapest: Pázmány University ePress, 2019, pp. 33–33.
This research has been partially supported by the European Union, co-financed by the European Social Fund (EFOP-3.6.3-VEKOP-16-2017-00002).

Multistate-switching based memristor modeling in a Python based SPICE-like circuit simulator

Dániel HAJTÓ
(Supervisor: György CSEREY)
Pázmány Péter Catholic University, Faculty of Information Technology and Bionics
50/a Práter street, 1083 Budapest, Hungary
hajto.daniel@itk.ppke.hu

***Abstract*—Memristors and memristive devices are stateful, non-linear units. To be able to design complex circuits using them, accurate models are necessary, which can be used by circuit simulators. Considering the small device size for most implementations quantum mechanical effects likely occur during operation, which implies that probabilistic modeling approach could produce more realistic memristor models. The current circuit simulators do not provide support for probabilistic models, therefore a new, improved circuit analyser is needed. In this work I provide a proof-of-the-concept implementation in Python which is partially compatible with $SPICE$ circuit file formats. A work-in-progress probabilistic memristor model is also presented.**

***Keywords*-memristor; memristor modeling; nonlinear dopant kinetics; circuit simulation**

I. Introduction

Memristors are subject of interest from their recent rediscovery in 2008 [1]. Since then many useful applications were created [2], [3], [4]. However, a single unified memristor model is yet to be accepted. One of the reasons is that the different implementations have significantly different characteristics. They vary in time scale - from ns to several s in writing/erasing speed -, resistance scale - from several Ω to $G\Omega$ - and number of states - from 2 states to practically infinite or analogous - as well as have various parasitic effects, for example non-linear characteristics without state change.

II. Multistate-switching based modeling

In the case of chalcogenide memristors, the memristive effect is created by nano-filament forming in the chalcogenide matter. The filaments are ions of the conductor plates or bars, which are conducting also.

The idea of the switching based modeling approach is to mimic the ion movements with switches. The weighed sum of all switches produces the state of the memristor.

Due to the lack of information about the exact structure of a given memristor device, the ion movement must be considered a probabilistic event on a given input voltage.

We can improve the model with the usage of multistate switches instead, which can describe more accurately the position of a given ion and thus its contribution to the state of the memristor.

A probabilistic switching based extension in the memristor model will result in stochastic equations. Modified Nodal Analysis can be applied, but it will result in Stochastic Differential Algebraic Equations ($SDAE$). Solving this class of equations is much harder and finding a good general solution is considered to be an open question [5] even today.

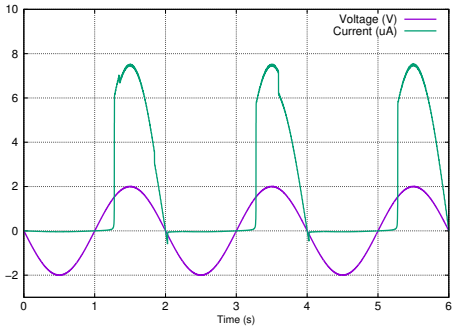

Fig. 1. Simulation result for the memristor model.

III. Results

A. Simulator

I have implemented a circuit simulator in which nonlinear and stochastic models can be created. It uses Modified Nodal Analysis as circuit analyser and Forward Euler method as differential equation solver. It uses the $SPICE$ input syntax with its basic elements and features. This consists the passive elements and basic circuit analysis methods like DC sweep or AC analysis.

B. Proposed model

I have implemented a general multistate-switching memristor model in this framework. An example simulation can be seen on Fig. 1 with one set of hyperparameters.

Acknowledgements

The author would like to acknowledge the support of Pázmány Péter Catholic University KAP R&D and equipment grants, as well as Hungarian state funding PPKE ITK EFOP-3.6.2-16-2017-00013, 3.6.3-VEKOP-16-2017-00002.

References

[1] Strukov, Dmitri B., Gregory S. Snider, Duncan R. Stewart, and R. Stanley Williams, *The missing memristor found*, nature 453, no. 7191, 2008.
[2] Li, Can, Miao Hu, Yunning Li, Hao Jiang, Ning Ge, Eric Montgomery, Jiaming Zhang et al., *Analogue signal and image processing with large memristor crossbars.*, Nature Electronics 1, no. 1, 2018.
[3] Ascoli, Alon, Dominik Baumann, Ronald Tetzlaff, Leon O. Chua, and Manfred Hild, *Memristor-enhanced humanoid robot control system–Part I: Theory behind the novel memcomputing paradigm.*, International Journal of Circuit Theory and Applications 46, no. 1, 2018.
[4] Baumann, Dominik, Alon Ascoli, Ronald Tetzlaff, Leon O. Chua, and Manfred Hild, *Memristor-enhanced humanoid robot control system–Part II: Circuit theoretic model and performance analysis.*, International Journal of Circuit Theory and Applications 46, no. 1, 2018.
[5] Schein, Oliver, and Georg Denk, *Numerical solution of stochastic differential-algebraic equations with applications to transient noise simulation of microelectronic circuits.*, Journal of Computational and Applied Mathematics 100, no. 1, 1998.

D. HAJTÓ, "Multistate-switching based memristor modeling in a Python based SPICE-like circuit simulator" in *PhD Proceedings – Annual Issues of the Doctoral School, Faculty of Information Technology and Bionics, Pázmány Péter Catholic University – 2019.* G. Prószéky, P. Szolgay Eds. Budapest: Pázmány University ePress, 2019, pp. 34–34. This research has been partially supported by the European Union, co-financed by the European Social Fund (EFOP-3.6.3-VEKOP-16-2017-00002).

Accelerating Charged Single alpha-helix on FPGA

.

Sam KHOZAMA
(Supervisors: Zoltán NAGY, Zoltán GÁSPÁRI)
Pázmány Péter Catholic University, Faculty of Information Technology and Bionics
50/a Práter street, 1083 Budapest, Hungary
khozama.sam@itk.ppke.hu

***Abstract*—Implementing and speeding up the bioinformatics algorithms which need a very fast and accurate results is the main advantage of reconfigurable architectures which can be used more efficiently in the comparing of conventional microprocessors with 32 or 64 bit representations. We have a new and huge amount of biological data generated each day. The procedure of analyzing and processing its algorithms takes a very long time in the normal CPUs. Low precision input data is the main characteristic of these algorithms in which it can be stored in 2-5 bits. By using such reconfigurable architecture like FPGA, so limited number of configurable logic is needed.**

I. Introduction

Charged single a-helix (CSAHs) form a recently recognized protein structural motif. Its existence and role are characterized in a few proteins only.To get reliable candidate CSAH motifs, we have two conceptually different computational methods which are capable of scanning large databases: SCAN4CSAH and FT_CHARGE. SCAN4CSAH is based on sequence features characteristic, whereas FT_CHARGE applies and utilizes Fourier transformation to charges along sequences. Field-programmable gate array (FPGA) based systems provide the potential for drastic improvement in the performance of data intensive applications. Acceleration different sequence search and sequence matching in bioinformatics algorithms like Smith-Waterman algorithm is the goal of using FPGA.

II. FT_CHARGE ALGORITHM

Both SCAN4CSAH and FT_CHARGE are used to detect charged single a-helix (CSAHs) motif and these two algorithms are totally conceptually different computational methods to analyze sequences of protein. while FT_CHARGE algorithm applies Fast Fourier transformation to charges along sequences, SCAN4CSAH algorithm is based on the characteristic of sequence features[6]. standard FASTA format is the input format for both algorithms. FASTA file involves of series of characters where each character represent one protein in a sequence. The analysis of biopolymer sequences utilizes Fourier transformation regularly.

As shown in figure 1, the first step in the system is Charge Correlation function and its results passed to the second block (Fast Fourier Transformation(FFT)).

III. FPGA IMPLEMENTATION

FPGA manufacturers offer very efficient signal processing libraries to utilize them in such blocks. Previous system was using FFT IP core from Xilinx CoreGenerator and the main goal was optimizing the computation of the charge correlation function to feed the FFT core efficiently. The previous implementation of FT_CHARGE algorithm was on a small FPGA, and it run in a reasonable time even with a large dataset. The only way to extend this solution is to create several units in parallel using a larger Xilinx ZENQ board.

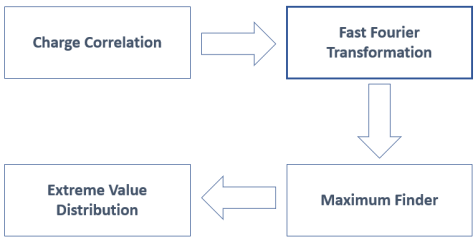

Fig. 1. The block diagram of the system

TABLE I
Area requirements of the system

	LUT	FF	Slice	BRAM	DSP
Correlation	14280	9430	5180	0	0
FFT	6810	1287	3200	5	0
Amplitude and max	6570	6400	2670	0	20
EVD fit	51170	41300	16930	10	300
Other(AXI-IC, DMAs, etc.)	37810	46210	13810	95	0
Complete system	116640	116210	41790	110	380

IV. FAST FOURIER TRANSFORMATION BLOCK

Fast Fourier Transformation by using The Cooley-Tukey Algorithm is the way of avoid using the Discrete Fourier Transformation which is incredibly slow!

Previously, the system used Xilinx FFT IP which do the transformation serially. So, 32 or 64 clock-cycles are required to load the samples. And the whole computation is done in 32 — 46 clock-cycles. In our case, we modified the charge correlation part to provide these data elements in parallel, which means: computation could be increased by 32 times.

For easier testability, we get MATLAB code and C code from the previous implementation. We created a complete (test bench) in Vivado HLS to load a valid sequence data to the system and process it and check whether the result is good or not.

V. CONCLUSION

We improved, in this paper, the proposed FPGA based system for speeding up a-helix detection algorithm by replicating the main three block as much as they fit a larger FPGA board. In addition to, implementing these several processing units in parallel which enables fast search on larger protein databases and run the whole system in a speed of 30 times more. Using the butterfly diagram and fixed-point representation save more area and time with almost the same accuracy.

References

[1] D. Süveges, Z. Gáspári, G. Tóth, L. Nyitray, *Charged single a-helix: a versatile protein structural motif, Proteins* , 74 (2009) 905–916.
[2] J. W. Cooley and J. W. Tukey *An algorithm for the machine calculation of complex Fourier series*, Math. of Computation, vol. 19, pp. 297–301, 1965.

S. KHOZAMA, "Accelerating Charged Single alpha-helix on FPGA" in *PhD Proceedings – Annual Issues of the Doctoral School, Faculty of Information Technology and Bionics, Pázmány Péter Catholic University – 2019.* G. Prószéky, P. Szolgay Eds. Budapest: Pázmány University ePress, 2019, pp. 35–35.
This research has been partially supported by the European Union, co-financed by the European Social Fund (EFOP-3.6.3-VEKOP-16-2017-00002).

A new technique for a better autofocus

Márton Zsolt KISS
(Supervisor:Ákos ZARÁNDY)
Pázmány Péter Catholic University, Faculty of Information Technology and Bionics
50/a Práter street, 1083 Budapest, Hungary
kisma1@itk.ppke.hu

***Abstract*—Digital holographic imaging is a good tool for automatic particle size and morphology measurements. Now, we present a new way to increase the accuracy of the autofocus. It is not another autofocus algorithm, but it can be used with different autofocus algorithms. This new method was tested with different autofocus algorithms, and its efficiency can be clearly observed. We used it in an in-line holographic setup, which was built to observe algae from algae cultures.**

***Keywords*-digital holography, autofocus, microscopy, real time measurements**

I. Introduction

Our aim was to have a better autofocus result to have a proper focus distance. With our approach we observe flowing samples that contain many point-like objects which are algae. From a captured hologram we can numerically reconstruct the images of the different objects that are in different depths.

Our idea was to modify the input images of the autofocus algorithm instead of the algorithm to have a better autofocus result. In the case of holography we apply numerical wave field propagation. It is known that rays connected to a higher numerical aperture have higher divergence angle. So we tested that if imaging is done only with these rays the accuracy of the focus distance measurement can be increased or not. We have to emphasize that these modified images are used only to determine the proper focus distance of an object. The original hologram and the proper focus distance are used to reconstruct the full image of an object for sample analyzes.

II. The theoretical background

First let observe an imaging using ray optics. Figure 1 a)-b) shows that if the numerical aperture (NA) is increased then the depth of field (δ) is decreased. They are in inverse proportion: $\delta \approx \frac{1}{NA}$ The numerical aperture is defined by the extremal rays diverging half angle (Θ). $NA = n * sin(\Theta)$ So drawing extremal rays the focus point can be pointed out more clearly as it can be seen compering Figure 1. a) to c). Leaving the focal point the extremal rays will spread more than the central rays. It is also known that the waist of a beam is smaller when the numerical aperture is bigger.

Because there is no way to increase the numerical aperture we decided to make the extremal rays more dominant, so we filter out the central rays that have usually higher intensity also as it can be seen in Figure 1 c). Without the central rays the image biased considerably, but the difference and so the contrast between the in focus and out of focus images will be bigger. Imaging without the central rays is imaging with a gappy wavefront.

We used holography for our measurements. The object's wavefront is captured as a thin digital hologram. We used angular spectrum method to emulate the propagation of the wave field. To make the reconstruction using only the extremal rays we can cut out the middle of the hologram of every object or also we can make a low frequency filtering. We chose the second solution. It is easier, and making on the full captured hologram it will done on every holograms of the objects.

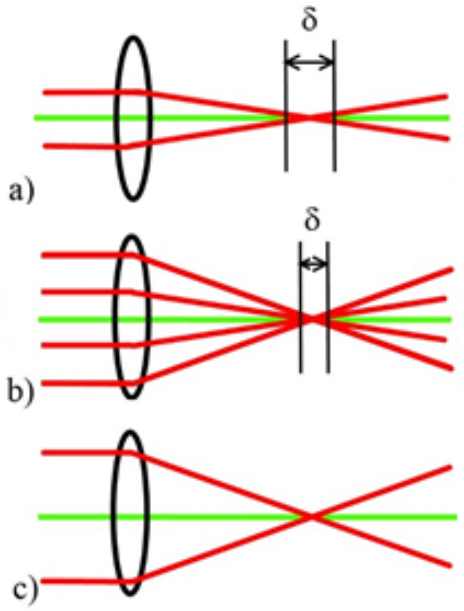

Fig. 1. a)-b) The connection between the numerical aperture (NA) and the depth of field. c) Cutting out the central rays, the effect of the extremal rays can be more dominant.

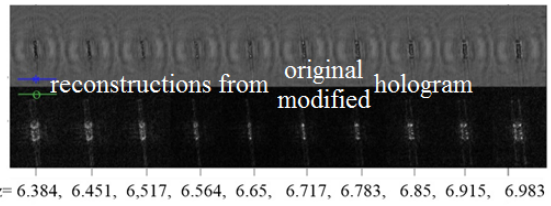

Fig. 2. Making the imaging without the central rays -the images that have a black background - will define more clearly where the focus is.

III. Results and conclusion

Using this filtering it is more obvious for human and for autofocus algorithms where the focus is. In Figure 2. we can see the reconstructions at different distances of an original and a modified holograms.

Acknowledgement

This article was fully presented in: SPIE, Photonoc West 2019. Conference, Proceedings Volume 10944, Practical Holography XXXIII: Displays, Materials, and Applications; 109440I (2019) https://doi.org/10.1117/12.2508896

M. KISS, "A new technique for a better autofocus" in *PhD Proceedings – Annual Issues of the Doctoral School, Faculty of Information Technology and Bionics, Pázmány Péter Catholic University – 2019.* G. Prószéky, P. Szolgay Eds. Budapest: Pázmány University ePress, 2019, pp. 36–36. This research has been partially supported by the European Union, co-financed by the European Social Fund (EFOP-3.6.3-VEKOP-16-2017-00002).

Monitoring of the physiological signals of newborn babies

Ádám NAGY
(Supervisor: Ákos ZARÁNDY)
Pázmány Péter Catholic University, Faculty of Information Technology and Bionics
50/a Práter street, 1083 Budapest, Hungary
nagy.adam@itk.ppke.hu

***Abstract*—Nowadays there is very intensive research in the field of remote measurement of physiological signals of neonatal. The motivation is the vulnerability of infants that is a big disadvantage of the touch sensors which are currently used in clinical applications. We have investigated several algorithms which can extract different signals from video records like breathing rate, pulse rate or SPO level of infants. In this paper, I will focus on extracting respiration of neonatal and the deep learning based identification of certain regions of interest on the baby like the belly, the chest etc.**

I. Introduction

The biggest challenge in the case of extraction of respiration rate (RR) of neonatal is that there are differences between the respiration of adults and newborn babies. The respiration of infants changes strongly in frequency and amplitude too. This is why we had to work out a new approach in order to measure it correctly. We propose two (optical flow based and SVD based) novel methods for RR monitoring and demonstrate their applicability by quantitative comparison to ground truth provided by human observer and ECG.

II. Extracting respiration signal

In both cases the input is a sequence of consecutive images (or a video record from the baby). It is based on sliding window and it calculates singular value decomposition in order to elicit breathing signal. The other approach is based on optical flow which is calculated between the consecutive images. The respiration signal itself is the mean absolute deviation from the background in the first case and the length of the average displacement vector in the second case.

III. Calculation of RR

we proposed two kinds of options for generating RR from the respiration signal. The first one is a sliding window based method that uses the Otsu algorithm to find the maximums of the signals. By counting them we can give the RR. The other solution is based on the auto correlation of the signal which return with a periodicity measure and the period itself.

IV. Validation of algorithm

We generated a Ground truth (GT) manually by a human observer who had to click the mouse each time breath motion (air in or out) was observed and we also recorded an ECG based ground truth where we measured the impedance change between the electrodes caused by the air volume changing in the lungs. During the validation we compared the result of our algorithms to the manual GT and the ECG based GT too.

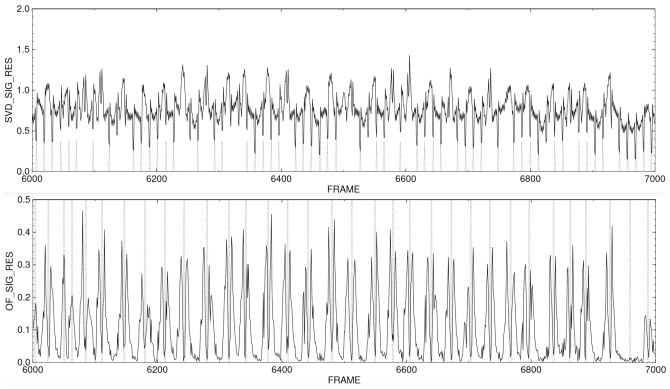

Fig. 1. The top figure above shows the result of SVD based RR monitoring method. The bottom figure displays the result of the Optical Flow based RR monitoring method.

V. Automatic ROI generation

During the validation it became obvious that only a smaller parts of the images provides us information about the respiration. However, the position of the region of interest can change in time. An automatic ROI detector is required. We know that the motion related to the respiration is localized in the belly in the case of newborn babies. As a consequence, we need to determine the position of the belly or the sides of the baby in the case when the baby is lying on its back. This is a segmentation task. We proposed UNET which is a deep learning architecture that can learn which pixels are related to the belly of the baby, which pixels to the arms, to the legs etc. However, it requires thousands of annotated images. Currently this annotation is happening by labelme.

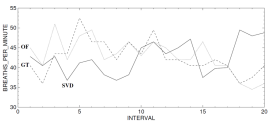

Fig. 2. Average respiration rates for intervals compared to the manual GT

References

[1] Stan Bircheld, *KLT: An Implementation of the Kanade-Lucas-Tomasi Feature Tracker*, http://cecas.clemson.edu/˜stb/klt, 2007,

[2] L.Cattani,D.Alinovi,G.Ferrari,R.Raheli,E.Pavlidis,C.Spagnoli,andF.Pisani. *Monitoring infants by automatic video processing: A unied approach to motion analysis*, Computers in Biology and Medicine, 80:158–165, 2017,

[3] D. Chetverikov and A. Axt *Approximation-free running svd and its application to motion detection*, Pattern Recognition Letters, 31:891–897 2010

Á. NAGY, "Monitoring of the physiological signals of newborn babies" in *PhD Proceedings – Annual Issues of the Doctoral School, Faculty of Information Technology and Bionics, Pázmány Péter Catholic University – 2019.* G. Prószéky, P. Szolgay Eds. Budapest: Pázmány University ePress, 2019, pp. 37–37. This research has been partially supported by the European Union, co-financed by the European Social Fund (EFOP-3.6.3-VEKOP-16-2017-00002).

Contextual calibration for UAV sense and aviod

Koppány PÁZMÁN
(Supervisor: Ákos ZARÁNDY)
Pázmány Péter Catholic University, Faculty of Information Technology and Bionics
50/a Práter street, 1083 Budapest, Hungary
pazman.koppany@itk.ppke.hu

***Abstract*—In this research, we investigated the applicability of contextual calibration for neural network based mono-camera vision systems of UAVs using simulated training data. We found that the further training of a network in an unknown environment did not decrease the quality of the network, furthermore, in the cases where the unknown environment was not sufficiently represented in the original training data, we observed an increased performance of the network.**

***Keywords*-transfer learning, contextual calibration**

I. Introduction

Sense and avoid (SAA) for unmanned areal vehicles (UAVs) stands for the detection of an intruder UAV coming in the general direction of our own UAV and determining if taking action in order to avoid collision is necessary. In this research, we focused on the first step of SAA, the identification of an intruder.

By contextual calibration, we mean the further on-line training of a neural network already trained for the intruder detection with calibration data of the actual flight. The motivation behind this method is that while we can train a network sufficiently before taking off, during a real flight, the UAV will be placed in an environment whose aspects are not covered completely by the training data set. Therefore, by feeding new negative examples, collected during the actual flight, to the network, we can adapt it to the current environment.

II. Experiments

Obtaining real flight videos is a costly and non-trivial task, especially with close encounters of UAVs, which is necessary for investigating the SAA problem. We used the publicly available CVPR video set [1], and beyond that, we set up a simulated experimental environment using Unreal Engine 4 with the Microsoft AirSim[1] plugin. We created three different skies and four terrains, whose combinations give us 12 different simulated setups.

The camera images are given to the preprocessing algorithm, proposed in [2], in order to select rectangular regions (ROIs), where an incoming UAV might be present. The cropped ROIs were used to train convolutional neural networks during the trainig stage, and durirng the evaluation phase, the ROIs proposed by the preprocess algorithm were inferred by the netwoks.

We performed two sets of experiments: in one set, the base networks were trained on the CVPR data, then evaluated and calibrated on the simulated data; in the other set, base networks were trained on subsets of the simulated data, where one of the sky or landscape types were left out, then evaluated and calibrated on the subset of the simulated data which contained the detail left out during the base training.

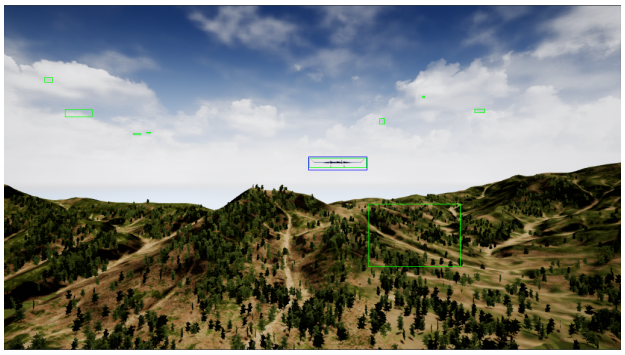

Fig. 1. The view of the landscape and sky created in Unreal Engine with an intruder UAV. The blue box marks the ground thruth, the ten green boxes are the ROIs which were considered to be most likely the intruder by the network.

We used two measures to assess the difference in performance between the base and the calibrated networks: the Area Under Curve value of Reciever Operating Characteristics (ROC AUC) and the normalized Discounted Cummulative Gain (nDCG). We concluded that the context calibration improves the AUC score when we trained the base networks on the CVPR data by 5.61% on average. In case of base networks trained on simulated data, although there is no significant change in the AUC scores, the nDCG values do increase from 0.93 to 0.934. These results mean that contextual calibration is most effective when the actual environment is not sufficiently represented in the original training data, but also a well-performing network can be slightly improved by it.

[1] An UE4 plugin that provides a realistic model of a drone and a car with cameras mounted on them. The camera image and a segmented image can be obtained in parallel with ease through an API. AirSim is available online at https://github.com/Microsoft/AirSim

Acknowledgements

I would like to express my gratitude, besides my supervisors, to ALEKSZIEV Rita and DARÓCZY Bálint, with whom we conducted the presented research in close cooperation.

References

[1] A. Rozantsev, V. Lepetit, and P. Fua, "Flying objects detection from a single moving camera," in *Proceedings of the IEEE Conference on Computer Vision and Pattern Recognition*, pp. 4128–4136, 2015.

[2] P. Bauer, A. Hiba, J. Bokor, and A. Zarandy, "Three dimensional intruder closest point of approach estimation based-on monocular image parameters in aircraft sense and avoid," *Journal of Intelligent & Robotic Systems*, vol. 93, pp. 261–276, Feb 2019.

K. PÁZMÁN, "Contextual calibration for UAV sense and aviod" in *PhD Proceedings – Annual Issues of the Doctoral School, Faculty of Information Technology and Bionics, Pázmány Péter Catholic University – 2019.* G. Prószéky, P. Szolgay Eds. Budapest: Pázmány University ePress, 2019, pp. 38–38.
This research has been partially supported by the European Union, co-financed by the European Social Fund (EFOP-3.6.3-VEKOP-16-2017-00002).

Local performance estimation of nonlinear rational systems in a convex computational framework using Finsler's lemma and affine annihilators

Péter POLCZ
(Supervisor: Gábor SZEDERKÉNYI)
Pázmány Péter Catholic University, Faculty of Information Technology and Bionics
50/a Práter street, 1083 Budapest, Hungary
polcz.peter@itk.ppke.hu

***Abstract*—We present an improved version of the previous results on induced $\mathcal{L}_2$ gain estimation for uncertain nonlinear rational systems. The storage function is searched in a general quadratic form of a rational state dependent vector generated from the linear fraction representation (LFR) realization of the system equation. By the means of an upper energy bound for the input signal, we give an invariant level set of the storage function as a guaranteed domain for local asymptotic stability (domain of attraction) and induced $\mathcal{L}_2$ norm smaller than or equal to $\gamma > 0$. In order to formulate convex linear matrix inequality (LMI) conditions for the dissipativity relations, Finsler's lemma is used with affine annihilators. The approach is illustrated on a second order benchmark systems.**

***Keywords*-linear parameter varying systems, global stability, Lyapunov functions, linear matrix inequalities**

I. Introduction

In many control problems, it is natural to involve finite-energy signals in the analysis and target induced $\mathcal{L}_2$ gain to measure the effect of disturbance attenuation. Hence, this metric is of potential interest for applications and can be quantified for a wide range of dynamic systems, linear or nonlinear problems [1].

In [2], Finsler's lemma [3] is borrowed to account for $\mathcal{L}_2$ performance estimation and robust nonlinear controller synthesis for rational uncertain nonlinear systems. By the introduction of an admissible disturbance set, the authors of [2] gave a local interpretation of the computed upper bound for the induced $\mathcal{L}_2$ norm. However, the exact definition for the admissible disturbance set is not fully covered.

In [4], we presented a numerical framework to compute an upper-bound for the induced $\mathcal{L}_2$ norm of linear parameter varying (LPV) system operator with rational parameter dependence. In [5], we proposed a numerical technique to design a passifying output projection mapping for asymptotically stable MIMO LPV systems.

In this research report, we start from the ideas of [2] and adapt the LMI relaxation techniques of [4] for nonlinear systems written in a quasi-LPV (qLPV) form to address local $\mathcal{L}_2$ gain estimation.

II. Problem formulation

We consider nonlinear input-output systems of the following qLPV form:

$$\Sigma : \begin{cases} \dot{x} = A(x)x + B(x)u, \text{ with } x(0) = 0 \\ y = Cx \end{cases} \tag{1}$$

where $x(t) \in \mathbb{R}^{n_x}$, $u(t) \in \mathbb{R}^{n_u}$ and $y(t) \in \mathbb{R}^{n_y}$ are the state, input and output signals, respectively. Matrices $A(x)$ and $B(x)$ are well-defined rational matrix functions in the state x.

The storage function for the dissipativity and local stability is searched in the following general quadratic form:

$$V(x) = x^T \mathbb{Q}(x) x = \pi^T Q \pi, \quad \text{with } \pi = \Pi x \text{ and } \mathbb{Q}(x) = \Pi^T Q \Pi, \tag{2}$$

where $\pi = \pi(x) \in \mathbb{R}^m$ and $\Pi = \Pi(x) \in \mathbb{R}^{m \times n_x}$ are well-defined rational vector respectively matrix valued functions of the state, and $Q \in \mathbb{R}^{m \times m}$ is a free symmetric matrix variable. Let $\Omega_\alpha \subset R^{n_x}$ denote the $V(x) \leq \alpha$ level set of the storage function. Vector $\pi(x)$ is generated from the LFR realization of the state transition matrix $A(x)$.

III. Contributions and summary

The main contribution is based on [2] and it is related to the local stability and dissipativity of system Σ. We show that local dissipativity [6, Definition 10.7.1] (over $\mathcal{X} \subset \mathbb{R}^{n_x}$) with respect to the supply rate $s(u, v) = \gamma^2 \|u\|^2 - \|y\|^2$ implies stability and γ upper bound for the induced $\mathcal{L}_2$ norm of system Σ for all input functions satisfying a concrete energy bound. Furthermore, we present a convex LMI approach to compute a local estimate for the induced $\mathcal{L}_2$ norm of a class of nonlinear systems. The quasi-LPV dynamic equation is considered in its linear fraction representation (LFR) form. The storage function is searched in a general quadratic form with a rational state dependent symmetric matrix. The structure of the storage function is generated from the LFR realization of the state transition matrix of the qLPV system equation.

Acknowledgements

This work together with the results presented in the submitted manuscript [4] and conference paper [5] were supported by the New National Excellence Program scholarship (ÚNKP-18-3-I-PPKE-9).

References

[1] H. K. Khalil, *Nonlinear systems*. Pearson Education, Prentice Hall, 2002.
[2] A. Isidori, *Nonlinear control systems II*. London, UK, UK: Springer-Verlag London, 1999.
[3] D. F. Coutinho, M. Fu, A. Trofino, and P. Danès, "L2-gain analysis and control of uncertain nonlinear systems with bounded disturbance inputs," *International Journal of Robust and Nonlinear Control*, vol. 18, no. 1, pp. 88–110, 2008.
[4] M. C. de Oliveira and R. E. Skelton, *Perspectives in robust control*, ch. Stability tests for constrained linear systems, pp. 241–257. Springer, 2001.
[5] P. Polcz, T. Péni, B. Kulcsár, and G. Szederkényi, "Induced $\mathcal{L}_2$ gain computation for rational LPV systems using Finsler's lemma and minimal generators," Preprint submitted to *Systems & Control Letters*, 2019.
[6] P. Polcz, B. Kulcsár, T. Péni, and G. Szederkényi, "Passivity analysis of rational LPV systems using Finsler's lemma," in *IEEE 58th Conference on Decision and Control*, Regular paper submitted in March, 2019.

P. POLCZ, "Local performance estimation of nonlinear rational systems in a convex computational framework using Finsler's lemma and affine annihilators" in *PhD Proceedings – Annual Issues of the Doctoral School, Faculty of Information Technology and Bionics, Pázmány Péter Catholic University – 2019.* G. Prószéky, P. Szolgay Eds. Budapest: Pázmány University ePress, 2019, pp. 39–39. This research has been partially supported by the European Union, co-financed by the European Social Fund (EFOP-3.6.3-VEKOP-16-2017-00002).

Nearest neighbours algorithms for high bandwidth PET image reconstruction on FPGA

Levente Márk SÁNTHA
(Supervisor: Zoltán NAGY, Ákos ZARÁNDY)
Pázmány Péter Catholic University, Faculty of Information Technology and Bionics
50/a Práter street, 1083 Budapest, Hungary
santha.levente.mark@itk.ppke.hu

***Abstract*—More and more efforts are taken in the field of medical imaging to speed up the image reconstruction and also to improve the quality of the results. A typical PET (Positron Emission Tomograph) scan measurement produces more than 10 Gigabyte of raw data. These are processed offline. Without an accelerator the processing time can be quite long. Furthermore a traditional computer can not be settled next to a medical sensor, because its size is too big, weight is too heavy and power consumption is too huge comparing with an embedded solution. With FPGAs these tasks can be handled faster and with low power consumption. The FPGAs are re-configurable systems thus different type of filters, reconstruction techniques are available on the same hardware.**

***Keywords*-PET, FPGA, Nearest neighbors algorithm, Binning**

I. Introduction

PET is a nuclear medicine imaging technique that provides detailed images from organic tissues. Isotopes, such as ($C^{11}, N^{13}, O^{15}, F^{18}$), are used during the process. These materials are emitting high energy photons during their decomposition. The half-life of these isotopes are quite short ($\sim$1 - 100 minutes). During the radioactive decay two photons are released in opposite direction. (A positron is emitted from the nucleus, and after a short path, it collides with an electron. After this they are destroyed, and the photons are emitted.) The detector needles sense these photons.

Some Photons do not reach the detector, or do not travel along straightly. This makes difficulties in imaging, as we can only use pairs of photons coming directly to the detector. All photons that have different energy or come from other directions are noise and must be filtered out during imaging.

Unfortunately the detectors are far from the ideal ones, therefore the first step is to determine the source needle of every event. This is a nearest neighbour problem where the inputs of the algorithm are:

- the anger coordinates of the needles determined during calibration of the module,
- the anger coordinates of the events detected during a measurement

and the output is:

- index of the closest needle to the event, if the distance of the event is equal to two or more needles then the needle with the lowest index is returned.

II. Voronoi cell

The most straightforward solution of the previous problem is to generate the Voronoi cell map around each needle and use this to find the closest needle of every event. The Voronoi map need to be computed only once, thus a simple brute force algorithm can be used by simply running trough all the anger coordinates and all the needles.

A sensor has $400 - 1521$ needles and its index is stored on 16 bits, therefore the resulting 1024×1024 sized Voronoi map representation requires 2 MB storage for each module. In nowadays PCs this look-up-table can fit into the cache memory providing fast access.

Because of the size and power consumption a microprocessor can not attached to each sensor module, thus an alternative hardware platform is needed FPGAs has high computation power and low power usage, but on the other hand they don't have enough internal memory to store the look-up table and off-chip memories have bad performance during random access. Thus the algorithm had to be modified to fit the requirements.

III. Quad tree approach

In a hierarchical volumetric data structure two dimensional spatial data sets can be efficiently stored. This is based on quad tree data structure [1]. The shape of the Voronoi cell are stored in a quad tree for compression of the look-up-table. During the build-up of the data structure we put non-overlapping squares of the same size ($2^n \times 2^n$, $n = 5$) on the Voronoi map. If there are different indexed Voronoi cells in the elements of a rectangle we try to cover the area by dividing the square into four parts. (Figure 1.) The methodology results in a quad tree, where the search time of the tree depends only on the number of the levels of the tree.

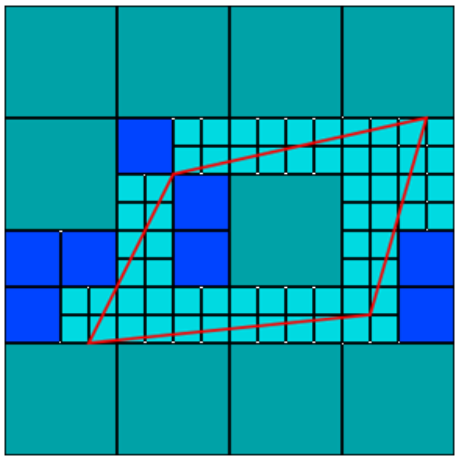

Fig. 1. Quad tree representation of a cell bounded by red line

References

[1] R. A. Finkel and J. L. Bentley, "Quad trees a data structure for retrieval on composite keys," *Acta Informatica*, vol. 4, pp. 1–9, Mar 1974.

L. SÁNTHA, "Nearest neighbours algorithms for high bandwidth PET image reconstruction on FPGA" in *PhD Proceedings – Annual Issues of the Doctoral School, Faculty of Information Technology and Bionics, Pázmány Péter Catholic University – 2019.* G. Prószéky, P. Szolgay Eds. Budapest: Pázmány University ePress, 2019, pp. 40–40. This research has been partially supported by the European Union, co-financed by the European Social Fund (EFOP-3.6.3-VEKOP-16-2017-00002).

The effects on cell attachment of surface nanostructuring of SU-8 thin films

Ágnes SZABÓ
(Supervisor: Zoltán FEKETE)
Pázmány Péter Catholic University, Faculty of Information Technology and Bionics
50/a Práter street, 1083 Budapest, Hungary
szabo.agnes@itk.ppke.hu

***Abstract*—By the implantation of neural interfaces the organism reacts to the foreign body with reactive gliosis. To reduce this negative response, the imitation of the structure of the extracellular matrix (ECM) may provide a solution to enhance the biocompatibility of neural electrodes. The aim of this study is to investigate how the cells react to various surface topography.**

***Keywords*-cell-surface interaction; nanostructuring; cell attachment**

I. Introduction

The immuneresponse of the brain tissue limits the currently used long-term central nervous system (CNS) electrodes. Both the performance of this sensors and stimulators and the integrity of the neural network are affected by this response. The activated actrocytes ultimately insulate the implants from the surrounding tissue [1]. The surrounding of the cells is the extracellular matrix, which has a an influence on attachment and also the behavior of neural cells [2]. Various groups studied the interaction between patterned surface and cells. It has been shown that the fill factor of micropillars influences cell development [3]; cells sense the depth of micro gratings [5]; the distance between a micropattern and soma of a neuron affects the neurite outgrowth [4]. Therefor the imitation of the structure of the ECM by topographical modification of the implant surface may provide a good solution.

II. Materials and Methods

SU-8 is a biocompatible epoxy-based negative photoresist, from which micrometric structures can be formed on silicon surface. SU-8 structures were patterned by standard photolithography and electron beam lithography.

On the patterned chip primer mouse actrocytes were seeded. The cultures were fixed after 24 or 48 hours. The details of the surface patterning and cell culturing are described in [6].

About the fabricated samples fluorescence microscopy images were made. Different patterns were fabricated - columns, lines and Meander. The images were taken with three channels - DAPI (nuclus), actin (structure protein), GFAP (glial specific protein).

III. Discussion

During this project, our goal is to investigate the changes in the attachment of the astrocytes in the presence of different patterns. The area, the perimeter of the cell is correlated with the attachment. Also the intensity of the different cells has information about the cell survival.

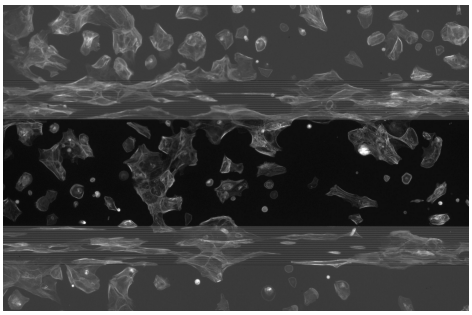

Fig. 1. Astrocytes on the fabricated SU-8 surface. Above and below the black area, parallel lines as micropatterns are located, which gives orientation of the seeded cells.

Acknowledgements

This research was supported by the National Science Foundation of Hungary (NKFIH K 120143).

References

[1] Jorfi, Mehdi, *Progress towards biocompatible intracortical microelectrodes for neural interfacing applications.* Journal of neural engineering 12.1 (2014): 011001.

[2] Piret, Gaeelle, *Support of neuronal growth over glial growth and guidance of optic nerve axons by vertical nanowire arrays.* ACS applied materials & interfaces 7.34 (2015): 18944-18948.

[3] Jeon, HoJun, *A mini-review: cell response to microscale, nanoscale, and hierarchical patterning of surface structure.* Journal of Biomedical Materials Research Part B: Applied Biomaterials 102.7 (2014): 1580-1594.

[4] Mahoney, Melissa J., *The influence of microchannels on neurite growth and architecture.* Biomaterials 26.7 (2005): 771-778.

[5] Chua, Jie Shi, *Extending neurites sense the depth of the underlying topography during neuronal differentiation and contact guidance.* Biomaterials 35.27 (2014): 7750-7761.

[6] Pongrácz, Anita, *Modification of Glial Attachment by Surface Nanostructuring of SU-8 Thin Films.* Multidisciplinary Digital Publishing Institute Proceedings. Vol. 2. No. 13. 2018.

Á. SZABÓ, "The effects on cell attachment of surface nanostructuring of SU-8 thin films" in *PhD Proceedings – Annual Issues of the Doctoral School, Faculty of Information Technology and Bionics, Pázmány Péter Catholic University – 2019.* G. Prószéky, P. Szolgay Eds. Budapest: Pázmány University ePress, 2019, pp. 41–41. This research has been partially supported by the European Union, co-financed by the European Social Fund (EFOP-3.6.3-VEKOP-16-2017-00002).

Reachability Analysis of Subconservative Reaction Networks

Gergely SZLOBODNYIK
(Supervisor: Gábor SZEDERKÉNYI)
Pázmány Péter Catholic University, Faculty of Information Technology and Bionics
50/a Práter street, 1083 Budapest, Hungary
szlobodnyik.gergely@itk.ppke.hu

***Abstract*—A computational solution is presented for the reachability problem of discrete state chemical reaction networks (d-CRNs), namely whether there exists a valid state transition (reaction) sequence between a prescribed pair of an initial and a target state. Considering the class of subconservative reaction network structures, the reachable set of a d-CRN can be characterized with well-defined simplexes. Upper bounds can also be derived for the possible length of cycle-free state transition sequences. We show that the reachability problem in the case of subconservative d-CRNs can be decided in the form an integer programming feasibility problem of well-decoupled time complexity. The proposed computational model is also employed for determining feasible series of reactions between given (sets of) states. Our findings are illustrated on a discrete state compartmental epidemiological model obeying conservation laws.**

This paper presents the results of [1,2] and can be considered as a brief summary of them.

***Keywords*-Discrete state reaction networks, reachability analysis, integer programming feasibility**

I. Summary

Assuming homogeneous mixing and large population size the dynamics of several biochemically motivated compartmental system can be described by means of continuous differential equation systems. However, if the population size is low, then a deterministic continuous differential equation based modeling approach does not give us satisfactory description of the qualitative dynamical behavior of the underlying system. In this case it becomes important to find an other mathematical representation capable of keeping truck the counts of individuals in different compartments. Discrete state models can be easily introduced so that the state variables correspond to the integer counts of individuals. In order to characterize the dynamical behavior of such a system discrete state continuous time Markov chain models are commonly introduced [3]. It has been shown that considering infinite volume limit, i.e. if the population size converges to infinity, the expected value of a continuous time Markov chain-based discrete state system is a deterministic continuous system on finite time intervals [3]. However, it is known that the long-term qualitative dynamical behavior of the continuous and discrete state models could be substantially different [3]. Hence it becomes important to examine the differences between the qualitative dynamical behavior of the two mentioned models with the same parametrization. It can be done through the so-called reachability analysis of the discrete state model, namely given a pair of initial and target states, decide whether it is possible to reach the target state from the prescribed initial one through a finite sequence of non-negative state transitions. Employing reachability analysis, one could identify anomalous states appearing in the discrete state model – such us extinctions of individuals from some compartment – that significantly differ from the qualitative dynamical behavior of the continuous system. We give a computational characterization of the reachability problem of discrete state Chemical Reaction Networks (d-CRN) [1,2]. The problem is reformulated in the form of an integer programming (feasibility) problem in order to decide the reachability and find feasible state transition sequences. The proposed computational approach relies on the discrete state equation describing the state transitions of the system. It is known that the existence of a non-negative integer solution for the state equation is a necessary condition of reachability. However, the integer program-based approach is NP-hard that highly confines our ability to examine complex systems of several compartments and transitions even in the case of additional constraints on the state transition sequences. We show how one can make use of some special structural properties of the underlying reaction network – such as conservativity laws – in order to relax the computational intractability of the problem. The results are illustrated on some well-known epidemiological models.

This paper is a brief review of the results detailed in [1,2].

References

[1] G Szlobodnyik, G Szederkényi, MD Johnston, "Reachability analaysis of subconservative discrete chemical reaction networks",MATCH Commun. Math. Comput. Chem., Vol. 81(3), pp. 705-736., 2019.

[2] G. Szlobodnyik and G. Szederkenyi, "Reachability Analysis of Low-Order Discrete State Reaction Networks Obeying Conservation Laws", Complexity, Vol. 2019, Article ID 1035974, 13 pages, 2019.

[3] D. F. Anderson, T. G. Kurtz, "Stochastic analysis of biochemical systems", Berlin Springer, 2015.

[4] H. W. Lenstra Jr., "Integer Programming with a Fixed Number of Variables", Mathematics of Operation Research, 8., 1983., 538-548.

G. SZLOBODNYIK, "Reachability Analysis of Subconservative Reaction Networks" in *PhD Proceedings – Annual Issues of the Doctoral School, Faculty of Information Technology and Bionics, Pázmány Péter Catholic University – 2019.* G. Prószéky, P. Szolgay Eds. Budapest: Pázmány University ePress, 2019, pp. 42–42. This research has been partially supported by the European Union, co-financed by the European Social Fund (EFOP-3.6.3-VEKOP-16-2017-00002).

.

PROGRAM 3
FEASIBILITY OF ELECTRONIC AND OPTICAL DEVICES, MOLECULAR AND NANOTECHNOLOGIES, NANO-ARCHITECTURES, NANOBIONIC DIAGNOSTIC AND THERAPEUTIC TOOLS

Head: Árpád CSURGAY

Implementation of neural networks in Fourier domain

András FÜLÖP
(Supervisors: András HORVÁTH, György CSABA)
Pázmány Péter Catholic University, Faculty of Information Technology and Bionics
50/a Práter street, 1083 Budapest, Hungary
fulop.andras@itk.ppke.hu

***Abstract*—Nearly 90% of computations in convolutional neural networks are the convolutions. The convolution in time domain is an element-wise multiplication in frequency domain. During my work the main project was to simulate a convolutional neural network in frequency domain, which can effectively solve machine learning tasks like image processing (classification) problems.**

***Keywords*-neural network; convolution; Fourier transform; frequency domain**

I. Introduction

The commonly used deep learning methods (deep learning has been successfully applied for example in large-scale automatic speech recognition, in natural language processing and in image processing as well) go through the same process. The algorithms apply a nonlinear transformation on inputs and use what they learn to create statistical models as outputs and the iterations continue until the outputs have reached an acceptable level of accuracy. [1] [2] [3] [4]

II. Convolutional neural networks

There are four main operations in convolutional neural network:

1) convolution
2) non-linearity (ReLU)
3) pooling (subsampling)
4) classification

III. Spectral pooling

Pooling refers to dimensionality reduction in convolutional neural networks to impose a capacity bottleneck and facilitate computation. Oren Rippel et al. introduced a new approach to pooling, the spectral pooling, which performs dimensionality reduction by projecting onto the frequency basis set and then truncating the representation. [5]

The spectral approach reduces several issues present in existing pooling strategies. For example, max pooling one major criticism is its poor preservation of information. It implies a very sharp dimensionality reduction by at least a factor of 4 every time it is applied on two-dimensional inputs. In addition, it does not utilize its capacity well to reduce approximation loss, since the maximum value in the window only reflects local information, and often does not represent well the contents of the window. [5]

In contrast, the spectral pooling preserves more information for the same number of parameters. It achieves this by utilizing the non-uniformity of typical inputs in their signal-to-noise ratio as a function of frequency. [5]

Fig. 1. Approximations for different pooling schemes, for different factors of dimensionality reduction. Spectral pooling projects onto the Fourier basis and truncates it as desired. [5]

IV. Summary

The convolution in time domain is element-wise multiplication in frequency domain, so we can use the Fourier transform in convolutional neural networks, because the 90% of computations in convolutional neural networks are the convolutions. [5]

Acknowledgements

I would like to thank my supervisors András Horváth and György Csaba for the continuous support of my work and for their expert advice. Without they precious support it would not be possible to conduct this research.

References

[1] Y. Bengio, A. C. Courville, and P. Vincent, "Unsupervised feature learning and deep learning: A review and new perspectives," *CoRR, abs/1206.5538*, vol. 1, p. 2012, 2012.
[2] Y. LeCun, Y. Bengio, and G. Hinton, "Deep learning," *nature*, vol. 521, no. 7553, p. 436, 2015.
[3] A. Krizhevsky, I. Sutskever, and G. E. Hinton, "Imagenet classification with deep convolutional neural networks," pp. 1097–1105, 2012.
[4] Y. LeCun, B. E. Boser, J. S. Denker, D. Henderson, R. E. Howard, W. E. Hubbard, and L. D. Jackel, "Handwritten digit recognition with a back-propagation network," in *Advances in neural information processing systems*, pp. 396–404, 1990.
[5] O. Rippel, J. Snoek, and R. P. Adams, "Spectral representations for convolutional neural networks," in *Advances in neural information processing systems*, pp. 2449–2457, 2015.

A. FÜLÖP, "Implementation of neural networks in Fourier domain" in *PhD Proceedings – Annual Issues of the Doctoral School, Faculty of Information Technology and Bionics, Pázmány Péter Catholic University – 2019.* G. Prószéky, P. Szolgay Eds. Budapest: Pázmány University ePress, 2019, pp. 44–44.
This research has been partially supported by the European Union, co-financed by the European Social Fund (EFOP-3.6.3-VEKOP-16-2017-00002).

A review of micromachined ultrasound transducers

Krisztián FÜZESI
(Supervisor: Miklós GYÖNGY)
Pázmány Péter Catholic University, Faculty of Information Technology and Bionics
50/a Práter street, 1083 Budapest, Hungary
fuzesi.krisztian@itk.ppke.hu

In ultrasound, employing higher frequency pulses leads to higher resolution. However, sound attenuation varies at least linearly with frequency, causing a limitation in penetration depth. There is also a significant loss of energy during the transformation between electrical and mechanical energy. For example, using a conventional PZT ultrasound transducer with 2 MHz center frequency, the signal loss could be approximated as over -100 dB assuming only 5 cm imaging depth [1]. Approximately 90 dB of this attenuation is due to the poor response of the transducer itself, with the rest being due to tissue attenuation.

Continuous development of integrated circuits and electrical components enabled the application of higher and higher frequencies in sonography as shorter (ns), and more precise high voltage (over 100 V) pulses could be emitted. For this reason, nowadays the bottleneck of ultrasound systems has become the use of conventional transducers.

Currently capacitive micromachined transducers (CMUT) dominate the field of research [2]. The second, most widespread type are piezoelectric micromachined transducers (PMUT). In some patents there are also MUTs utilizing magnetic field changes (MMUT). These three types of MUTs are presented in details below.

The CMUT arrays are built up from micromachined semiconductor cells, where in receive mode the electrodes converts sound waves into modulated capacitance and in transmit mode a capacitive charge is modulated to vibrate the membrane of the device and emit a sound wave. [2, 3]

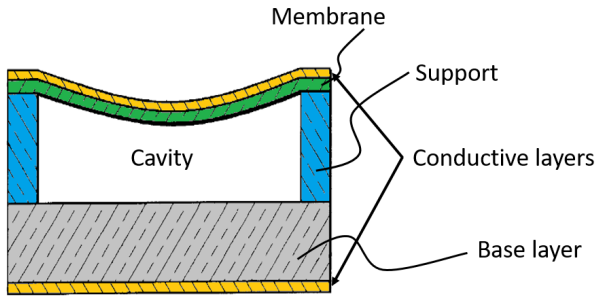

Fig. 1. Schematics of a typical CMUT cell. The figure is adopted from [3]. Base layer of the cell is made of silicon or glass substrates, indicated with gray. An insulating support is added to the base layer which is made of silicon oxide or silicon nitride, indicated with blue. A membrane (indicated with green) is built on the support to form a dielectric cavity. The membrane is made of silicon nitride and the cavity could be filled with air or gas or (as the most usual solution) be evacuated. On the top and bottom, a conductive film made of e.g. gold or platinum is formed (indicated with yellow). These two electrodes are separated with the cavity to form a capacitance. A change in capacitance cause the membrane to vibrate, and inversely, as an incoming wave vibrates the membrane, the capacitance is changing what could be detected.

Since the small size of CMUTs, it is desirable to have as good electromechanical coupling and sensitivity as for conventional transducers. In CMUTs, considering conventional mode the highest sensitivity could be achieved, when the membrane is distended, in other words, when the conductive layers are as close as possible (which means distance in the order of a micron or less). Thus, CMUTs are usually operating with a bias voltage (or charge), which must be carefully controlled to maintain high sensitivity, but avoiding short-circuiting the transducer itself or non quadratic behavior. [3]

Typical sensitivity of a CMUT can be comparable to (300 nV/Pa [4]) that of PZT based resonators (225 nV/Pa [1]). The electromechanical coupling in CMUTs is a function of the applied bias voltage. When reaching the collapse point of a CMUT, the electromechanical coupling approaches unity. In contrast, in a PZT based resonator has a coupling factor <0.55 [5].

Q number, and thereof -6 dB fractional bandwidth of CMUTs could vary greatly; one of the lowest value reported is 20% [4], while Sawaby et al. [6] reported 130%.

Due to increased coupling and good sensitivity CMUTs can have lower energy consumption than conventional transducers, which could be a key advantage and anticipate a break-through of the segment of portable ultrasound devices. However, it is important to note that similar to conventional transucers, higher voltage is needed (over 100V) to maintain required bias voltage. [2, 7]

References

[1] H.-Y. Tang, *Interface Electronics for Ultrasonic Transducers*. PhD thesis, UC Berkeley, 2016.

[2] K. Brenner and et. al., "Advances in capacitive micromachined ultrasonic transducers," *Micromachines*, vol. 10, p. 152, Feb 2019.

[3] J. D. Fraser, "Capacitive micromachined ultrasonic transducers," Sept. 3 2002. US Patent 6,443,901.

[4] T. L. Christiansen and et. al., "3-d imaging using row–column-addressed arrays with integrated apodization—part ii: Transducer fabrication and experimental results," *IEEE transactions on ultrasonics, ferroelectrics, and frequency control*, vol. 62, no. 5, pp. 959–971, 2015.

[5] X. Jiang and et. al., "Monolithic ultrasound fingerprint sensor," *Microsystems & Nanoengineering*, vol. 3, p. 17059, 2017.

[6] A. Sawaby and et. al., "A wireless implantable ultrasound array receiver for thermoacoustic imaging," in *2018 IEEE Symposium on VLSI Circuits*, pp. 189–190, IEEE, 2018.

[7] A. D. Leone, D. U. Ghisu, and F. Quaglia, "Reception and transmission circuit for a capacitive micromachined ultrasonic transducer," Mar. 17 2016. US Patent App. 14/750,312.

K. FÜZESI, "A review of micromachined ultrasound transducers" in *PhD Proceedings – Annual Issues of the Doctoral School, Faculty of Information Technology and Bionics, Pázmány Péter Catholic University – 2019.* G. Prószéky, P. Szolgay Eds. Budapest: Pázmány University ePress, 2019, pp. 45–45. This research has been partially supported by the European Union, co-financed by the European Social Fund (EFOP-3.6.3-VEKOP-16-2017-00002).

A Review of Super-Resolution Techniques on Computed Tomography images

Janka HATVANI
(Supervisor: Miklós GYÖNGY)
Pázmány Péter Catholic University, Faculty of Information Technology and Bionics
50/a Práter street, 1083 Budapest, Hungary
hatvani.janka@itk.ppke.hu

***Abstract*—Computed tomography is one of the most common medical imaging techniques. A higher radiation dose is necessary for obtaining images of better signal-to-noise ratio, increased resolution and less artifacts, but will on the other hand expose the patient to a higher risk for health. This means that post-processing algorithms improving the quality of the obtained images would be advantageous for giving better diagnosis with a low radiation dose. This article investigates such post-processing super-resolution algorithms, including iterative sparsity-based optimization techniques, tensor factorization and deep-learning.**

***Keywords*-limited angle CT, iterative techniques**

I. Introduction

Computed tomography (CT) is a wide-spread diagnostic imaging tool for mapping the 4D structure of the body. However, it has alarming carcinogenic potential. Thus, decreasing the dose of the ionizing radiation would be beneficial for making this diagnostic tool safer. Post-processing single image super-resolution algorithms (SISR) have the advantage of increasing the image quality without changing the hardware. Large size of 3D images require increased computational capacity, demanding new calculation methods. In this paper some commonly used SISR algorithms are introduced, namely regularizations using alternating direction method of multipliers (ADMM), tensor factorization (TF) based methods, and convolutional neural networks (CNNs).

II. SISR algorithms

The ground truth of CT images can be estimated with a micro-CT (μCT) scan, giving a sufficient resolution, but can be used only *ex vivo*. A tooth extracted for health reasons can be imaged in HR μCT and the LR dental cone beam CT (CBCT) too. In the image degradation model for SISR methods the HR image $\boldsymbol{X} \in \mathbb{R}^{I\times J\times K}$ is corrupted by a decimation operator D with rate r, a blurring kernel H, and some added noise $\boldsymbol{N}$, resulting in the LR image $\boldsymbol{Y} \in \mathbb{R}^{I/r\times J/r\times K/r}$ such that

$$\overline{\boldsymbol{Y}} = DH\overline{\boldsymbol{X}} + \overline{\boldsymbol{N}} \tag{1}$$

The above degradation model can be extended by some regularizers based on prior information. With ADMM this constrained problem can be transformed into a series of unconstrained subproblems [1], which will be minimized alternating between the split variables. The obvious bottleneck of this technique is the size of the image: matrix H can be extremely large in real-life scenarios, especially in the 3D case.

One advantage of TF is that it does not need to unfold the image of interest into a 2D matrix as in the above mentioned method. As a consequence, this method avoids any loss of information about the locality of the image pixels. On the other hand, the size of matrices during calculation will remain small, leading to a fast solution. The idea is to decompose the image of interest using its canonical polyadic decomposition (CPD). [2] This factorization will simplify complex operations, such that the memory requirement of the algorithm can be kept low.

In a CNN the connections between layers realize convolutions (its outputs are the features), making these structures shift-invariant. [3] After training the learned features will be extracted from the LR image, and using a non-linear mapping the HR image will be reconstructed. In biomedical imaging the main challenge is the collection of data for sufficient training. In our work 2D axial slices of the 3D volume were enhanced this way and afterwards the 3D volume was rebuilt for analyzis. [4]

III. Discussion

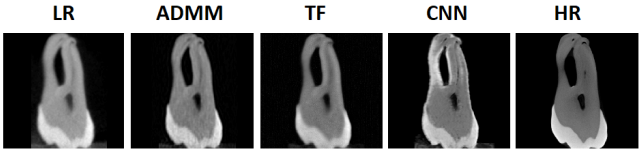

Fig. 1. Effect of the different algorithms on the CBCT (LR) coronal slice of an inferior molar tooth. The picture was scaled to the size of the HR image.

Examining the images in Fig. 1 it can be seen that all methods give an output with higher contrast and better defined cavities. The ADMM solution has piece-wise constant regions and enlarged cavities. The CNN gave the sharpest edges but it is vertically stripy, the outer edges of the teeth are lighter and jagged. The TF method is closest to the HR image. The ADMM is the slowest (5 hr runtime), followed by deep learning (3 days training but 75 s inference). The TF algorith only took 151 s (10 iterations), making it in this sense the most promising of all three algorithms.

References

[1] F. Shi, J. Cheng, L. Wang, P.-T. Yap, and D. Shen, "LRTV: MR image super-resolution with low-rank and total variation regularizations," vol. 34, no. 12, pp. 2459–2466, 2015.

[2] L. Chiantini and G. Ottaviani, "On generic identifiability of 3-tensors of small rank," *SIAM Journal on Matrix Analysis and Applications*, vol. 33, no. 3, pp. 1018–1037, 2012.

[3] C. Dong, C. C. Loy, K. He, and X. Tang, "Learning a deep convolutional network for image super-resolution," in *Proc. 13th European Conf. Computer Vision (ECCV)*. Zurich, Switzerland: Springer, Sep. 6–12, 2014, pp. 184–199.

[4] J. Hatvani, A. Horvath, J. Michetti, A. Basarab, D. Kouame, and M. Gyongy, "Deep learning-based super-resolution applied to dental computed tomography," *IEEE Transactions on Radiation and Plasma Medical Sciences*, pp. 1–1, 2018, in Press.

J. HATVANI, "A Review of Super-Resolution Techniques on Computed Tomography Images" in *PhD Proceedings – Annual Issues of the Doctoral School, Faculty of Information Technology and Bionics, Pázmány Péter Catholic University – 2019.* G. Prószéky, P. Szolgay Eds. Budapest: Pázmány University ePress, 2019, pp. 46–46. This research has been partially supported by the European Union, co-financed by the European Social Fund (EFOP-3.6.3-VEKOP-16-2017-00002).

Review of detection and segmentation methods on ultrasound images

Péter MAROSÁN
(Supervisor: Miklós GYÖNGY PhD)
Pázmány Péter Catholic University, Faculty of Information Technology and Bionics
50/a Práter street, 1083 Budapest, Hungary
marosan.peter@itk.ppke.hu

***Abstract*—Ultrasound imaging is a widely-used diagnostic modality in medicine. Computer-aided detection and segmentation (CADS) techniques give reliable support for experts, due to the ever growing quality of images and the exponentially growing computational capacity of processors. Ultrasound imaging-based segmentation of a region of interest (ROI) is frequently accomplished by a two-step framework. While the first step of the framework stands for the coarse localization of the ROI, the second step extracts the fine boundary of the required feature. The work describes the detailed process flow of this two-step framework and reviews the most relevant detection and segmentation techniques, grouping them by their applicability in the process flow.**

***Keywords*-ultrasound; computer vision; automated; detection; segmentation**

I. Introduction

Ultrasound-based imaging has become an essential medical diagnostic modality in the last decades. Similarly to other imaging modalities, CADS techniques play an important role in ultrasound-based examinations too. Automated detection and segmentation methods can aid surgery planing, but they can also help tissue classification tasks by providing accurate boundary delimitation of the ROI with valuable knowledge about the shape of lesions.

II. General pipeline for detection and segmentation

The pure detection and segmentation pipeline stands from two main steps, such as the coarse region localization and the fine boundary delimitation. It has to be declared that ultrasound segmentation techniques are commonly applied on pre-processed images, so noise filtering or image enhancement are also permanent steps of the process flow. The final step of the framework is usually the evaluation of the results. Figure 1. illustrates the steps by a certain example of the left ventricle.

III. Review of techniques

Segmentation techniques can be grouped based on which step of the main pipeline is their primary application field. By this division, one can determine three groups of techniques, such as the ones, which are performing on coarse region detection, approaches for fine boundary delimitation and universal ones, which can give an effective solution for both issues. The collection of these techniques is remarkably bases on the review articles of Noble et al. [1] and Meiburger et al. [2].

A. Coarse region detection

Coarse region detection techniques are commonly robust for different imaging devices, parameters, noise or artefacts; but not necessarily accurate and precise. Typical methods for region detection are superpixel or patch-based techniques, texture-based approaches or data-mining.

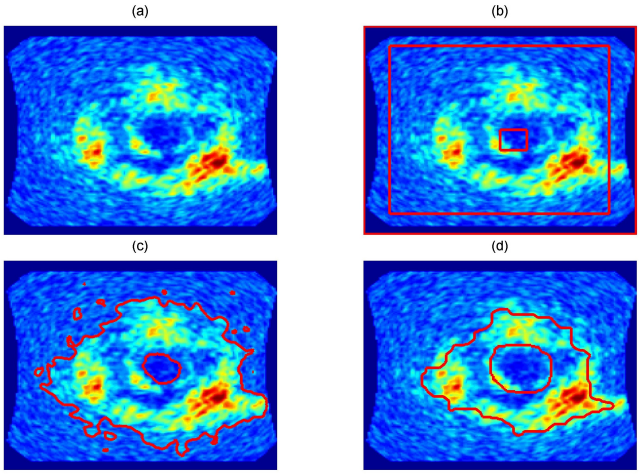

Fig. 1. Illustration of the general lesion detection and segmentation pipeline; (a) Ultrasound record of left ventricle. (b) Initial rough detection (c) Intermediate step (d) Boundary refinement.

B. Fine boundary delimitation

Boundary refinement related methods usually work with pre-defined lesion seeds, extracted automatically or with human interaction. Due to their primary application field, this kind of techniques do not require significant robustness against noise or other kind of artefacts, they can focus on accurate boundary refinement. Fine boundary segmentation can be achieved by applying active contour model-based techniques, edge-tracking & gradient based methods or optimization techniques for instance.

C. Universal approaches

Previously, all the techniques were presented, which can perform well on coarse region localization or boundary refinement, but not on both tasks. At the same time, some techniques can be applied efficiently on all steps of the framework or they can even fuse the different steps into a single one. Shape priors, local statisticspixel intensity-based techniques, transform-basedmodeling or Neural Networks and Deep Learning approaches belong to this group.

References

[1] A. Noble and D. Boukerroui, "Ultrasound image segmentation: a survey," *IEEE Transactions on Medical Imaging*, vol. 25, pp. 987–1010, aug 2006.
[2] K. M. Meiburger, U. R. Acharya, and F. Molinari, "Automated localization and segmentation techniques for B-mode ultrasound images: A review," *Computers in Biology and Medicine*, vol. 92, pp. 210–235, jan 2018.

P. MAROSÁN, "Review of detection and segmentation methods on ultrasound images" in *PhD Proceedings – Annual Issues of the Doctoral School, Faculty of Information Technology and Bionics, Pázmány Péter Catholic University – 2019.* G. Prószéky, P. Szolgay Eds. Budapest: Pázmány University ePress, 2019, pp. 47–47. This research has been partially supported by the European Union, co-financed by the European Social Fund (EFOP-3.6.3-VEKOP-16-2017-00002).

In vivo and in vitro representation of sharp wave-ripple associated dendritic signals

Zsolt MEZRICZKY
(Supervisor: Balázs RÓZSA)
Pázmány Péter Catholic University, Faculty of Information Technology and Bionics
50/a Práter street, 1083 Budapest, Hungary
mezriczky.zsolt@itk.ppke.hu

Hippocampus is the key brain region in memory processes. The local field potentials from the hippocampus indicate different physiological states. Sharp wave-ripples (SPW-Rs) appear during slow wave sleep and consummatory behaviour and have an important role in memory formation and consolidation [1]. They also participate in navigation: SPW-R activity can be detected at decision making and replay of the spatial map [2]. SPW-R resulted by well synchronized activity of pyramidal cells and interneurons, as cell assemblies [3].

These oscillatory events can be associated with various dendritic activities. My colleagues previously proved the presence of SPW-R associated dendritic signals on parvalbumin (PV) containing interneurons with two-photon microscopy in vitro. Regenerative Ca2+ spikes appear on the apical dendrites of PV neurons in the CA1 region of hippocampus during SPW-Rs. These dendritic spikes (dSpikes) can be separated from back propagating action potentials (bAPs) based on somatic activity. These dSpikes originate from dendritic hot spots and spread out in the lateral dendritic zones and are initiated independently from the soma, unlike bAPs, that originate from the soma. The important role of L-type Ca2+ channels were also described in the mediation of dSpikes [4].

In vitro measurements have some limitations in the case of dendritic measurements. Because of the morphology of their dendrites, PV interneurons in the hippocampus are easily damaged during slicing, therefore the measurement of the basal dendrites is problematic. We are able to measure the basal dendrites in situ in awake animals with two photon microscopy. However, two-photon three-dimensional acousto-optical measurements allow us to measure many cells in high volume or the whole dendritic arborization of a single neuron with fast scanning methods [5].

The SPW-R associated dendritic spikes in the hippocampus were not previously investigated in vivo. Our technical apparatus with electrophysiological recording allows us to investigate the dendritic signals during SPW-R oscillation. To prove our hypothesis, in vitro methods are also available (whole-cell patch clamp recording). The following questions arise: Do we find evidence about dSpikes in the basal dendrites of PV neurons in the hippocampus? Can we separate the dendritic signals in basal dendrites? Do the regenerative events show correlation with SPW-R? Which ion channels are responsible for the Ca2+ responses on dendrites?

In this work we used in vivo methods to demonstrate different dendritic signals during SPW-Rs in awake mice. Using two-photon acousto-optical microscopy we separated the bAPs from the dSpikes in awake mice. We found correlation between the SPW-Rs and dSpikes in vivo. I found an in vitro method to separate dSpikes from bAPs using a patch clamp recording

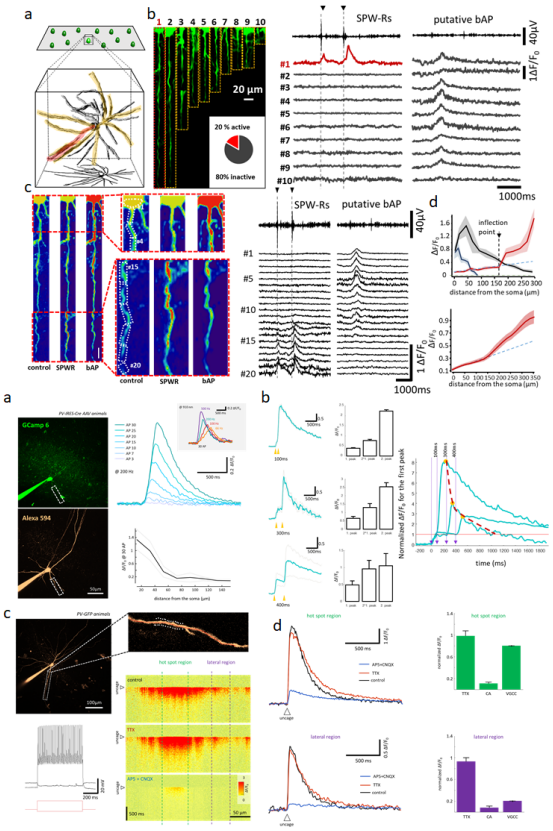

and glutamate uncaging technique and proved the role of the voltage gated Ca2+ channels in the case of dSpikes in vitro.

Acknowledgements

I would like to thank for the help of Balázs Chiovini, Dénes Pálfi, Gábor Juhász and Linda Sulcz-Judák in my work.

References

[1] Buzsaki G. Hippocampal sharp wave-ripple: A cognitive biomarker for episodic memory and planning. Hippocampus. 2015 Oct;25(10):1073-188.

[2] O'Neill J, Pleydell-Bouverie B, Dupret D, Csicsvari J. Play it again: reactivation of waking experience and memory. Trends Neurosci. 2010 May;33(5):220-9

[3] Buszaki G.Neural syntax: Cell assembles, synassambles and readers Neuron. 2010 Nov 4;68(3):362-85.

[4] 4. Chiovini B, Turi GF, Katona G, Kaszás A, Pálfi D, Maák P, Szalay G, Szabó MF, Szabo G, Szadai Z, Káli S, Rózsa B. Dendritic spikes induce ripples in parvalbumin interneurons during hippocampal sharp waves. 2014. Neuron. 82(4):908-24

[5] 5. Szalay G, Judák L, Katona G, Ócsai K, Juhász G, Veress M, Szadai Z, Fehér A, Tompa T, Chiovini B, Maák P, Rózsa B. Fast 3D Imaging of Spine, Dendritic, and Neuronal Assemblies in Behaving Animals. 2016. Neuron. 92 (4): 723-738

Zs. MEZRICZKY, "In vivo and in vitro representation of sharpwave-ripple associated dendritic signals" in *PhD Proceedings – Annual Issues of the Doctoral School, Faculty of Information Technology and Bionics, Pázmány Péter Catholic University – 2019.* G. Prószéky, P. Szolgay Eds. Budapest: Pázmány University ePress, 2019, pp. 48–48. This research has been partially supported by the European Union, co-financed by the European Social Fund (EFOP-3.6.3-VEKOP-16-2017-00002).

3D two-photon imaging of putative visual cortical functional modules

Zsófia VARGA-MEDVECZKY
(Supervisor: Balázs RÓZSA)
Pázmány Péter Catholic University, Faculty of Information Technology and Bionics
50/a Práter street, 1083 Budapest, Hungary
zsofia.varga-medveczky@itk.ppke.hu

***Keywords*-bundle; dendritic bundle; apical dendrite; visual cortex; two-photon miroscopy**

I. Introduction

Structural and functional evidence suggests that the nervous system is organized in a modular fashion. It is supposed that, at least at the structural level, the fundamental unit of the cortical organization is a group of interconnected neurons that share a certain set of properties and extend vertically through the cortical layers to form a column. These cortical columns are sometimes referred to as modules [1].

On a developmental basis, nearby pyramidal cells in the cortex send their apical dendrites to the upper layers in groups [2]. The groups of dendrites that emerge together are called bundles. The dendritic bundles consist of 5-10 apical dendrites of pyramidal cells and their cell bodies which are located in the deep layers (layer V-VI). These structural units are most easily imaged in layers III and IV but with proper methods the dendritic bundles could also be identified in layer II. The definition of the limits of a dendritic bundle raises a number of methodological issues. Depending on the sensitivity and resolution of the used technique, bundles can vary in the number and size of the constituent dendrites [3] [4].

Dendritic bundles could be easily found across the cortical areas, such as primary visual cortex, somatosensory and motor cortex. These structural units have been investigated in detail in the cerebral cortex of many different mammalian species, including mouse, rat, monkey and human also. It is reported that in the visual cortex, the mean spacing between modules was found to be 60 μm in the rat, 56 μm in the cat and 23 μm in the rhesus monkey. Bundles are clearly visible with two-photon microscopy in vivo. The fluorescent labeling enables the visualization from the deep layers to the surface [3] [4].

Functional properties of the cells in different visual cortical layers are characterized, but their important input units the dendrites forming bundles, due to technical obstacles are much less well known. Using the latest developed scanning methods in the Rózsa Laboratory, we have the opportunity to functionally image those bundles in awake behaving animals engaged in a visual task. The work promises to reveal relations between the functional properties of units forming bundles in the primary visual cortex, but also may shed light on the computational intricacies of this important input device of the visual cortex. We intend to be among the first research groups to be able to image the full length of the apical dendrites and compare the activities of the grouped units.

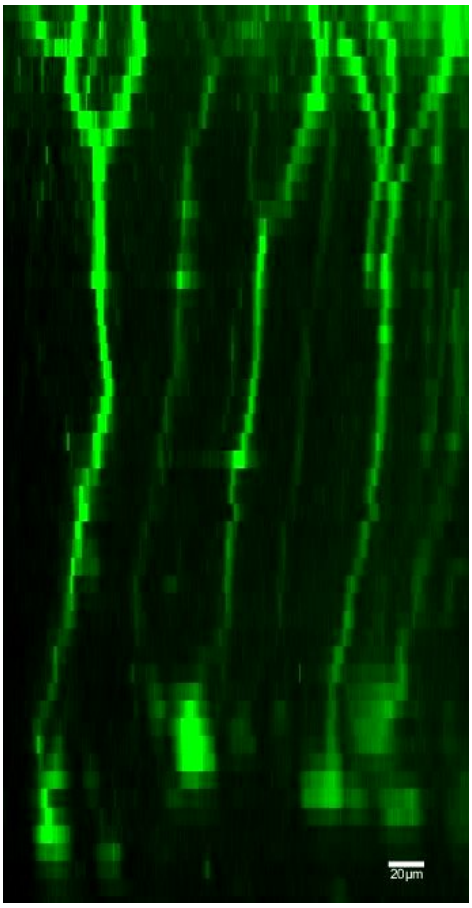

Fig. 1. Two-photon image from the primary visual cortex showing fluorescent pyramidal cells with bundling apical dendrites

References

[1] V. B. Mountcastle, "The organization of the neocortex," *Brain*, 1997.

[2] P. Rakic, "Specification of cerebral cortical areas," *Science*, 1988.

[3] G. M. Innocenti and A. Vercelli, "Dendritic bundles, minicolumns, columns, and cortical outputunits," *Frontiers in Neuroanatomy*, 2010.

[4] P. Krieger, T. Kuner, and B. Sakmann, "Synaptic connectons betweeen layer 5b pyramidal neurons in mouse somatosensory cortex are independent o apical dendrite bundling," *The Journal of Neuroscience*, 2007.

Zs. VARGA-MEDVECZKY, "3D two-photon imaging of putative visual cortical functional modules" in *PhD Proceedings – Annual Issues of the Doctoral School, Faculty of Information Technology and Bionics, Pázmány Péter Catholic University – 2019.* G. Prószéky, P. Szolgay Eds. Budapest: Pázmány University ePress, 2019, pp. 49–49. This research has been partially supported by the European Union, co-financed by the European Social Fund (EFOP-3.6.3-VEKOP-16-2017-00002).

.

PROGRAM 4
HUMAN LANGUAGE TECHNOLOGIES, ARTIFICIAL UNDERSTANDING, TELEPRESENCE, COMMUNICATION

Head: Gábor PRÓSZÉKY

Prominent color detection in images via hierarchical color aggregation

András GELENCSÉR
(Supervisors: Kristóf KARACS, Péter SZOLGAY)
Pázmány Péter Catholic University, Faculty of Information Technology and Bionics
50/a Práter street, 1083 Budapest, Hungary
gelencser.andras@itk.ppke.hu

***Abstract*—Universal color recognition algorithms work differently from the human color perceptional system. The classical methods quantize all the colors of the whole image with some algorithm, and choose the color classes with the biggest population to find characteristic colors. In our case, we want to find the most significant colors for human observer. There is no warranty, that the color class with the most occurrence will draw people's attention. We propose a new method based on hierarchical grouping, called color aggregation, according to the features of the color classes which are the results of the color quantization. The proposed framework can determine good prominent color candidates.**

***Keywords*-color; prominent color; color aggregation**

I. Introduction

Colors play an important role in our everyday life, as they provide complex information on the surrounding world [**?**]. However, precise identification of colors is an ill-posed problem in image processing task. Most relevant algorithms make a naive analysis of the input pixels. If we try to find the dominant or most vibrant colors on an image, these methods can give reasonable answers; however, in some cases human observers may pick colors differently.
Our aim is to develop a method that can locate the good prominent color candidates in the input, similarly to human color vision. This kind of intelligent behavior inherently requires semantic knowledge, but even using low level visual analysis an acceptable level of accuracy can be achieved in a number of applications, which can support visually impaired people or attention modeling surveillance.

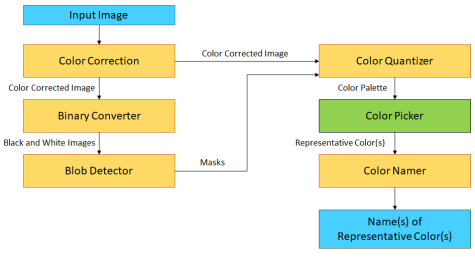

Fig. 1. Schematic representation of the proposed method.

II. Algorithm Framework

The joint operation of several algorithms is needed to find the prominent color of the input image. Figure **??** serves as the easy review of the system. We created a modular build for the various task. On the one hand we can supervise the process easier, on the other hand, since there is multiple solution for many problem class, the framework is easy to modify, improve or exchange an algorithm to a similar one.

Fig. 2. Difference between the prominent color and the dominant colors of a sample image. People will look for apples in the fruit tree, so the prominent color will be a shade of red for human observers (on the left). Image processing techniques work with color statistics and are more apt to acquire the most frequent colors of the image. Five dominant colors of the picture are shown on the right.

First we perform some Color Correction tasks to eliminate the disturbing artifacts on the image (illumination, shading, glance) and bring all image to standard daylight illumination [**?**]. Then, according to the task at hand, we process either the whole image as classical approaches do and find global color statistical information, or use only the visually interesting part of the image, determined with blob detection techniques [**?**]. The next step to reduce the color space with a color quantizer method only to a limited number of colors (Color Palette), which will represent the original pixel colors appropriately. In possession of the collected color data we define different color aggregation functions, which determine the representative colors from the features of the palette colors with various aspects. The winner prominent color candidate will be converted to text form to easily communicate verbally to the visually impaired user.

III. Conclusion

We presented a pipeline for the extraction of the prominent color of real world images with the primary goal of target aware color recognition using only statistical tools. But all aggregation functions considered so far return insensible results on some more complex inputs. Our hypotesis that the quantized color cluster features could give a clue to find better prominent color candidates, but these features depends from the input image.
We develop a basic color namer method, but it need some improvement according to the state-of-the-art, because sometimes disturbing color mismatching occurs.

References

[1] Fairchild, M D, *Color Appearance Models*, John Wiley and Sons, 2005
[2] E. Provenzi, M. Fierro, *Colour Constancy Beyond the Classical Receptive Field*, IEEE Tran. on Patt.A. And MI., 2007, vol 16., no.1, p. 162-171
[3] Radványi, M and Karacs, K, *Autonomous detection of information patterns through hierarchical peeling*, 2013 ECCTD, 2013, p. 1-4

A. GELENCSÉR, "Prominent color detection in images via hierarchical color aggregation" in *PhD Proceedings – Annual Issues of the Doctoral School, Faculty of Information Technology and Bionics, Pázmány Péter Catholic University – 2019.* G. Prószéky, P. Szolgay Eds. Budapest: Pázmány University ePress, 2019, pp. 52–52. This research has been partially supported by the European Union, co-financed by the European Social Fund (EFOP-3.6.3-VEKOP-16-2017-00002).

Increasing Agility in Learning through Better Novelty Representation

András Attila SULYOK
(Supervisors: Kristóf KARACS, Péter SZOLGAY)
Pázmány Péter Catholic University, Faculty of Information Technology and Bionics
50/a Práter street, 1083 Budapest, Hungary
sulyok.andras.attila@itk.ppke.hu

I. Introduction

In the Reinforcement Learning (RL) problem setting, the goal is to teach an agent to maximise its reward based on interactions with its environment. This framework is general enough for a number of engineering problems with an appropriate choice of reward function. The disadvantage is that there is very little information for the agent to go on: it is hard to design a reward function that matches the design goals and speeds up learning. It usually involves domain knowledge, and deceptive rewards must be avoided [1].

Therefore, most tasks are described with sparse rewards: usually zero unless the goal state is achieved, or 1 as long as the agent exhibits the desired behaviour and -1 when it does not. To aid learning and achieve more robust policies, one can encourage exploration with intrinsic rewards, similar to curiosity in humans [2].

II. Background

The environment in an RL problem is a Markov Decision Process (MDP) [3], that is, an $(\mathcal{S}, \mathcal{A}, \mathcal{P})$ triplet, where $\mathcal{S}$ is the set of states the agent can be in, $\mathcal{A}$ is the set of actions the agent can choose from and $\mathcal{P}(S_{t+1}, R_{t+1} \mid S_t, A_t)$ describes the environment dynamics, which determines the state at time $t+1$ given a state and action at time t. It also determines the reward R_{t+1} given in response to S_t and A_t. This reward, the *extrinsic reward* is simply a number, usually bounded. It represents the goal of the agent: higher reward is given to the expected behaviour.

Intrinsic reward [2] is another type of reward, which the agent calculates for itself and is used to aid or speed up the learning process.

The agent is modelled by its policy $\pi(a \mid s)$ that represents the probability for each state of choosing a specific action. The goal of the agent is to find a policy that maximises the expected cumulative reward (the return): $\mathbb{E}_{(R_{t+1})\sim\pi,\mathcal{P}}\{\sum_t R_{t+1}\}$. It is usually found using an optimisation process.

One idea is to learn the expected return for each state s and action a with an appropriate function approximator: $Q_\theta : \mathcal{S}\times\mathcal{A} \to \mathcal{R}$ with parameter vector $\theta \in \mathbb{R}^k$. This is trained by running an exploration policy (this generates the training samples), and using semi-gradient descent with a loss that minimises the difference between the Q values of successive states (Deep Q-Network algorithm).

Another approach is to represent the policy itself (π_θ), and directly perform gradient ascent on the expected return (policy gradient).

III. Exploration

The problem with learning based on the extrinsic reward alone is that it is usually sparse and contains little information as to which direction the agent should update its policy. This can be mitigated by, for example, active exploration: to visit as much of the state and action spaces as possible, in order to find the best rewards. Depending on the abstraction level of the data, one can encourage exploration in many ways.

Exploration of different actions is aided by not always choosing the optimal action, but exploring alternatives: either by explicit formulation with separate exploration policies (ϵ-greedy, Boltzmann-exploration), or adding an entropy term to the loss function of the represented policy to delay putting too much likelihood to perceived optimal actions. Exploration in action space is incremental: only small perturbations in the policy space are evaluated.

Exploration of different states is aided by adding an intrinsic reward for encountering new states; this is used in curiosity-based learning [2]. When the reward does not depend on the current state only (as it does in, for example, goal-based tasks), intrinsic reward can be based on an aggregation of the states along the trajectory, as proposed, for example, in the novelty search algorithm [1].

Explicit exploration of rewards of different trajectories is rarely formulated, but every exploration in a non-stationary environment (arising, for example, from the presence of multiple learning agents) can be thought of as exploring whether the reward the agent can achieve now is good enough or is there a better one?

But what constitutes as novel, especially in state space where the number of observed dimensions is oftentimes much higher than the actual number of free parameters of the state? A problem often emerging with rewarding novel states is the *noisy TV problem*: an agent can get an infinite supply of rewards just by staying in a state in which its observations are essentially random (for example, staying in a room with a TV displaying white noise). What we want to achieve is to, while exploring, separate the useful features of the observations from those that change meaninglessly: we want to transform the states into features that are useful for exploration (and perhaps use this feature to enhance the policy/Q model).

References

[1] J. Lehman and K. O. Stanley, "Abandoning objectives: Evolution through the search for novelty alone," *Evolutionary computation*, vol. 19, no. 2, pp. 189–223, 2011.
[2] Y. Burda, H. Edwards, A. Storkey, and O. Klimov, "Exploration by random distillation," in *Submitted to International Conference on Learning Representations*, 2019.
[3] R. S. Sutton and A. G. Barto, *Reinforcement learning: An introduction*. MIT press, 2 ed., 2018.

A. SULYOK, "Increasing Agility in Learning through Better Novelty Representation" in *PhD Proceedings – Annual Issues of the Doctoral School, Faculty of Information Technology and Bionics, Pázmány Péter Catholic University – 2019.* G. Prószéky, P. Szolgay Eds. Budapest: Pázmány University ePress, 2019, pp. 53–53. This research has been partially supported by the European Union, co-financed by the European Social Fund (EFOP-3.6.3-VEKOP-16-2017-00002).

.

PROGRAM 5
ON-BOARD ADVANCED DRIVER ASSISTANCE SYSTEMS

Heads: Csaba REKECZKY, Ákos ZARÁNDY

Incorporating topological information in loss function for image segmentation

Jalal Al-Afandi
(Supervisor: András Horváth)
Pázmány Péter Catholic University, Faculty of Information Technology and Bionics
50/a Práter street, 1083 Budapest, Hungary
alafandi.mohammad.jalal@itk.ppke.hu

***Abstract*—The rapid advancement of neural network has long reached the application of image segmentation starting with medical images until object tracking and surveillance. Beside network architecture, the size of the training dataset and parameters tuning, one of the main factor for the success of object segmentation is loss function. Comparing the ground truth with the network prediction is intrinsic for back propagation to work with gradient descent. A pixel wise loss function is usually used where the back propagation don't take the neighboring pixels into consideration and disregarding the topological information encompassed in the shape of each object. We are working on a new loss function which penalize the value and shape discrepancies of the predicted object.**

I. Introduction

Image segmentation is now well spread in the applications of machine learning. Thus, we can obtain more information than image classification or even object detection with bounding boxes. The applications of Image segmentation vary from medical images to self-driving cars. Using neural network, the algorithm depends on the selected architecture i.e SegNet, RetinaNet or U-Net, parameters tuning, selected dataset and a metric to compare the network output to the optimal, ideal ground truth.

The loss is inherently a scalar for a condensed value presenting the resemblances and the discrepancies between the High-dimensional features. Beside information compression, loss should be resilient to noisy features. Although the loss has to allow comparison, it should be robust against noise.

In current applications most of image segmentation approaches do use a pixel wise loss i.e. L1, L2, Smooth-L1[1] or cross entropy which don't take pixels position into consideration.

The loss will be zero for a perfect solution and it will increase with respect to the number of misclassified pixels. The location of the misclassified pixels should matter, a circle with 50 pixels in the middle of the object should have more penalty than a 50 individual pixels scattered all over the image. More over, misclassification in the center of the object or even far away form the object should have bigger loss than misclassification near the border of the object.

The most frequently applied metrics for image comparison are Hamming and Hausdorff distances.

Hamming distance computes the number of differing pixels between two images while Hausdorff distance is inferred solely by topological differences between the objects which is not used in practice because of its susceptibility to noisy pixels.

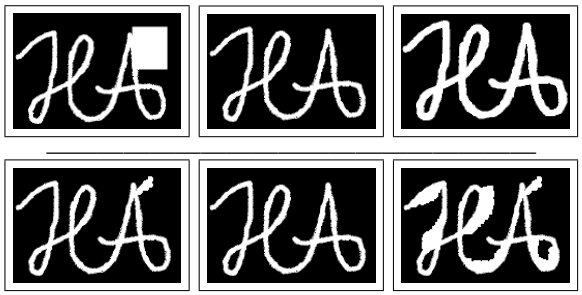

Fig. 1. The images in the first row demonstrate the contradiction between the Hamming distance and subjective human judgments while the images in the second row demonstrate the contradiction between Hausdorff distance and subjective perception

II. Wave metric

To over come the limitation of commonly used loss functions, we are working on a topological loss function which will encompass the shape of the object. The idea was inspired by [2] where We can start from the intersection with small weights and then propagate the values reaching the union. While our wave is propagating, we will increase the penalty.

References

[1] M. Schmidt, G. Fung, and R. Rosales, "Fast optimization methods for l1 regularization: A comparative study and two new approaches," in *European Conference on Machine Learning*. Springer, 2007, pp. 286–297.

[2] I. Szatmári, C. Rekeczky, and T. Roska, "A nonlinear wave metric and its cnn implementation for object classification," *Journal of VLSI signal processing systems for signal, image and video technology*, vol. 23, no. 2-3, pp. 437–447, 1999.

M. ALAFANDI, "Incorporating topological information in loss function for image segmentation" in *PhD Proceedings – Annual Issues of the Doctoral School, Faculty of Information Technology and Bionics, Pázmány Péter Catholic University – 2019.* G. Prószéky, P. Szolgay Eds. Budapest: Pázmány University ePress, 2019, pp. 56–56. This research has been partially supported by the European Union, co-financed by the European Social Fund (EFOP-3.6.3-VEKOP-16-2017-00002).

Solving K-SAT Problems with Continuous Time Neural Networks

Dóra Eszter BABICZ
(Supervisors: András HORVÁTH, Csaba REKECZKY)
Pázmány Péter Catholic University, Faculty of Information Technology and Bionics
50/a Práter street, 1083 Budapest, Hungary
babicz.dora.eszter@itk.ppke.hu

NP complete problems are efficiently (polynomial time) checkable, but the worst-case complexity of finding a solution is exponential on Turing machines [1]. Because every NP-complete problem can be transformed into a Boolean satisfiability (*k*-SAT) in polynomial time, it increases the relevance of solving these types of problems [2]. Boolean satisfiability problems are a type of constraint satisfaction problems and are considered to be one of the hardest. Converting an NP-complete problem to a Boolean satisfiability (*k*-SAT) problem - can be done in polynomial time. *k*-SAT problems contain conjunctive normal formulas of variables in which every conjunction contains *k* number of variables. It was shown in [3] that *k*-SAT problems can be solved with analogue dynamics, avoiding local traps, and also in polynomial time, but with an exponentially increasing power consumption.

The definition of the *k*-SAT problem is the following: there are given *N* Boolean variables $x_i \in \{0, 1\}$ and a propositional formula $\mathcal{F}$ which is a conjugation form of *M* constraints C_i. Each constraint is a disjunctive form of *k* variables x_i or their negations $\bar{x_i}$. Solving this kind of problem means finding an assignment of the variables where all clauses (constraints) are satisfied.

The form of the dynamics used in the circuits are very similar to regular cellular neural network dyanmics and are the following:

$$\frac{\mathrm{d}x_i(t)}{\mathrm{d}t} = -x_i(t) + \sum_j w_{ij} f(x_j(t)) + u_i \qquad (1)$$

where x_i is the state value (activation potential) of the cell, *f(x)* is the output function of the neuron (usually sigmoid), u_i is the input or bias of the neuron and w_{ij} are connection weights between cells i and j.
The Continuous-time recurrent neural network can be defined on a bipartite graph with two type of nodes/cells. One is called the "*s*-type" and represents the variables of *k*-SAT. Their state value will be denoted by s_i, *i*=1,...,*N* and the output function is defined as the following:

$$f(s_i) = \frac{1}{2}(\mid s_i + 1 \mid - \mid s_i - 1 \mid) \qquad (2)$$

The output of $f(s_i)$ = 1 is assigned to x_i Boolean variable when it is $TRUE$ (x_i = 1) and if the variable is $FALSE$ (x_i = -1), then $f(s_i)$ = -1, but between these two extrema, any continuous value is allowed, meaning *f*(s_i) $\in$ [-1,1]. The self-coupling parameter will be a fixed value w_{ii} = *A* and the input is u_i = 0 $\forall i$.
The other type of the cells represent the constraints of *k*-SAT with value a_m, *m*=1, ..., *M* and with the output function of:

$$g(a_m) = \frac{1}{2}(1 + \mid a_m \mid - \mid a_m - 1 \mid) \qquad (3)$$

The "*a*-type" cells determine the impact of a clause at a given moment on the dynamics of the state (*s*) variables. When the clause is true, then *g*(a_m) = 0 and *g*(a_m) = 1 if it is false. For these cells the self coupling w_{mm} = *B* and the input is u_m = *u* = 1 - *k* where k is the number of variables in the clause, in this case $k = 3$.

The dynamics fulfill the following requirements:

- They have continuous-time dynamics
- All states, constraints and variables remain bounded
- The derivative of the dynamics is zero if and only if the formula is satisfied
- Starting from a chosen initial condition the system converges to a solution without getting trapped

The proof of the last two points along with a more detailed description can be found in [4]. An example problem in conjunctive form is the following:

$$(\neg A_1 \vee A_2 \vee V) \wedge (A_1 \vee \neg A_2 \vee V) \wedge (A_1 \vee A_2 \vee \neg V) \wedge (\neg A_1 \vee \neg A_2 \vee \neg V) \wedge (\neg C \vee H \vee G) \wedge (D \vee H \vee F)$$

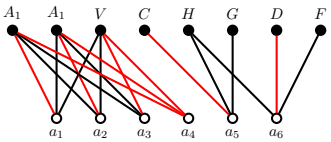

Fig. 1. Bipartite graph of the example problem

References

[1] Michael, R. Garey, and S. Johnson David. "Computers and intractability: a guide to the theory of NP-completeness." WH Freeman and Co., San Francisco (1979).
[2] Cook, Stephen A. "The complexity of theorem-proving procedures." Proceedings of the third annual ACM symposium on Theory of computing. ACM, 1971.
[3] Ercsey-Ravasz, Maria, and Zoltan Toroczkai. "Optimization hardness as transient chaos in an analog approach to constraint satisfaction." Nature Physics 7.12 (2011): 966-970.
[4] Molnar, Botond, Zoltan Toroczkai, and Maria Ercsey-Ravasz. "Continuous-time neural networks without local traps for solving Boolean satisfiability." Cellular Nanoscale Networks and Their Applications (CNNA), 2012 13th International Workshop on. IEEE, 2012.

D. BABICZ, "Solving K-SAT Problems with Continuous Time Neural Networks" in *PhD Proceedings – Annual Issues of the Doctoral School, Faculty of Information Technology and Bionics, Pázmány Péter Catholic University – 2019.* G. Prószéky, P. Szolgay Eds. Budapest: Pázmány University ePress, 2019, pp. 57–57. This research has been partially supported by the European Union, co-financed by the European Social Fund (EFOP-3.6.3-VEKOP-16-2017-00002).

Brick Segmentation in Masonry Walls by a CNN-based Watershed Algorithm

Yahya IBRAHIM
(Supervisor: Csaba BENEDEK)
Pázmány Péter Catholic University, Faculty of Information Technology and Bionics
50/a Práter street, 1083 Budapest, Hungary
ibrahim.yahya@itk.ppke.hu

***Abstract*—Artificial intelligence techniques have been increasingly used in many image-based documentations and survey applications. In archeology sites, brick segmentation is considered as an important first step in the analysis of masonry wall images. However, it is highly challenging to find a widely adoptable solution for the extreme variety of walls categories. In this paper, a new technique which combines the strength of deep learning (U-Net) for brick seed localization, and the Watershed algorithm for accurate instance segmentation is proposed, a new dataset is created for training the network and evaluating our results. The quantitative evaluation both at instance and at pixel level is provided showing the advantages of the proposed method, providing average F1-scores above 80%.**

***Keywords*-Documentation application; Brick segmentation; Deep learning; U-Net; Watershed**

I. SUMMARY

In this paper a novel image-based automated brick segmentation approach is presented, the U-Net is adopted to generate the marker for the Watershed process, which provides as output the accurate contours of the individual bricks, and also separates them from the mortar regions. We also introduce a new manually annotated dataset of many masonry images which consists of 162 hand-labeled images. Fig. 1 shows the dataflow of our approach, by showing the results of the subsequent filtering steps for an input image.

In an earlier study Riveiro et. al. [1] present an automatic color-based algorithm for segmenting masonry structures, based on an improved marker-controlled Watershed. Oses et. al. [2] use an automatic image-based delineation method for classification of built heritage masonry to determine the necessary degree of protection in different buildings. We provide the Quantitative evaluation both at an instance and at a pixel level, and the results are compared to two reference methods proposed for wall delineation in Table. I. We can confirm, that our method can detect the outlines of the bricks with high accuracy (above 80%) for any types of walls.

Further work will focus on making tests on an extended dataset, and performance comparison of different CNN architectures (like SegNet, FCN, etc.) for the problem. Another relevant research chapter may deal with wall classification, age or architectural style.

ACKNOWLEDGEMENT

This work was supported by the National Research, Development and Innovation Fund (grants NKFIA K-120233 and KH-125681), and by the Szechenyi 2020 Program (grants EFOP-3.6.2-16-2017-00013 and 3.6.3-VEKOP-16-2017-00002). Budapest, Hungary.

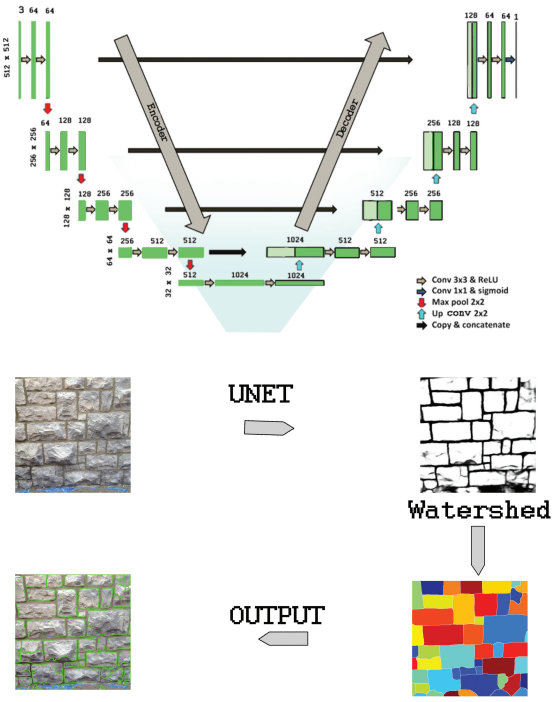

Fig. 1: Dataflow of our method: U-Net model, The Watershed output, The final output.

REFERENCES

[1] B. Riveiro, B. Conde, H. Gonzalez, P. Arias, and J. Caamaño, "Automatic creation of structural models from point cloud data: The case of masonry structures," *ISPRS Annals of Photogrammetry, Remote Sensing and Spatial Information Sciences*, vol. II-3/W5, pp. 3–9, 8 2015.

[2] N. Oses, F. Dornaika, and A. Moujahid, "Image-based delineation and classification of built heritage masonry," *Remote Sensing*, vol. 6, no. 3, p. 1863–1889, Feb 2014. [Online]. Available: http://dx.doi.org/10.3390/rs6031863

TABLE I: Evaluation of the delineation step. Comparison of state-of-the-art methods and our proposed U-Net-based approach.

Method	F1-score (%)	Precision (%)	Recall(%)
Riveiro method [1]	23.65	37.04	17.71
Oses method [2]	22.58	39.57	16.91
Proposed method	**81.57**	**81.16**	**82.14**

Y. IBRAHIM, "Brick Segmentation in Masonry Walls by a CNN-based Watershed Algorithm" in *PhD Proceedings – Annual Issues of the Doctoral School, Faculty of Information Technology and Bionics, Pázmány Péter Catholic University – 2019.* G. Prószéky, P. Szolgay Eds. Budapest: Pázmány University ePress, 2019, pp. 58–58. This research has been partially supported by the European Union, co-financed by the European Social Fund (EFOP-3.6.3-VEKOP-16-2017-00002).

Improving image quality of bone scintigraphy using artificial intelligence

Ákos KOVÁCS[1, 2]
(Supervisors: András HORVÁTH[1], Tamás BÜKKI[2])
[1]Pázmány Péter Catholic University, Faculty of Information Technology and Bionics
50/a Práter street, 1083 Budapest, Hungary
[2]Mediso Kft.
3 Laborc street, 1037 Budapest, Hungary
kovacs.akos@itk.ppke.hu

***Abstract*—Bone scintigraphy, which is a medical imaging technique, has been an important part of the diagnosis of certain disease groups for decades. Improving image quality of these measurements can help in diagnostics, and can reduce the required radiopharmacon dosage or the time requirement of the measurement.**

In the last year I have implemented multiple solution for noise reduction, lesion generation, detection and segmentation. I have experimented with various neural networks in TensorFlow and made steps for a noise filtering artificial network implementation not only for bone scintigraphy, but for SPECT as well.

***Keywords*-medical imaging; SPECT; AI; artificial intelligence; bone scintigraphy**

I. Introduction

Bone scintigraphy, which is a medical imaging technique, has been an important part of the diagnosis of certain disease groups for decades. The gamma photons from the radiopharmaceuticals in the patient's body are detected after direction filtration. The gamma detectors do not rotate, so we get only planar measurements about the radiopharmacon distribution. [1]

II. Comparison of different loss functions for medical image segmentation

One task with working bone scintigraphy measurements to segment bone structures. I have implemented several solution for this.

- Traditional method: adaptive threshold with manual corrections
- Neural network based segmentation, using:
  - L1 loss function
  - Binary cross-entropy
  - A novel loss function

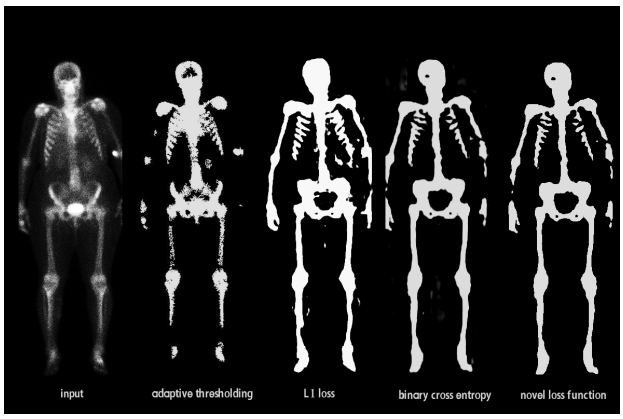

Fig. 1. Comparison of different losses for segmentation on a test image.

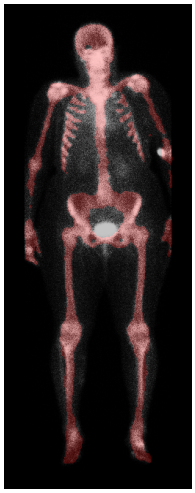

Fig. 2. Neural network's result with a novel segmentation loss function.

III. Conclusions and further plans

With using this novel loss function one can achieve better segmentation quality. The outlier false segments are disappeared. These results are promising so in the future we will segment more images manually to get a larger database for training a more precise network.

Acknowledgement

SUPPORTED BY THE ÚNKP-18-3 NEW NATIONAL EXCELLENCE PROGRAM OF THE MINISTRY OF HUMAN CAPACITIES

References

[1] M. N. Wernick and J. N. Aarsvold, *Emission Tomography: The Fundamentals of PET and SPECT*. Elsevier, Dec. 2004. Google-Books-ID: R5slur_hdfEC.

Á. KOVÁCS, "Improving image quality of bone scintigraphy using artificial intelligence" in *PhD Proceedings – Annual Issues of the Doctoral School, Faculty of Information Technology and Bionics, Pázmány Péter Catholic University – 2019.* G. Prószéky, P. Szolgay Eds. Budapest: Pázmány University ePress, 2019, pp. 59–59. This research has been partially supported by the European Union, co-financed by the European Social Fund (EFOP-3.6.3-VEKOP-16-2017-00002).

Challenges in track to track sensor fusion using neural networks

Lóránt KOVÁCS
Supervisors: Ákos ZARÁNDY, Viktor TIHANYI
Pázmány Péter Catholic University, Faculty of Information Technology and Bionics
50/a Práter street, 1083 Budapest, Hungary
kovacs.lorant@itk.ppke.hu

I. Introduction

Every object has to be known in the local neighborhood of an autonomous vehicle. The sensor fusion algorithms are responsible for this task. They construct a model of the local surroundings of the vehicle from the gathered sensor data. There are conventional approaches [1], [2], and neural network based methods [3], [4]. The performance of the different approaches have to be comparable.

II. Conventional sensor fusion

A fusion algorithm was implemented following Houenou et al., described in [1]. The description of the implementation is available in [5]. This previous paper also describe a suitable comparison metric for evaluating the fusion algorithm performance. The Multiple Object Tracking Benchmark (MOTChallenge) [6] is used for the basis of the evaluation, including the CLEAR metrics [7] and a some track quality measures introduced by Wu and Nevatia in [8].

This sets the [6] and the MOTChallenge: The Multiple Object Tracking Benchmark as a guideline for this evaluation. Two sets of measures are used in this approach: the CLEAR metrics [7], and a set of track quality measures [8]. The MOTChallenge benchmark environment is available

III. Sensor fusion using neural networks

To train a neural network, a large training dataset is required, where all the inputs have their desired output values in pair. Unfortunately, this is currently not available for my research. But, if a proper network is trained on the conventional fusion method's input and output, the robustness and the sensor dependency of the conventional and the neural approaches can be investigated.

Behind having enough relevant data for training and testing, the key issue is the *proper network*. Can it be implemented using only feed forward neurons? How many hidden layers are required? Is a fully connected network suitable for this problem? Instead of handling the fusion task independently on each frame, can the results be more accurate or even relevant if the input data is handled with the temporal correspondence existing among the consecutive measurements?

These questions are under investigation, the results are going to be published soon.

Acknowledgements

This research is supported by the *Foundation for the Hungarian Vehicle Technology Education*. The support of the Széchenyi 2020 Program, of the Human Resource Development Operational Program, of the Program of Integrated Territorial Investments in Central-Hungary and of the European Structural and Investment funds (EFOP-3.6.2-16-2017-00013, 3.6.3-VEKOP-16-2017-00002 and EFOP-3.6.2-16-2017-00002) are gratefully acknowledged. Supported by the ÚNKP-18-3-I-PPKE-122 New National Excellence Program of the Ministry of human capacities.

References

[1] A. Houenou, P. Bonnifait, V. Cherfaoui, and J. F. Boissou, "A track-to-track association method for automotive perception systems," *IEEE Intelligent Vehicles Symposium, Proceedings*, pp. 704–710, 2012.

[2] H. Cho, Y.-W. Seo, B. V. Kumar, and R. R. Rajkumar, "A multi-sensor fusion system for moving object detection and tracking in urban driving environments," in *2014 IEEE International Conference on Robotics and Automation (ICRA)*, pp. 1836–1843, IEEE, may 2014.

[3] P. Kasnesis, C. Z. Patrikakis, and I. S. Venieris, "PerceptionNet: A Deep Convolutional Neural Network for Late Sensor Fusion," in *Advances in Intelligent Systems and Computing*, vol. 868, pp. 101–119, 2019.

[4] L. Vargas-Meléndez, B. L. Boada, M. J. L. Boada, A. Gauchía, and V. Díaz, "A sensor fusion method based on an integrated neural network and Kalman Filter for vehicle roll angle estimation," *Sensors (Switzerland)*, vol. 16, no. 9, 2016.

[5] L. Kovacs, L. Lindenmaier, H. Nemeth, V. Tihanyi, and A. Zarandy, "Performance evaluation of a track to track sensor fusion algorithm," in *CNNA 2018; The 16th International Workshop on Cellular Nanoscale Networks and their Applications*, pp. 1–2, Aug 2018.

[6] A. Milan, L. Leal-Taixe, I. Reid, S. Roth, and K. Schindler, "MOT16: A Benchmark for Multi-Object Tracking," pp. 1–12, mar 2016.

[7] R. Stiefelhagen, K. Bernardin, R. Bowers, R. T. Rose, M. Michel, and J. Garofolo, "The CLEAR 2007 Evaluation," in *Multimodal Technologies for Perception of Humans*, vol. 4625 LNCS, pp. 3–34, Berlin, Heidelberg: Springer Berlin Heidelberg, 2008.

[8] Bo Wu and R. Nevatia, "Tracking of Multiple, Partially Occluded Humans based on Static Body Part Detection," in *2006 IEEE Computer Society Conference on Computer Vision and Pattern Recognition - Volume 1 (CVPR'06)*, vol. 1, pp. 951–958, IEEE, 2006.

L. KOVÁCS, "Challenges in track to track sensor fusion using neural networks" in *PhD Proceedings – Annual Issues of the Doctoral School, Faculty of Information Technology and Bionics, Pázmány Péter Catholic University – 2019.* G. Prószéky, P. Szolgay Eds. Budapest: Pázmány University ePress, 2019, pp. 60–60. This research has been partially supported by the European Union, co-financed by the European Social Fund (EFOP-3.6.3-VEKOP-16-2017-00002).

Online Targetless Camera-LIDAR calibration

.

Balázs NAGY
(Supervisor: Csaba BENEDEK)
Pázmány Péter Catholic University, Faculty of Information Technology and Bionics
50/a Práter street, 1083 Budapest, Hungary
nagy.balazs@itk.ppke.hu

***Abstract*—In this paper we propose an end-to-end, automatic camera-Lidar calibration approach for self driving vehicle navigation. The main idea is to moving from the image domain to the 3D space by generating a point cloud using a structure from motion (SFM) pipeline. As a core step of the algorithm we introduce an object level alignment to transform the point clouds into a common coordinate system. Finally, based on the SFM pipeline and the result of the point cloud alignment we calculate the correspondence between the image domain and the 3D Lidar point cloud.**

***Keywords*-calibration; LIDAR; point cloud; camera**

I. Introduction

State of the art autonomous systems [1] equipped with 3D Lidar and high resolution cameras perceive accurate visual information from the scene. While Lidar sensors provide strong 3D geometric information and they are not limited by the lighting conditions, high resolution cameras extract color and texture information to complete the recorded data.

However, accurate Lidar and camera calibration is essential for robust data fusion, so sensor fusion and calibration are one of the most studied fields in autonomous driving related computer vision. Though several Lidar-camera calibration approaches exist in the literature, however the process of these calibration steps are often very complex, cumbersome and usually they are also very time consuming.

A. Related works

In the literature we can distinguish target based and target less calibration techniques. [3] detects holes on planar object, [2] uses one Lidar-image pair with multiple chessboards. However target based calibration methods are time consuming, because of the complex setups requiring that the calibration objects must be seen concurrently by the Lidar and the camera from different views. Target less approaches extract some features, lines or planars [4] from the raw image and the point cloud data without any target objects to to find correspondences between the different domains.

II. The proposed approach

To avoid feature (SIFT, line and planar segments) detection from very different domains we modify a state-of-the-art SFM pipeline to generate point clouds from the image sequences recorded by the moving vehicle and we perform an object level alignment between the Lidar and the generated point clouds. During the SFM pipeline we calculate transformation T_1 which projects the points of the generated point cloud onto the corresponding image pixels. In the next step we align the point clouds in object level [5] and we estimate a transformation T_2 which transform the Lidar point cloud to the coordinate system of the generated one. At this stage we can project the points of the Lidar point cloud directly onto the image domain using transformation T_1 and we save the mapping between the corresponding 3D points and the 2D pixel coordinates. Finally, using T_2 inverse we transform back the Lidar point cloud to the original position and using the saved 2D-3D mapping information we calculate transformation T_3 which is able to project the original Lidar point cloud directly onto the 2D image domain.

(a) Prop. fully aut. targetless approach. (b) Semi aut. target based approach.

Fig. 1. Qualitative comparison of the proposed online LIDAR-camera self-calibration approach and a state-of-the-art offline calibration algorithm.

III. Conclusion

This paper proposed a targetless camera-LIDAR sensor self-calibration approach using 2D-3D data fusion, that can be performed on the fly, and updated periodically during the data capturing process, thus eliminating the need of lengthy offline sensor calibrations.

IV. Acknowledgment

This work was supported by the National Research, Development and Innovation Fund (grants NKFIA K-120233 and KH-125681), and by the Széchenyi 2020 Program (grants EFOP-3.6.2-16-2017-00013 and 3.6.3-VEKOP-16-2017-00002). Balázs Nagy was also supported by the ÚNKP-18-3 New National Excellence Program of the Ministry of Human Capacities.

References

[1] D. L. Rosenband, *Inside Waymo's self-driving car: My favorite transistors*, Symposium on VLSI Circuits, 20-22, 2017.
[2] Andreas Geiger, Frank Moosmann, Omer Car, Bernhard Schuster, *Automatic camera and range sensor calibration using a single shot*, IEEE International Conference on Robotics and Automation, 3936-3943, 2012.
[3] Martin Velas, Michal Spanel, Zdenek Materna, Adam Herout, *Calibration of RGB Camera With Velodyne LiDAR*, 2014.
[4] Davide Scaramuzza, Ahad Harati, Roland Siegwart, *Extrinsic self calibration of a camera and a 3D laser range finder from natural scenes*, IEEE/RSJ International Conference on Intelligent Robots and Systems, 4164-4169, 2007.
[5] B. Nagy, C. Benedek, *Real-time point cloud alignment for vehicle localization in a high resolution 3D map*, Workshop on Computer Vision for Road Scene Understanding and Autonomous Driving (ECCV), 2018.

B. NAGY, "Online Targetless Camera-LIDAR calibration" in *PhD Proceedings – Annual Issues of the Doctoral School, Faculty of Information Technology and Bionics, Pázmány Péter Catholic University – 2019.* G. Prószéky, P. Szolgay Eds. Budapest: Pázmány University ePress, 2019, pp. 61–61. This research has been partially supported by the European Union, co-financed by the European Social Fund (EFOP-3.6.3-VEKOP-16-2017-00002).

Adversarial Attack Resilience of Neural Networks

Franciska Sára RAJKI
(Supervisor: András HORVÁTH)
Pázmány Péter Catholic University, Faculty of Information Technology and Bionics
50/a Práter street, 1083 Budapest, Hungary
rajki.franciska.sara@itk.ppke.hu

***Abstract*—Adversarial attacks intentionally modify the inputs to cause deep neural networks to make incorrect predictions. These attacks create perturbations on physical objects that fool image classifiers under a variety of real-world conditions. Such attacks pose a risk to deep learning models used in safety-critical systems such as self-driving cars. [1] Our approach was to make a network, which has high accuracy and is also better in ignoring adversarial attacks than a simple convolutional neural network.**

I. Summary

A classical example for adversarial attack is stickering a stop sign. This small change which is negligible to humans can cause a neural network embedded self-driving car to misclassify or ignore the sign, which can lead to serious accidents. This is called an adversarial sticker attack. [1] Eykholt et al. introduced two different adversarial attack method, the disappearance and the creation attacks. The latter one fools the network into recognizing an object, which is not represented while the other one fools the network to misclassify represented objects. [1] Brown et al. presented a method to create the so-called adversarial patches. The patches are universal because they can be used to attack any scene, robust because they work under a wide variety of transformations, and targeted because they can cause a classifier to output any target class. These adversarial patches can be printed, added to any scene, photographed, and presented to image classifiers; even when the patches are small, they cause the classifiers to ignore the other items in the scene and report a chosen target class. [2] I implementedan a neural network which is similar to an autoencoder. It performs a domain-to-domain transformation. An autoencoder is a neural network consisting of two parts, an encoding side and a decoding side. The input of the network is also the expected output of it. We made sure that our network works properly on several datasets. We had the feasibility test on the MNIST dataset of handwritten numbers[3]. To make sure that our network also works on something more complex we also tried the network on the INRIA dataset of persons[4] and part of the cifar-10 dataset [5]. The network has a high accuracy, and is also better in fending off adversarial attacks than a similarly clever convolutional network.

References

[1] K. Eykholt, I. Evtimov, E. Fernandes, B. Li, A. Rahmati, F. Tramèr, A. Prakash, T. Kohno, and D. Song, "Physical adversarial examples for object detectors," *CoRR*, vol. abs/1807.07769, 2018.
[2] T. B. Brown, D. Mané, A. Roy, M. Abadi, and J. Gilmer, "Adversarial patch," *CoRR*, vol. abs/1712.09665, 2017.
[3] Y. LeCun, "The mnist database of handwritten digits," *http://yann. lecun. com/exdb/mnist/*, 1998.
[4] N. Dalal and B. Triggs, "Histograms of oriented gradients for human detection," in *Proceedings of the 2005 IEEE Computer Society Conference on Computer Vision and Pattern Recognition (CVPR'05) - Volume 1 - Volume 01*, CVPR '05, (Washington, DC, USA), pp. 886–893, IEEE Computer Society, 2005.
[5] A. Krizhevsky, V. Nair, and G. Hinton, "Cifar-10 (canadian institute for advanced research),"
[6] I. Goodfellow, J. Shlens, and C. Szegedy, "Explaining and harnessing adversarial examples," in *International Conference on Learning Representations*, 2015.

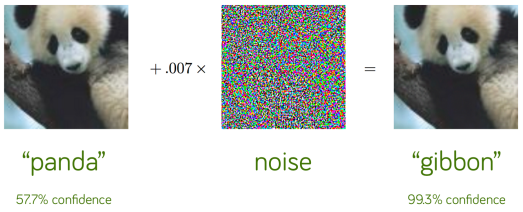

Fig. 1. Image misclassified because of adversarial noise attack. [6]

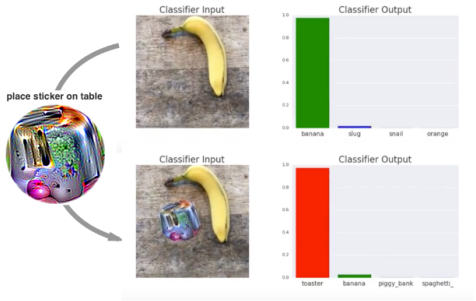

Fig. 2. Image misclassified because of adversarial patch attack. [2]

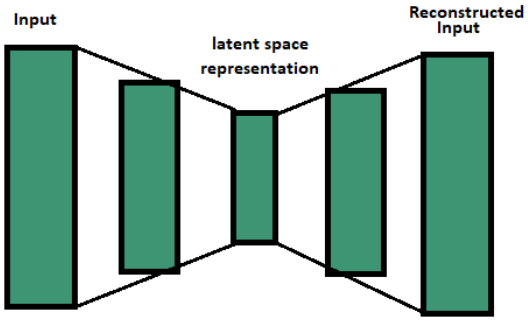

Fig. 3. Autoencoder structure.

F. RAJKI, "Adversarial Attack Resilience of Neural Networks" in *PhD Proceedings – Annual Issues of the Doctoral School, Faculty of Information Technology and Bionics, Pázmány Péter Catholic University – 2019.* G. Prószéky, P. Szolgay Eds. Budapest: Pázmány University ePress, 2019, pp. 62–62.
This research has been partially supported by the European Union, co-financed by the European Social Fund (EFOP-3.6.3-VEKOP-16-2017-00002).

APPENDIX

PROGRAM 1: Bionics, Bio-inspired Wave Computers, Neuromorphic Models	
Name	**Supervisor**
Luca Anna BORS	Franciska ERDŐ PhD
Suchana CHAKRAVARTY	Attila CSIKÁSZ-NAGY DSc
Veronika CSILLAG	Imre FARKAS MD PhD, Zsolt LIPOSITS MD DSc
Ward FADEL	István ULBERT MD DSc, Lucia WITTNER MD PhD
Bianka Vivien FARKAS	Zoltán GÁSPÁRI PhD, Tamás HEGEDŰS PhD
Tünde Éva GAIZER	Attila CSIKÁSZ-NAGY DSc
Anna HAJDARA	Miklós GYÖNGY PhD, Balázs MAYER PhD
Zita HARMAT	Zoltán GÁSPÁRI PhD
Zsófia Etelka KÁLMÁN	Zoltán GÁSPÁRI PhD
Bence Márk KEÖMLEY-HORVÁTH	Attila CSIKÁSZ-NAGY DSc, István Zoltán REGULY PhD
Csaba Márton KÖLLŐD	István ULBERT MD DSc
Marcell MISKI	Attila CSIKÁSZ-NAGY DSc
Máté MOHÁCSI	Tamás FREUND MHAS, Szabolcs KÁLI PhD
Eszter NAGY-KANTA	Zoltán GÁSPÁRI PhD
Mihály SZŰCS	Kristóf IVÁN PhD
Luca TAR	Tamás FREUND MHAS, Szabolcs KÁLI PhD
Moutz WAHDOW	István ULBERT MD DSc

PROGRAM 2: Computer Technology Based on Many-core Processor Chips, Virtual Cellular Computers, Sensory and Motoric Analog Computers	
Name	**Supervisor**
Nawar Kadhem AL-HEMEARY	Gábor SZEDERKÉNYI DSc, György CSEREY PhD
Gábor Dániel BALOGH	István Zoltán REGULY PhD
Áron CSERKASZKY	Péter SZOLGAY DSc
Attila FEJÉR	Péter SZOLGAY DSc
Dániel HAJTÓ	György CSEREY PhD
Sam KHOZAMA	Zoltán NAGY PhD, Zoltán GÁSPÁRI PhD
Márton Zsolt KISS	Ákos ZARÁNDY DSc
Ádám NAGY	Ákos ZARÁNDY DSc
Koppány PÁZMÁN	Ákos ZARÁNDY DSc
Péter POLCZ	Gábor SZEDERKÉNYI DSc
Levente Márk SÁNTHA	Ákos ZARÁNDY DSc, Zoltán NAGY PhD
Ágnes SZABÓ	Zoltán FEKETE PhD
Gergely SZLOBODNYIK	Gábor SZEDERKÉNYI DSc

PROGRAM 3: Feasibility of Electronic and Optical Devices, Molecular and Nanotechnologies, Nano-architectures, Nanobionic Diagnostic and Therapeutic Tools	
Name	**Supervisor**
András FÜLÖP	György CSABA PhD, András HORVÁTH PhD
Krisztián FÜZESI	Miklós GYÖNGY PhD
Janka HATVANI	Miklós GYÖNGY PhD
Péter MAROSÁN	Miklós GYÖNGY PhD
Zsolt MEZRICZKY	J. Balázs RÓZSA PhD
Zsófia VARGA-MEDVECZKY	J. Balázs RÓZSA PhD

PROGRAM 4: Human Language Technologies, Artificial Understanding, Telepresence, Communication	
Name	**Supervisor**
András GELENCSÉR	Kristóf KARACS PhD, Péter SZOLGAY DSc
András Attila SULYOK	Kristóf KARACS PhD, Péter SZOLGAY DSc

PROGRAM 5: On-board Advanced Driver Assistance Systems	
Name	**Supervisor**
Mohammad Jalal ALAFANDI	András HORVÁTH PhD
Dóra Eszter BABICZ	Csaba REKECZKY PhD, András HORVÁTH PhD
Yahya IBRAHIM	Csaba BENEDEK PhD
Ákos KOVÁCS	Tamás BÜKKI PhD, András HORVÁTH PhD
Lóránt KOVÁCS	Ákos ZARÁNDY DSc, Viktor TIHANYI PhD
Balázs NAGY	Csaba BENEDEK PhD
Franciska Sára RAJKI	András HORVÁTH PhD